Copy No. 101

NASA CR-132669

A FUSELAGE/TANK STRUCTURE STUDY FOR ACTIVELY COOLED HYPERSONIC CRUISE VEHICLES

Active Cooling System Analysis

By James E. Stone

Prepared under Contract No. NAS1-12995
McDonnell Aircraft Company (MCAIR)
McDonnell Douglas Corporation, St. Louis, Mo. 63166
for
NATIONAL AERONAUTICS AND SPACE ADMINISTRATION
Langley Research Center, Hampton, Va. 23865

FOREWORD

This report summarizes the results of "A Fuselage/Tank Structure Study For Actively Cooled Hypersonic Cruise Vehicles" performed from 11 March 1974 through 30 June 1975 under National Aeronautics and Space Administration Contract NAS-1-12995 by McDonnell Aircraft Company (MCAIR), St. Louis, Missouri, a division of McDonnell Douglas Corporation.

The study was sponsored by the Structures and Dynamics Division with Dr. Paul A. Cooper as Study Monitor and Mr. Robert R. McWithey as Alternate Study Monitor.

Mr. Charles J. Pirrello was the MCAIR Study Manager with Mr. Allen H. Baker as Deputy Study Manager. The study was conducted within MCAIR Advanced Engineering which is managed by Mr. Harold D. Altis, Director, Advanced Engineering Division. The study team was an element of Advanced Systems Concepts, supervised by Mr. Dwight H. Bennett.

The basic purpose of this study was to evaluate the effects of fuselage cross section (circular and elliptical) and structural arrangement (integral and non-integral tanks) on the performance of actively cooled hypersonic cruise vehicles. The study was conducted in accordance with the requirements and instructions of NASA RFP 1-08-4129 and McDonnell Technical Proposal Report MDC A2510 with minor revisions mutually agreed upon by NASA and MCAIR. The study was conducted using customary units for the principal measurements and calculations. Results were converted to the International System of Units (S.I.) for the final report.

This is one of three reports detailing the technical results of the study. The other two reports are "Aircraft Design Evaluation," Reference (1), and "Structural Analysis," Reference (2).

The primary contributor to the contents of this report was James E. Stone. Assistance was provided by Roland L. Hansen and Ralph L. Herring.

TABLE OF CONTENTS

LIST OF ILLUSTRATIONS

LIST OF ABBREVIATIONS AND SYMBOLS

Symbol	Definition
A	Area
B/O	Boiloff, fuel
Btu	British Thermal Unit
cfm	Cubic feet per minute
D	Diameter
ECS	Environmental Control System
ϵ	Emissivity
°F	Degrees Fahrenheit
FS	Fuselage Station
ft	Feet
g	Grams
GH_2	Gaseous Hydrogen
GN_2	Gaseous Nitrogen
h	Heat transfer coefficient, convective
H_2	Hydrogen
HP	Horsepower
hr	Hour
h_v	Heat of vaporization, latent
in	Inch
Ins	Insulation
J	Joule
K	Kelvin
L	Length
lbf	Pounds Force
lbm	Pounds Mass
LE	Leading Edge
LH_2	Liquid Hydrogen
m	Meter
$\dot{m}$	Coolant flowrate
min	Minute
Mn	Mach number
mph	Miles per hour
N	Newton

LIST OF ABBREVIATIONS AND SYMBOLS (Continued)

Symbol	Definition
N_2	Nitrogen
NM	Nautical Mile
O.W.E.	Operating Weight, Empty
P	Pitch, Pressure
Pa	Pascal
pcf	Pounds mass per cubic foot
psi	Pounds force per square inch
$\dot{Q}$	Integrated heating rate = $\int \dot{q} dA$
$\dot{q}$	Heating rate per unit area
s, sec	Second
T	Temperature
t	Thickness
TOGW	Takeoff Gross Weight
T/O	Takeoff
TPS	Thermal Protection System
W	Watt
Wt	Weight
X	Distance, thickness
Λ	Leading Edge Sweep Angle
Prefixes	
c	Centi (10^{-2})
k	Kilo (10^{3})
m	Milli (10^{-3})
M	Mega (10^{6})
Δ	Difference
Subscripts	
avg	Average
b	Bond, adhesive
c	Coolant
ins	Insulation
max	Maximum
s	Skin
t	Tube

1. INTRODUCTION

This report, entitled "Active Cooling System Analysis," presents the thermodynamic design and analytical studies conducted for the three aircraft concepts described in Reference (1). The results of these studies were utilized in the design refinement of each concept, in which final weights and performance were determined. In general, while there were some differences in the thermodynamic analyses, the analytical effort for all three concepts was quite similar.

This effort was primarily directed toward two goals. These were:

a. Definition of an active cooling system (Figure 1) to satisfy the requirement of maintaining the aircraft's entire surface area at temperatures below 394 K (250°F) at Mach 6. (An unlimited fuel heat sink availability was assumed, as specified in the Statement of Work.)

b. Design of a hydrogen fuel tankage thermal protection system (TPS) that results in maximum aircraft range.

Effort on Concept 1 (circular, wing-body/non-integral tankage) was initially directed toward the first goal. The tankage TPS was designed after the fuselage structural arrangement had been established. This procedure was reversed for Concept 2 (circular, wing-body/integral tankage) and Concept 3 (elliptical, blended-body/integral tankage). Trade studies of eight candidate TPS arrangements were conducted for these concepts. The most promising concept was recommended to NASA and approved for further study. The Concept 2 and 3 active cooling systems were then defined. The results of the thermodynamic studies are summarized in Section 2.

Design requirements, discussed in Section 3, strongly influenced the thermodynamic studies. The intent of the study was to provide preliminary sizing data and to insure compatible comparisons of the three aircraft concepts being studied. Therefore the specific cooling systems derived are not to be considered optimized designs.

Section 4 describes the establishment of design heat loads for each concept, including determination of the minimum heat load flight profile. Detailed heating rates at various surface locations are provided, in addition to the total design airframe heat loads.

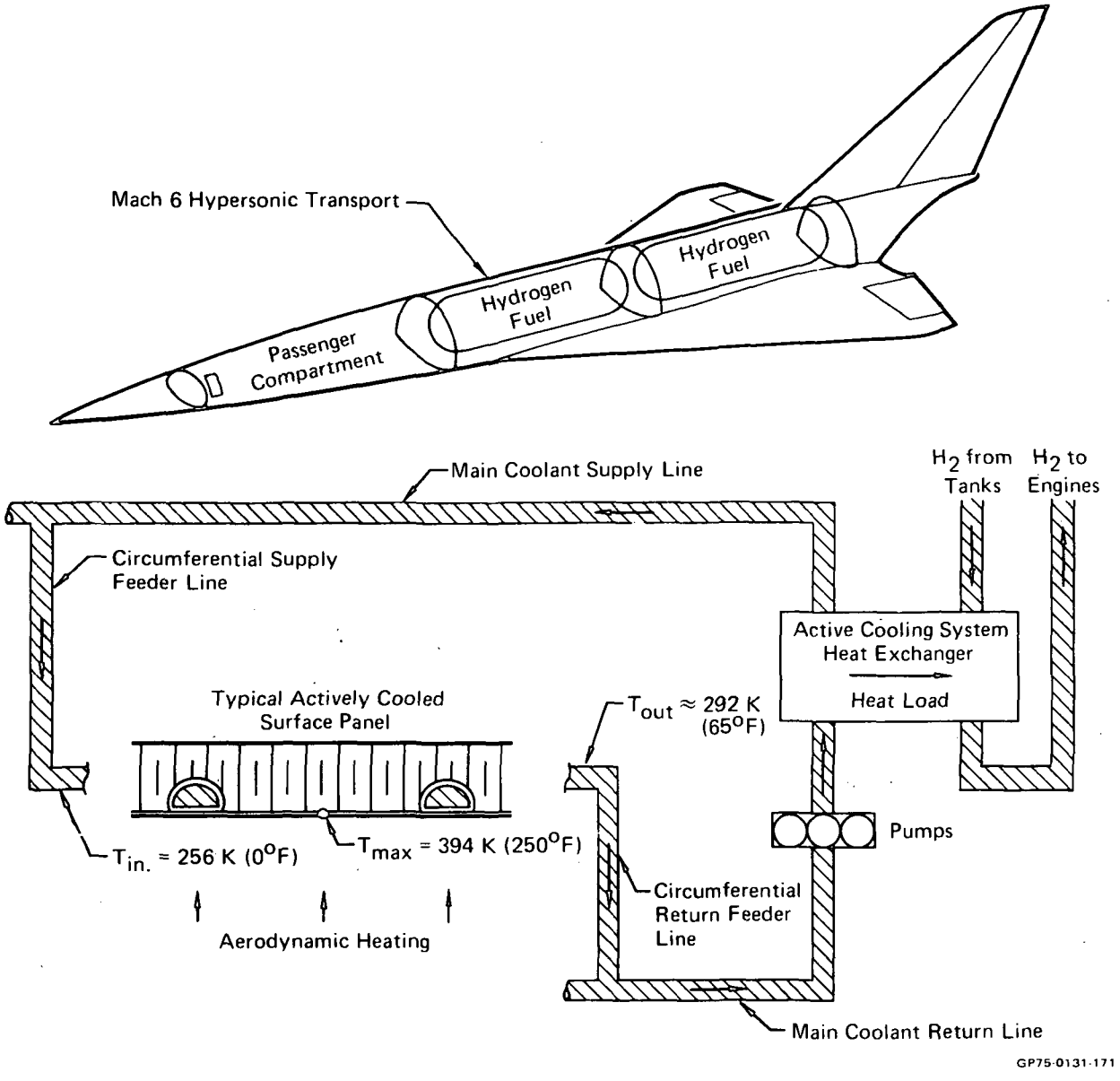

FIGURE 1
AIRFRAME SURFACE ACTIVE COOLING SYSTEM

Section 5 describes the techniques used to establish the coolant flowrates. These requirements were determined at various aircraft locations and integrated to yield total values. Subsystem cooling requirements were determined as discussed in Section 6, and added to the airframe cooling requirements to establish total design heat loads and coolant flowrates. The subsystems

considered were the environmental control system (ECS), hydraulic system, and electrical power system. The coolant distribution system routing arrangement and the locations of major components were then defined and cooling system weights were computed, as discussed in Section 7.

Analyses of the tankage thermal protection systems are discussed in Section 8. The procedure used to design the non-integral tankage TPS for Concept 1 is discussed first. Then, the eight candidate TPS concepts considered for integral tankage (Concepts 2 and 3) are described. The sizing techniques used and comparative data to a baseline TPS concept are discussed. The candidate TPS recommended to NASA is identified, along with the selection rationale. Section 8 also discusses an analysis conducted to size the gaseous nitrogen system used to purge the voids between tankage and the surface structure to avoid a buildup of gaseous hydrogen and water vapor condensation.

Some thermodynamic observations and considerations for this class of aircraft are discussed in Section 9. Significant thermodynamic conclusions derived from these studies are summarized in Section 10 along with recommedations for future investigation. The results of this entire study are summarized in Reference (3).

2. SUMMARY OF FINAL ACTIVE COOLING SYSTEM DESIGNS

Thermodynamic characteristics of the actively cooled thermal protection systems established for the three aircraft concepts are summarized in this section. Design heat loads and coolant flowrate requirements are defined for each major structural section and for the total system. Cooling system weights are summarized at the major component level.

As previously stated, it was assumed that an unlimited fuel heat sink capacity was available. However, by using the actual heat sink capacity available at realistic engine fuel flowrates, only about one-half of the design heat loads could have been accommodated. If less than the entire airframe surface area had been cooled, the weight of the active cooling system would have been lower, but weight increases would have been reflected elsewhere, for insulation, additional structural shielding, etc. These weights could tend to balance out, so overall aircraft weight may not be greatly affected.

Weight penalties have been calculated for TPS-related insulation and fuel boiloff. The TPS concepts shown were refined by trade studies which maximized the aircraft range for each concept.

Reference (4) specified a number of configuration/structural arrangement tradeoffs to be conducted in the study. The aircraft design evaluations are given in Reference (1) and the structural analyses tradeoffs presented in Reference (2). During the thermodynamic studies it became evident that significant thermodynamic performance drivers also existed. For example, as discussed in Section 4.2, the selection of a trajectory profile must be examined with care, and tailored to the requirements imposed on the active cooling system. Also, as discussed in Section 4.3, there may be overall aircraft penalties associated with cooling large areas subject to high heating rates, such as the nacelle, even if an unlimited heat sink is available. In summary, these studies revealed certain areas for further meaningful investigation. These areas are identified in References (1) and (2) as well as this report.

2.1 CONCEPT 1

The thermodynamic design characteristics of the circular, wing-body/non-integral tankage aircraft are summarized in Figure 2. Concept 1 was used in preliminary studies to determine the fuel weight, which was then held

constant in all three concepts. This aircraft was also used for the trajectory and nacelle cooling tradeoffs discussed in Sections 4.2 and 4.3.

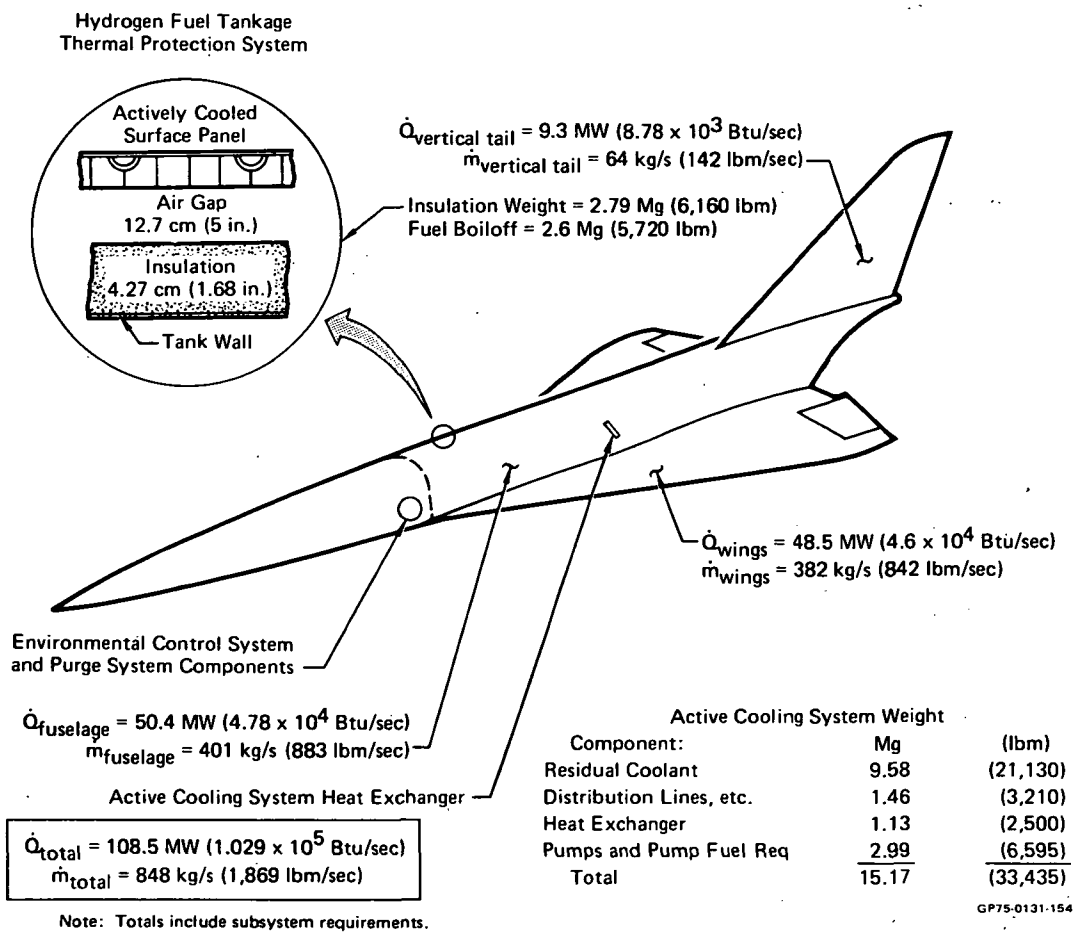

FIGURE 2
THERMODYNAMIC SUMMARY, CONCEPT 1

2.2 CONCEPT 2

Figure 3 summarizes the thermodynamic characteristics of the circular, wing-body/integral tankage aircraft. Since the moldline contours reflect only minute changes from Concept 1, the active cooling system characteristics are nearly identical. TPS arrangement reflects the result of the integral tankage TPS concept tradeoff study presented in Section 8. This arrangement is thermodynamically similar to the non-integral tankage TPS arrangement shown in Figure 2. The larger gap between the panel and insulation in Concept 1 results from a requirement for panel support frames. Concept 2 panels are not primary structure.

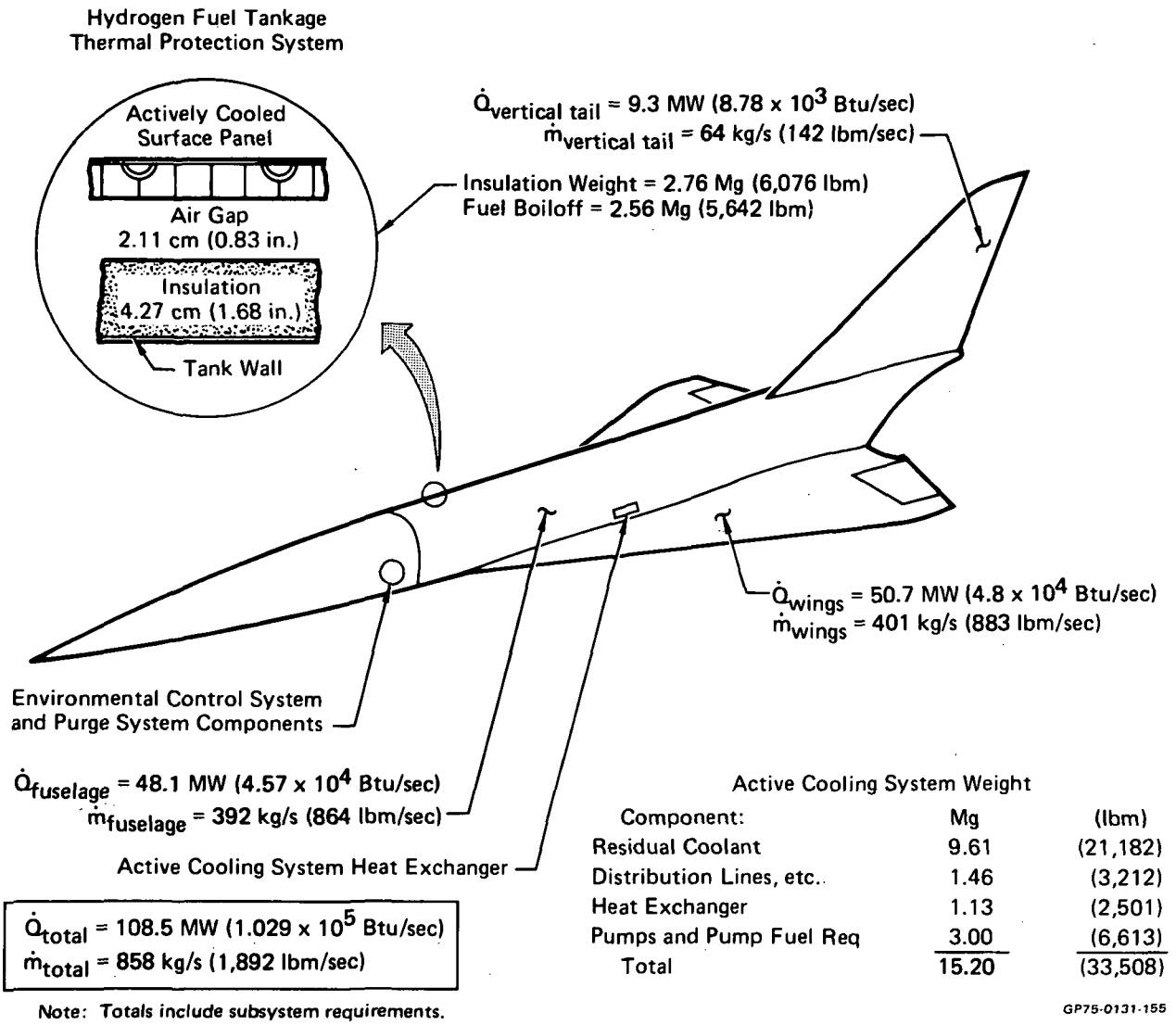

Active Cooling System Weight

Component:	Mg	(lbm)
Residual Coolant	9.61	(21,182)
Distribution Lines, etc.	1.46	(3,212)
Heat Exchanger	1.13	(2,501)
Pumps and Pump Fuel Req	3.00	(6,613)
Total	15.20	(33,508)

FIGURE 3
THERMODYNAMIC SUMMARY, CONCEPT 2

2.3 CONCEPT 3

Elliptical, blended-body/integral tankage aircraft thermodynamic characteristics are summarized in Figure 4. Compared to Concepts 1 and 2, the active cooling system requirements are significantly lower. This is attributable to the smaller surface area. Due to the significantly different fuselage shaping and volume utilization, the arrangement of cooling system components is considerably different. This difference, discussed in Section 7.1, was reflected in the thermodynamic study results.

The Concept 3 tankage TPS is similar to that shown for Concept 2 but the insulation is slightly thicker, because of the different range sensitivity of Concept 3. Total insulation and fuel boiloff weights are also higher because of the larger surface areas associated with elliptical, bubble tankage.

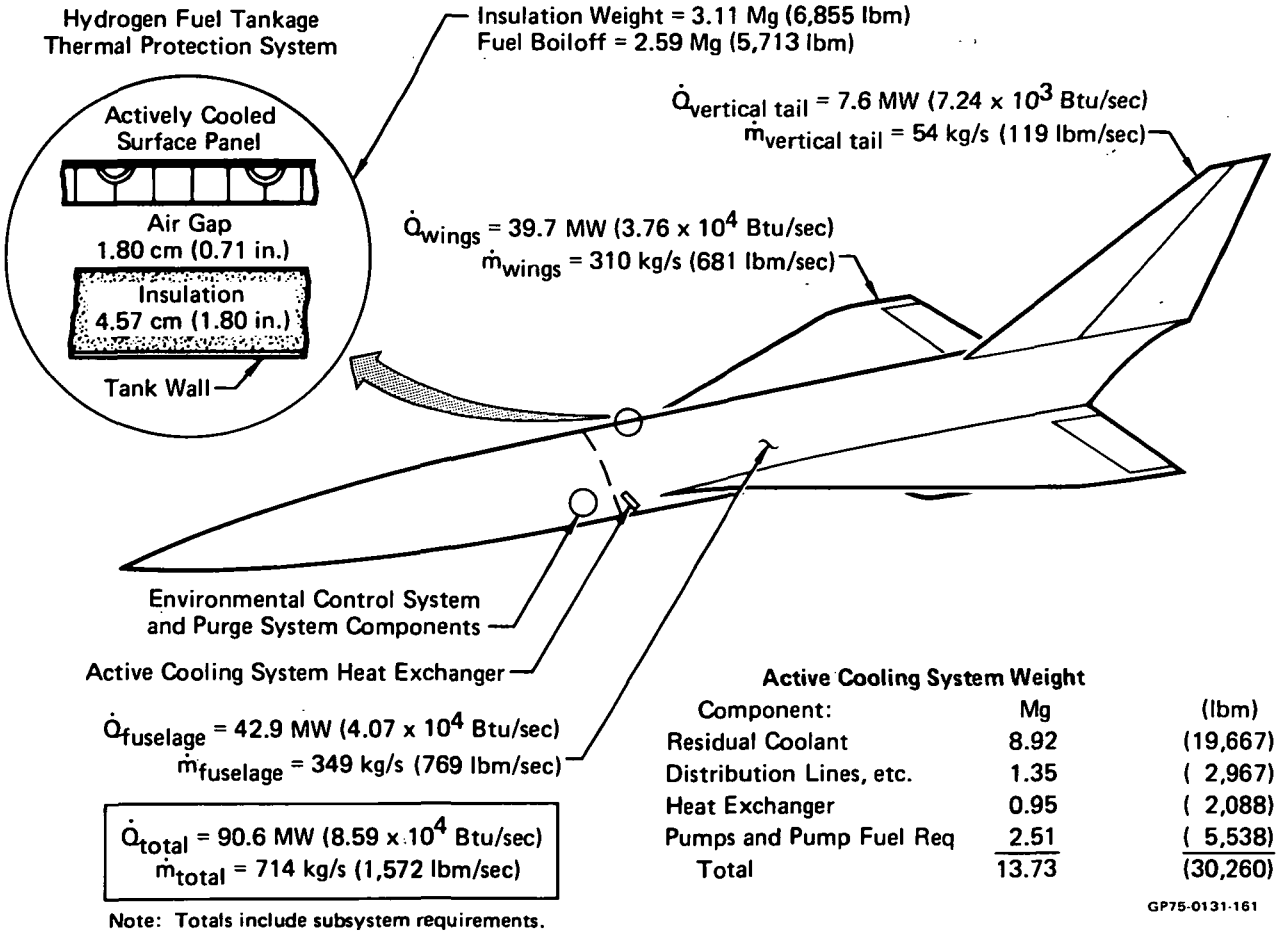

Active Cooling System Weight

Component:	Mg	(lbm)
Residual Coolant	8.92	(19,667)
Distribution Lines, etc.	1.35	(2,967)
Heat Exchanger	0.95	(2,088)
Pumps and Pump Fuel Req	2.51	(5,538)
Total	13.73	(30,260)

GP75-0131-161

FIGURE 4
THERMODYNAMIC SUMMARY, CONCEPT 3

3. THERMAL DESIGN REQUIREMENTS AND GUIDELINES

Ground rules, assumptions, and requirements used in the study are presented in this section, along with other thermodynamic considerations. In a few instances, deviations to Reference (4) requirements were approved by NASA. In addition, some study guidelines were established to facilitate the analyses. When possible, the results of previous studies, such as Reference (5), and current related studies, such as Reference (6), were used to establish these guidelines. The bases used for thermodynamic evaluation of the study aircraft are summarized in Figure 5.

	CRITERIA PERTINENT IN DETERMINING:			
	ABSORBED HEAT LOAD	COOLING SYSTEM SIZE	SUBSYSTEM REQ'S	TANKAGE TPS REQ'S
1. Requirements imposed by Reference (4):				
a. Airframe structural arrangement shall include an active cooling system over the entire surface area of the vehicle.	X	X		
b. Surface structural material will be maintained below 394 K (250°F).	X	X	X	X
c. Aluminum shall be the primary structural material.	X	X		
d. Engine fuel flow requirements shall be assumed adequate for vehicle cooling.	X	X		
e. Active cooling system for non-integral tank configurations and for the wings and tail surfaces of the integral tank configurations shall be similar to the water-glycol system described in References (5), (7), and (8).		X		
f. Passenger compartment pressures shall be as required by Reference (9).			X	
g. Several active cooling systems compatible with integral tankage, including three concepts defined in Reference (4), shall be screened and compared on the basis of a simplified assessment of system weight and volume utilization.		X		X

FIGURE 5

THEROMODYNAMIC EVALUATION BASIS

	CRITERIA PERTINENT IN DETERMINING:			
	ABSORBED HEAT LOAD	COOLING SYSTEM SIZE	SUBSYSTEM REQ'S	TANKAGE TPS REQ'S
h. Configurations with an intervening void space between the tankage structure and outer surface structure shall be purged with dry nitrogen gas at a maximum pressure of 3.45 kPa (0.5 psi) gage.				X
i. External cryogenic insulation shall be a closed cell freon-blown, fiberglass reinforced, polyurethane foam having a thermal conductivity of 187 mW/m·K (0.13 Btu in/hr ft^2°F) and a density of 64.1 kg/m^3 (4 lbm/ft^3).				X
j. Internal cryogenic insulation density shall be the same as external insulation but the thermal conductivity shall be based on the assumption that hydrogen gas has permeated the insulation.				X
k. Active cooling system weight shall include fuel boiloff, insulation, distribution system, heat exchanger, pump, and pump fuel weights.		X		X
2. Deviations to requirements: Justification:				
a. Requirement 1-a. - Nacelle surface area not actively cooled but designed as hot structure. Excessive penalties associated with cooling this relatively small area of the airframe. Discussed in Section 4.	X	X		

FIGURE 5 (Continued)

		CRITERIA PERTINENT IN DETERMINING:			
		ABSORBED HEAT LOAD	COOLING SYSTEM SIZE	SUBSYSTEM REQ'S	TANKAGE TPS REQ'S
b. Requirement 1-e. - Methanol-water solution selected as coolant rather than water-glycol.	Reference (6) studies indicate payoff with methanol-water and this selection provides compatibility between these studies. Discussed in Section 5.		X		
c. Requirement 1-i. - External cryogenic insulation thermal conductivity reflects variation with temperature rather than constant value.	More realistic assumption that removes undue conservatism in analyses. Discussed in Section 8.				X
3. Guidelines established:	Justification:				
a. Cooling system design pressure = 1.03 MPa (150 psi) absolute	Influenced by results presented in Reference (5).		X		
b. Coolant supply temperature = 256 K (0°F).	Influenced by Reference (6) results.		X		
c. Nominal panel size = 1.22 m x 6.10 m (4 ft x 20 ft)	Considered by MCAIR producibility department as being the largest size panel compatible with handling considerations.		X		

FIGURE 5 (Continued)

		CRITERIA PERTINENT IN DETERMINING:			
		ABSORBED HEAT LOAD	COOLING SYSTEM SIZE	SUBSYSTEM REQ'S	TANKAGE TPS REQ'S
d.	Panel coolant tube I.D. = 8.64 mm (0.34 in)	Influenced by Reference (6) results. Analyses to optimize tube diameter considered beyond the scope of this study.	X		
e.	Engine inlet duct walls cooled with hydrogen fuel to super-alloy material temperature limits.	Decision discussed in Section 9.	X		
f.	A one-hour ground hold time added to basic trajectory.	Included to provide realistic sizing criteria for hydrogen tankage thermal protection and purge system requirements.			X
g.	Thermal conductivity of internal cryogenic insulation = 0.9 times that of gaseous hydrogen.	Based on available information reflecting effect of hydrogen gas permeation of assumed insulation material.			X
h.	Hydrogen fuel is loaded at normal boiling point temperature of 20.3 K (-423°F).	Compatible with fuel tank pressure of 138 kPa (20 psi) gage specified by Reference (4).			X

FIGURE 5 (Continued)

4. AIRFRAME SURFACE HEATING RATES

Airframe surface heating rates were determined so that the active cooling system requirements could be established. Local surface heating rates ($\dot{q}$), combined with structural requirement considerations, established the tube spacing in the panel and the flowrate requirements. With this information, the weight of the structural panel and the residual coolant within the panel was determined.

Integrating the local heating rates with respect to area ($\dot{Q}$) provided the instantaneous heating rate to be absorbed by the coolant. The summation of these heating rates over the entire cooled airframe surface provided the total cooling system design heat load. The total heat load influenced the size of cooling system components and established the amount of heat sink required. Panel coolant flowrate requirements and airframe geometry are the prime factors that influenced the size of the coolant distribution system.

This section summarizes the techniques used to establish parametric surface heating rates. The total airframe heat loads and the component weight of the active cooling system were then estimated for the design conditions related to the baseline trajectory of the Mach 6 transport. Two trade-offs were conducted to arrive at the selected design condition. The ascent trajectory was examined to define a flight profile that maximized aircraft range. A trade-off involving nacelle surface cooling requirements was also conducted.

The local heating rates at numerous locations on the aircraft surfaces are presented in this section.

4.1 ANALYTICAL TECHNIQUES

External surface heating rates are influenced by Mach number, altitude, and aircraft geometry. Preliminary analyses indicated that a trade-off of potential ascent trajectory profiles would be required to establish the design condition. To aid in this study, parametric heating rate data were generated to reflect the effects of design altitude on local heating rates at various surface locations.

The assumptions and analytical techniques used to predict the aerodynamic heating inputs to cooled panels are discussed below. The resultant data were applicable on all three aircraft concepts.

To be consistent with the requirement of a maximum structural temperature of 394 K (250°F) and the use of aluminum as the primary structural material,

heating rates were based on an average surface temperature of 366 K (200°F). This value is an approximation, based on an allowable skin temperature gradient between points midway between tubes and points immediately above tubes, of 56 K (100°F), but it can be shown that at Mach 6, a deviation of 11 K (20°F) in surface temperature will affect the calculated heating rates by only 1%. Therefore, the assumed value was considered accurate enough for calculating surface heating rates.

Heating rates to the cooled structure were determined by taking the difference between the aerodynamic heating input and the external surface thermal radiation loss. The estimated radiation loss of 204 W/m^2 (0.018 Btu/sec ft^2), based on an aluminum surface emissivity of 0.2, was small relative to the Mach 6 aerodynamic heating inputs, which average about 29.5 kW/m^2 (2.6 Btu/sec ft^2).

A range of altitudes from 28 km (92,000 feet) to 36.6 km (120,000 feet) (per the preliminary flight envelope for Mach 6 conditions) was considered during the parametric studies. Variations in surface deflection angle (defined as the angle the referenced surface makes relative to the free stream velocity vector) from -24° to 30° were considered. The surface deflection angle at each location was determined by adding the geometric angle relative to the wing chord line to the instantaneous angle of attack of the aircraft. A range of characteristic surface lengths of up to 107 m (350 ft) was considered. This encompasses any location on the study vehicles.

Heating rates in undisturbed flow regions removed from stagnation regions were determined based on Eckert's reference enthalpy method for laminar flow and the Spalding and Chi correlation for turbulent flow. Turbulent heating rates were based on a virtual origin at the onset of transition, with a transition length equal to the laminar run length. Transitional heating rates were determined by assuming a straight line relationship between the final fully laminar heating rate and the first fully developed turbulent heating rate. Transition lengths computed for windward and leeward surfaces are presented in Figures 6 and 7 respectively.

Local flow conditions used in determining aerodynamic heating characteristice were based on real gas, wedge flowfield and Prandtl-Meyer expansion relationships.

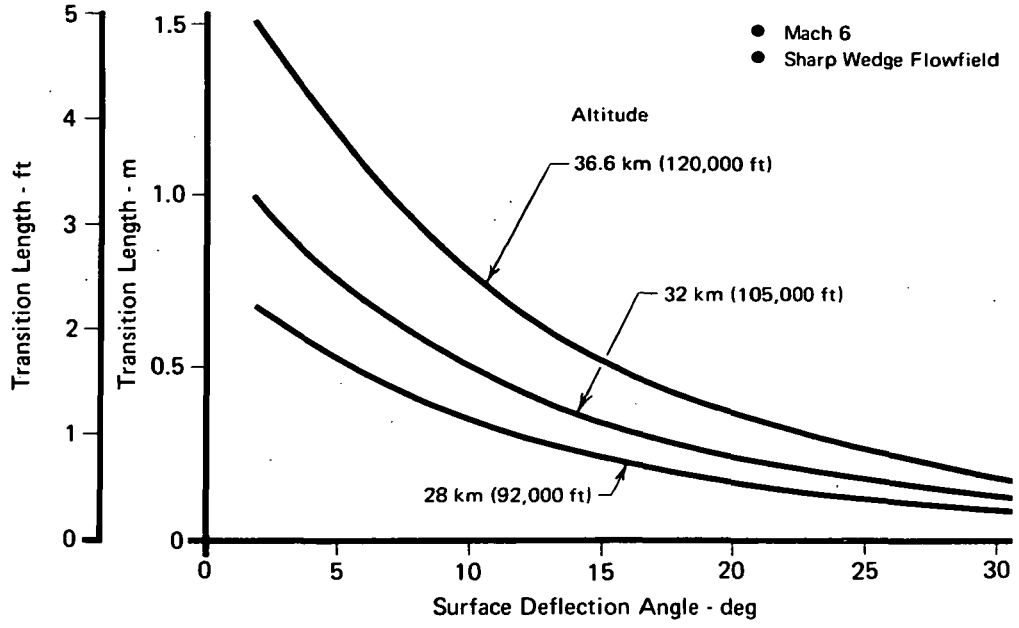

FIGURE 6
TRANSITION LENGTH, WINDWARD SURFACES

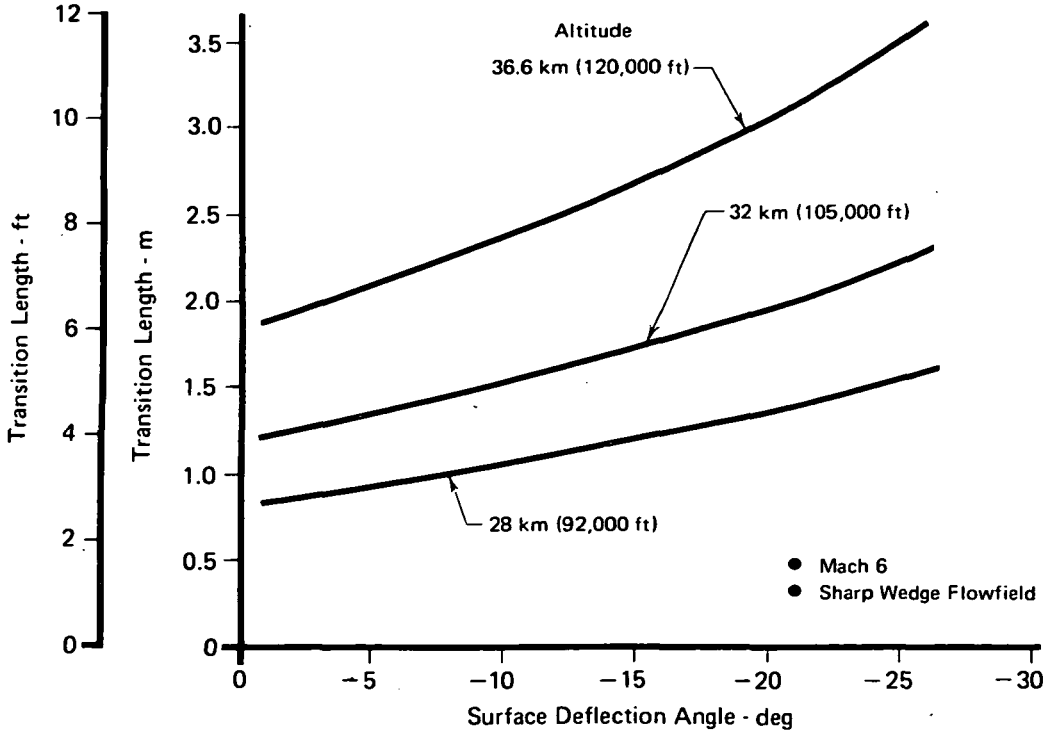

FIGURE 7
TRANSITION LENGTH, LEEWARD SURFACES

Examination of the proposed aircraft configurations revealed that most areas were readily adaptable to wedge flowfield simulation. Even though the fuselage forebodies are essentially elliptical in shape, the lower surfaces are nearly flat. Only the fuselage upper surfaces and forebody sidewalls deviate significantly from flat surfaces. To determine if body shape characteristics would significantly affect the analyses, some conical flowfield heating rates were determined for comparison. At most comparable points (equal body length and wedge/half-cone deflection angle) the calculated local heating rates were slightly higher (by as much as 15%) using a wedge flowfield. This is attributable to the higher local Reynolds numbers that result from higher local static pressures associated with wedge flowfields. Since analysis of aerodynamic heating rates, in conjunction with body shape considerations would have required sophisticated methods, with an apparently small payoff, subsequent analyses considered only wedge flowfield heating rates yielding conservative results.

Most leeward surfaces are exposed to expansion flowfields. Numerous heat transfer correlations have shown that considering fully expanded flow on leeward surfaces using Prandtl-Meyer relationships results in underprediction of heating rates. Conversely, consideration of non-expanded flow introduces significant conservatism. For these studies, leeward flow conditions were based on an effective expansion angle. Data correlations from sources such as Reference (10) indicate that at Mach 6, for a turbulent boundary layer, a maximum effective expansion angle of approximately 6° should be considered before flow separation occurs. Other unpublished MCAIR test data correlations indicate that, at Mach 6, a ratio of effective to actual expansion angle of 1/4 provides a conservative, yet reasonable, data fit. For this study, all leeward surface expansion angles were corrected to effective angles by a 1/4 factor while using Prandtl-Meyer relationships. This correction was applicable to determination of transition length and heating rate.

Figure 8 presents typical surface heating rates predicted for windward body locations while Figure 9 shows rates predicted for leeward body locations. Only fully turbulent flow heating rate estimates are presented in Figures 8 and 9.

Stagnation point heating rates were computed using Fay and Riddell's three-dimensional stagnation theory. Heating rates on the fuselage nose tip were determined by considering a cosine distribution away from the stagnation

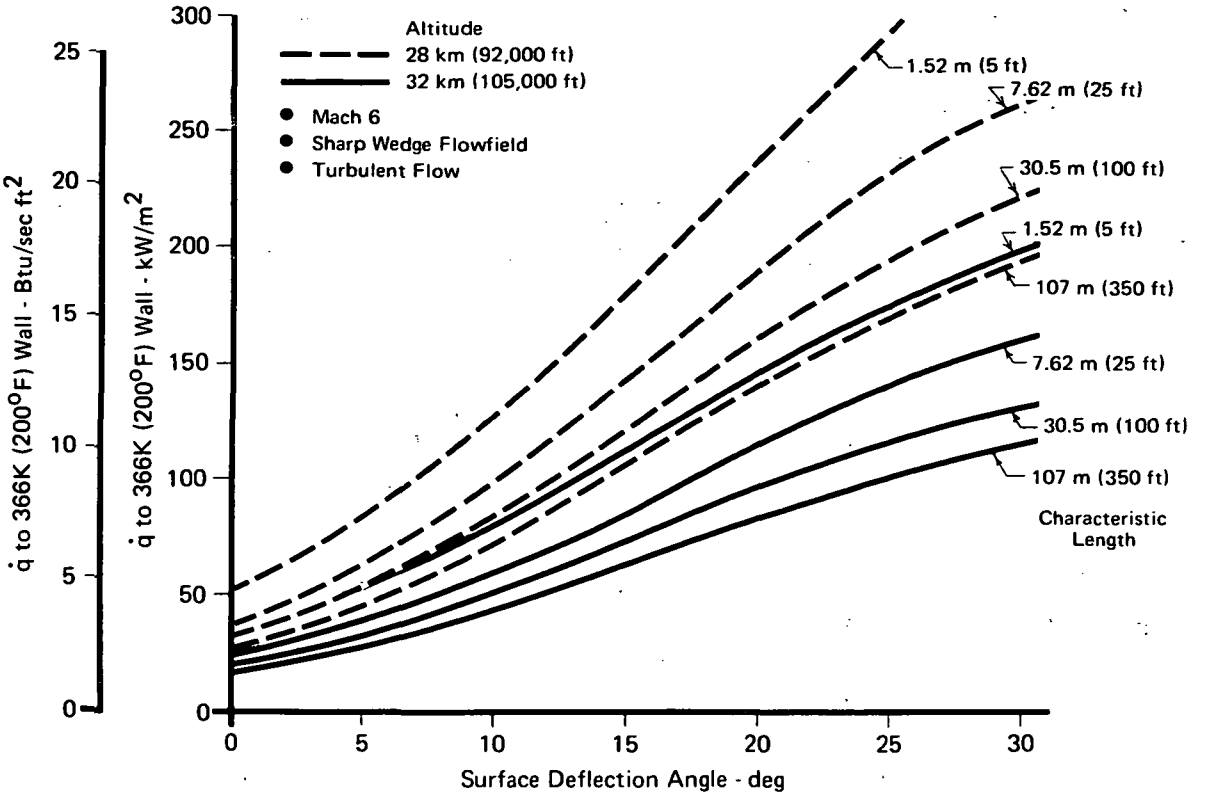

FIGURE 8
WINDWARD SURFACE HEATING RATES

GP75-0131-67

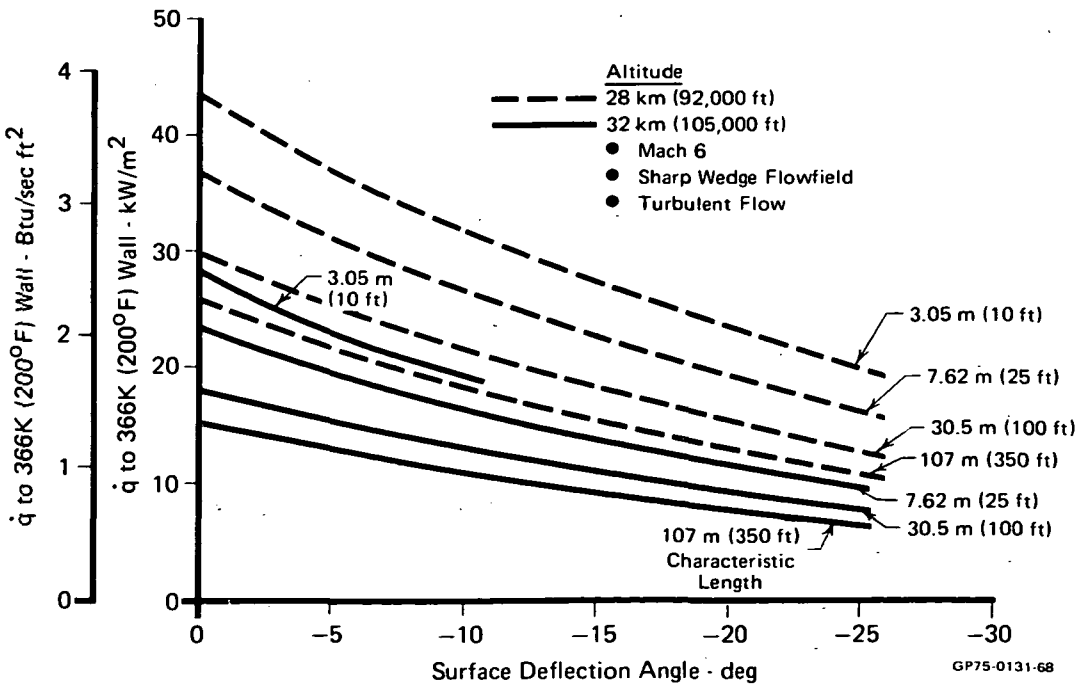

GP75-0131-68

FIGURE 9
LEEWARD SURFACE HEATING RATES

point, with a curve fairing to the heating rate data associated with the regions aft of the nose. Heating rates on the stagnation line of the wing and tail leading edges were determined by first correcting for two-dimensional flow by dividing the 3-D data by $\sqrt{2}$ and then accounting for sweep angle by applying a factor of the cosine of the angle raised to the 1.2 power. Heating rates away from the stagnation line were treated like those for the nose tip. Stagnation point heating rates are presented in Figure 10.

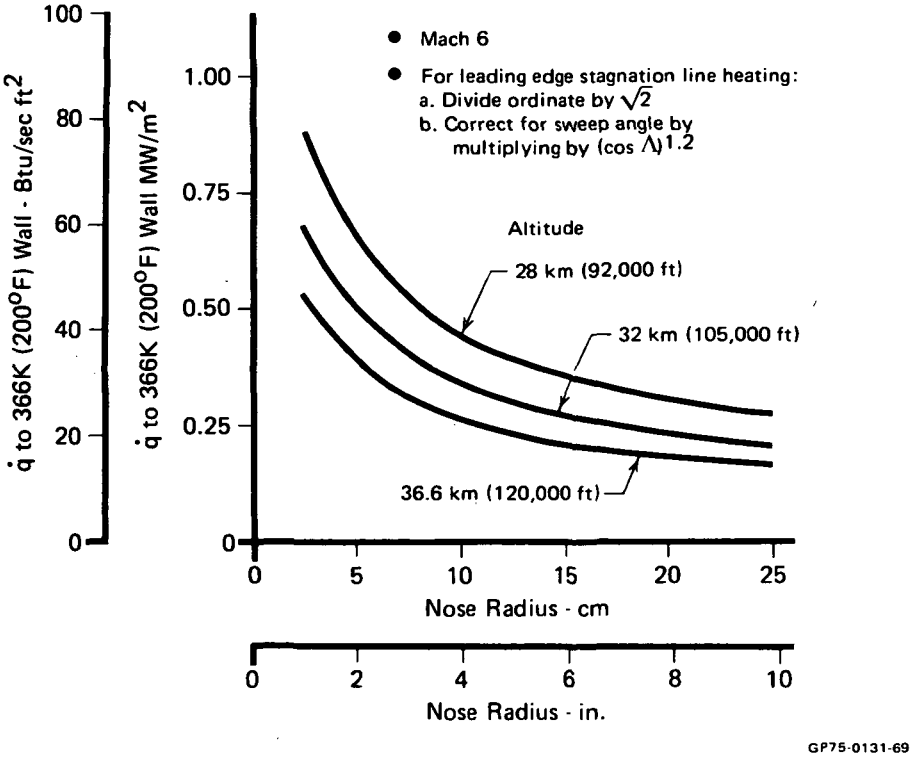

FIGURE 10
STAGNATION POINT HEATING, HEMISPHERICAL NOSE

4.2 ASCENT TRAJECTORY TRADE-OFF

It was necessary to establish a common cooling system design condition for Concepts 1, 2, and 3 to provide a consistent basis for configuration comparison. A decision was made to establish the cooling system design condition as that point in the nominal flight trajectory where the total heat absorbed by the cooling system was a maximum. The transient effects of maneuvers on cooling system design were not considered.

Examination of preliminary trajectory profiles revealed that maximum heating would occur during ascent at the lowest altitude at which Mach 6 was attained. Originally, an ascent trajectory considered aerodynamically optimum (consistent with structural limitations) was investigated. As indicated in Figure 11, this involved following a path from Mach 4 to Mach 6 that maintained a constant maximum inlet diffuser pressure of 896 kPa (130 psi) absolute. Mach 6 was attained at 28 km (92,000 ft). A constant Mach number climb to the 32 km (105,000 ft) cruise altitude concluded the ascent.

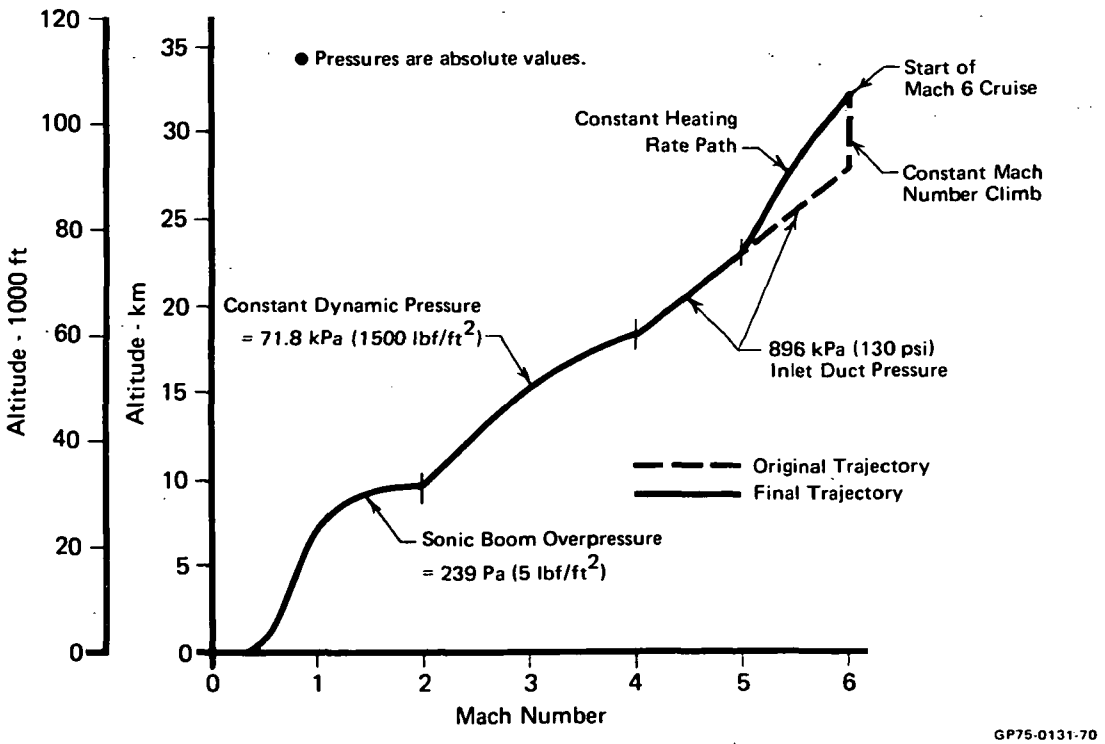

FIGURE 11
FLIGHT TRAJECTORY

Heat loads for Concept 1 were estimated using Mach 6, 28 km (92,000 ft), and an angle of attack of 4° as the design condition. Following a procedure as discussed in Section 4.4, a total heat load of 205 MW (6.99 x 10^8 Btu/hr) was determined. This resulted in an active cooling system weight, determined using the procedure discussed in Section 7, of 25 Mg (55,173 lbm). This weight was about twice the anticipated value for cooling system weight. Therefore, the significance of design point selection was investigated.

Heat loads were then estimated for Concept 1 using the start of cruise, 32 km (105,000 ft), as the design condition. For this condition, angle of attack is 7°. A total heat load of 143 MW (4.87×10^8 Btu/hr) was determined. A corresponding cooling system weight of 18.7 Mg (41,185 lbm) was estimated.

This considerable difference prompted a more thorough investigation of the ascent trajectory. Closer examination revealed that, on the constant inlet diffuser pressure path, the airframe heating rates attained at Mach 5 were essentially equal to those attained at the Mach 6 start of L/D_{max} cruise condition. Thus, the assumed original ascent trajectory forced the aircraft to pass through a condition which imposes a heating rate more than 40% greater than that heating rate associated with sustained cruise conditions. This is reflected in Figure 12.

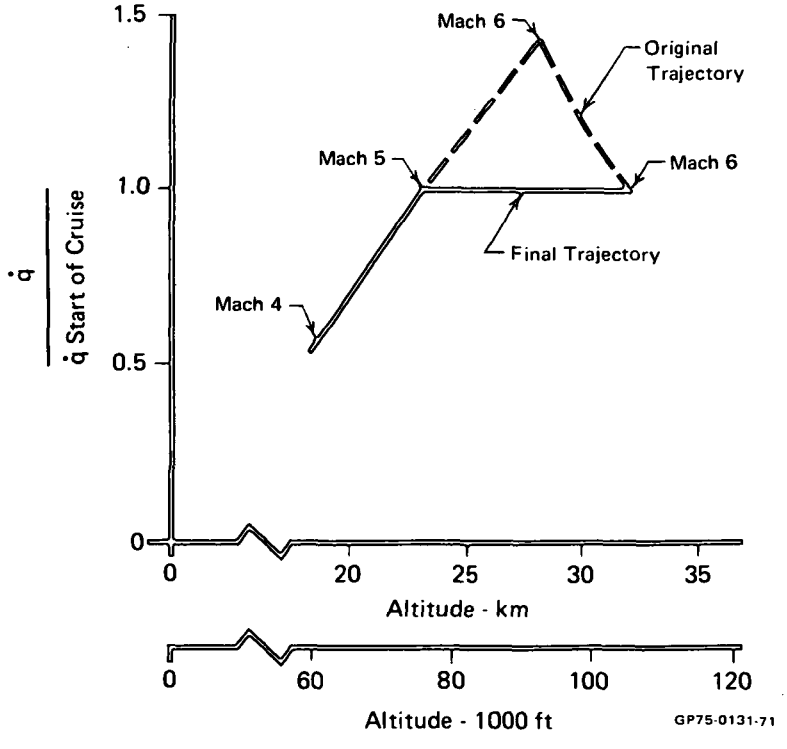

FIGURE 12
EFFECT OF ASCENT TRAJECTORY ON HEATING RATES

For a comparison, the effect of modifying the ascent trajectory to follow a constant heating path from Mach 5 to Mach 6 was investigated. This modification is reflected in Figures 11 and 12. The trade-off between these ascent trajectories is summarized in Figure 13. Although the modified trajectory incurs a range penalty of 76 km (41 NM) as a result of nonoptimum aerodynamic performance, range is increased 365 km (197 NM) because of a reduction in active cooling system weight of 6.35 Mg (13,988 lbm). This reduction was obtained from the range sensitivity to weight relationship shown in Figure 14. The net gain of 289 km (156 NM) clearly justified the selection of the modified trajectory. Thus, the initiation of Mach 6 cruise condition was selected as the design condition for the thermodynamic analyses of the three study aircraft configurations.

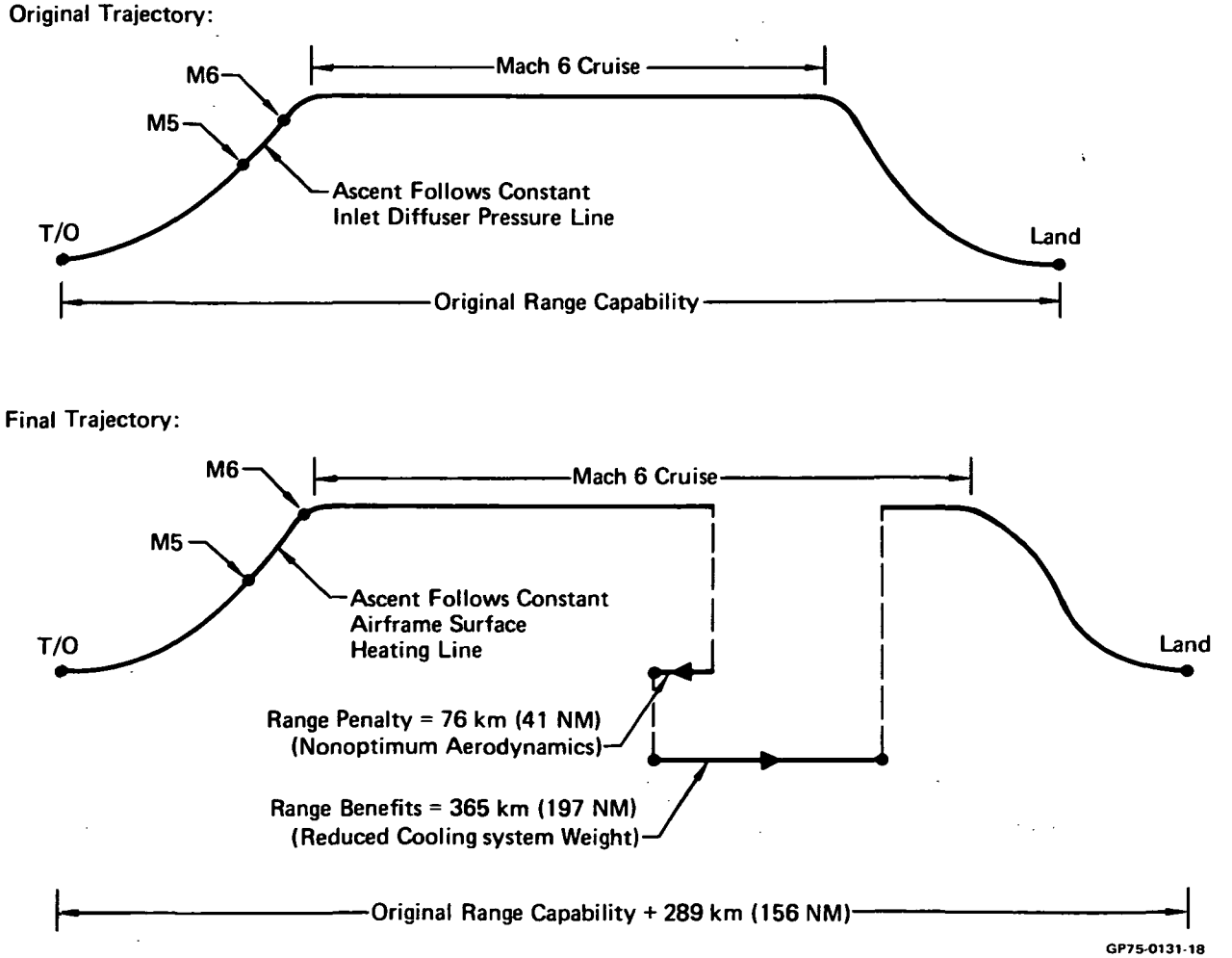

FIGURE 13
COMPARISON OF PROPOSED ASCENT TRAJECTORIES

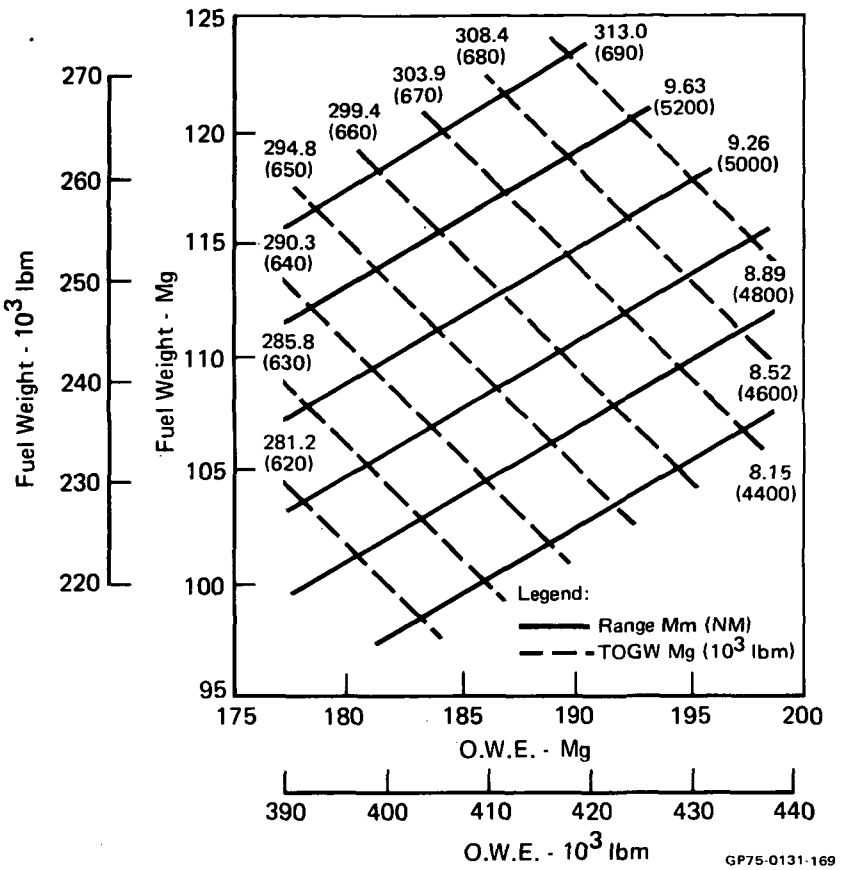

Notes:

1. Changes in O.W.E. (including total fuel weight) must reflect a 9% increment for a structural growth factor.
2. Changes in total and/or usable fuel weight may be read directly.

FIGURE 14
RANGE SENSITIVITY, CONCEPT 1

Reflecting on the results of this trade study, it becomes obvious that this class of aircraft is quite sensitive to design conditions. Designing for a transient or localized condition must be avoided as much as possible. In this case, designing to the originally assumed trajectory would have resulted in a large and heavy active cooling system which would have been significantly overdesigned for most of the mission.

4.3 NACELLE COOLING TRADE-OFF

Although a significant reduction in active cooling system weight had been obtained, the system weight still appeared high. Based on the information contained in Reference 5, a system weight on the order of 13.6 Mg (30,000 lbm) had been anticipated, rather than the resultant weight of 18.7 Mg (41,185 lbm).

One obvious difference in the original Concept 1 analysis was that consideration was given to cooling the surface area of the engine nacelle module. An examination of the heat load distributions for Concept 1, based on the final design condition, indicated that 23.8% of the total airframe heat load was attributable to cooling the nacelle, whereas nacelle wetted surface area of 381 m^2 (4100 ft^2) represented only 9.4% of the total airframe wetted surface area.

There are numerous reasons why the heating rates on the nacelle surface were much higher.

- The nacelle is located on the lower surface.
- Most surface locations are reasonably near a boundary layer attachment location.
- Flow in the boundary layer diverter region is subsonic and therefore local adiabatic wall temperatures approach total temperature.
- The external inlet ramps are positioned at high deflection angles.
- Heating to the panels in some regions includes conduction from the internal duct walls in addition to external aerodynamic heating (as discussed in Section 9.1).

All of these factors combine to impose extreme cooling requirements for the nacelle surfaces.

To establish the significance of the requirement to cool the nacelle region, the Concept 1 configuration was evaluated with and without this requirement. With the nacelle cooled, the cooling system weight was determined to be 18.7 Mg (41,185 lbm). Deleting the nacelle cooling requirement reduced the cooling system weight to 15.2 Mg (33,435 lbm) or a decrease of 3.52 Mg (7750 lbm). On the other hand, designing the nacelle as hot structure increased the structural weight by 1.13 Mg (2484 lbm). The net decrease was therefore 2.39 Mg (5266 lbm). This weight decrease increases range by 137 km (74 NM).

In addition to penalizing aircraft performance, cooling the nacelle surface offers many practical design problems. Routing coolant lines across the fuselage/nacelle interface would present difficulties. Designing cooling lines into the external inlet duct ramps and sidewalls would be complex and probably would result in volumetric penalties. Obviously, these complexities would also be reflected in high manufacturing cost. Taking all of these factors into

account a requirement to cool the nacelle surface areas could not be justified as being cost-effective. Therefore, subsequent analyses of Concepts 1, 2, and 3 considered hot structure for the engine nacelle module.

4.4 DESIGN HEAT LOADS - CONCEPTS 1, 2 AND 3

To size the active cooling systems for each configuration, it was necessary to establish the total heat load. In addition, to estimate cooled panel sizes and coolant flowrate requirements, the distribution of local heating rates required definition.

The parametric data discussed in Section 4.1 were used to generate generalized heating rates at the design condition of Mach 6, 32 km (105,000 ft) altitude, 7° angle of attack, as justified in Section 4.2. These generalized heating rates are presented in Figures 15 and 16. Figure 16, reflecting the effects of boundary layer transition from laminar to turbulent flow for regions near boundary layer development regions, was based on Figures 6 and 7.

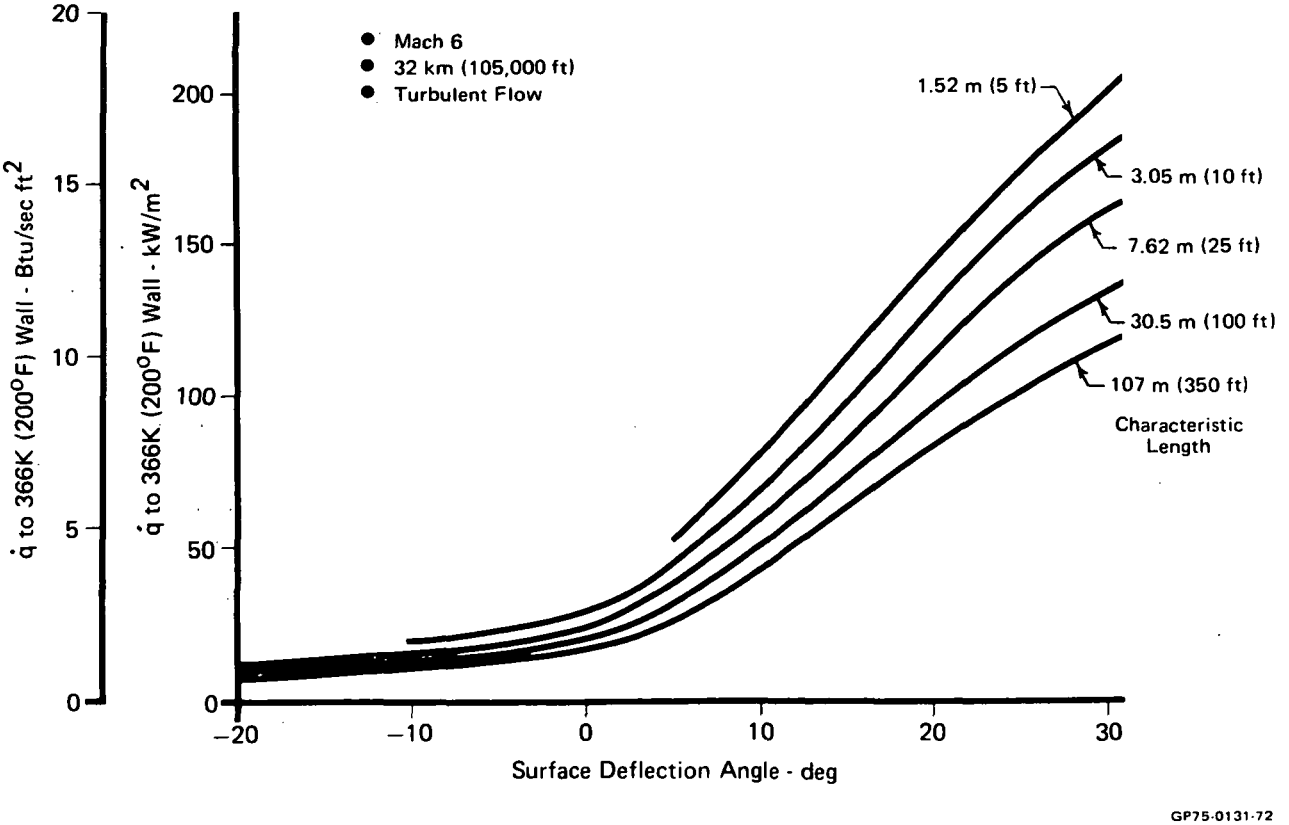

FIGURE 15
AFT LOCATION DESIGN HEATING RATES

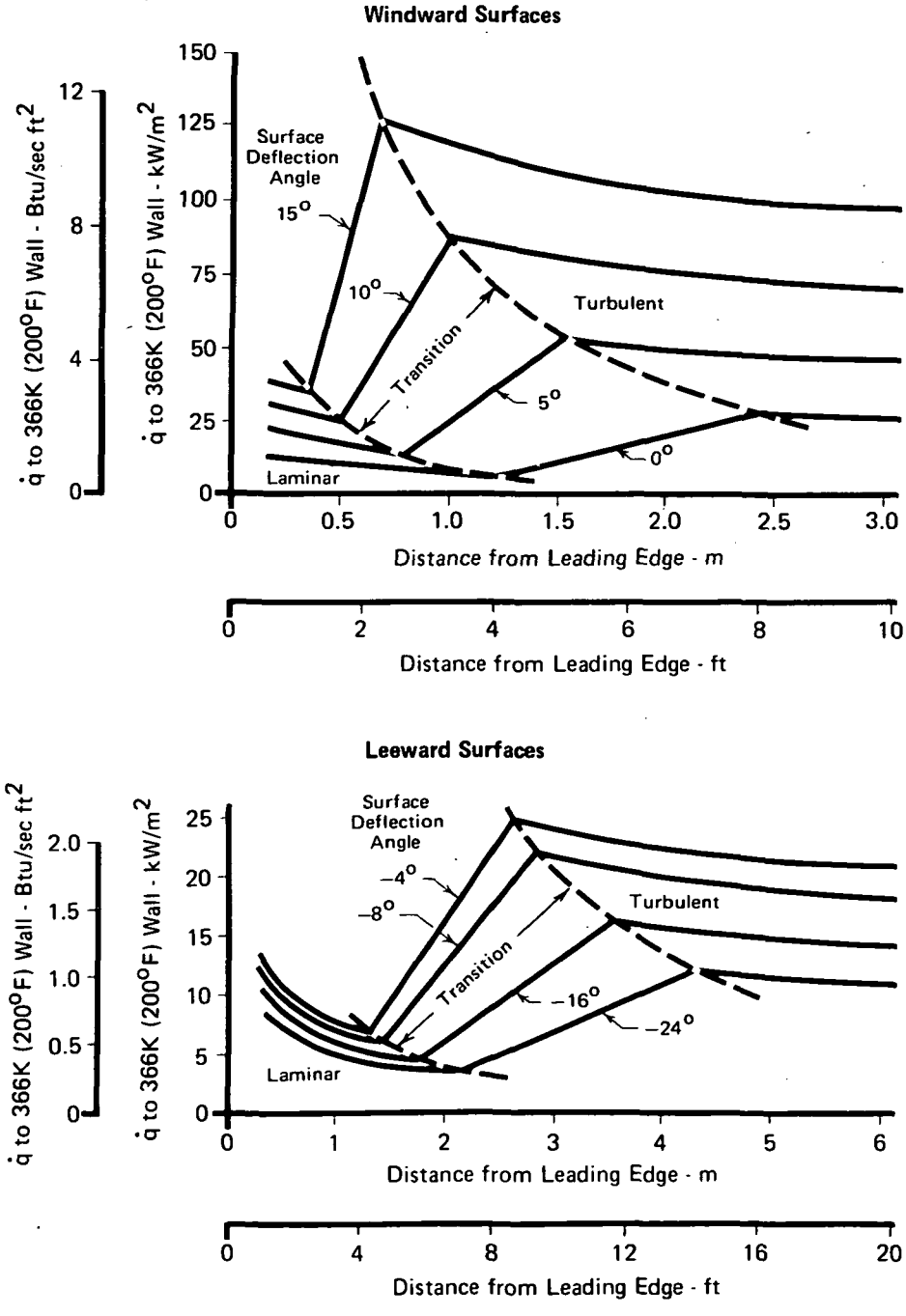

GP75-0131-121

FIGURE 16
FORWARD LOCATION DESIGN HEATING RATES
Mach 6
32 km (105,000 Ft) Altitude

Heating zones were defined over the surface area of each aircraft configuration. These zones were established in such a manner as to reflect significant variations in local heating rates without creating an unnecessary number of zones to manage. The fuselage of each configuration was divided into zones that reflected differences in distance from the nose and variations in upper, side, and lower surface deflection angles. The zones on wings and vertical tail surface areas were distinctly defined to reflect the effect of distance from leading edges and, in the case of wings, differences between upper and lower surface heating.

Figure 17 shows the heating zones defined for Concept 1. Thirty-one zones were used to cover the fuselage. Eight heating zones were used for the wings (including elevons) and three zones for the vertical tail. The figure indicates zones only on one side of the aircraft. The zones shown in Figure 17 were also applicable to Concept 2, although the areas involved varied since the latter configuration has a slightly smaller fuselage cross-section.

Concept 3 is significantly smaller than Concepts 1 and 2 and required a separate definition of heating zones as shown in Figure 18. To differentiate among upper, side, and lower surface heating effects on the forward fuselage, a zonal definition was established as indicated in Figure 18. Forward of FS 48.8 m (160 ft) waterline extremes for these zones were determined by finding 45° tangency points on the moldline. Between FS 48.8 m (160 ft) and FS 54.9 m (180 ft) an arbitrary line connecting the waterlines to the wing surfaces was drawn so that aft of FS 54.9 m (180 ft) no side surface heating effects are defined. Remaining regions of the Concept 3 configuration were treated in a manner similar to that used for Concepts 1 and 2.

Figures 19, 20, and 21 contain the following information for each heating zone on all three concepts.

a) Location,

b) Surface area (aircraft total),

c) Maximum heating rate,

d) Average heating rate over the zone, and

e) Zonal heating rate (product of the average heating rate and the area).

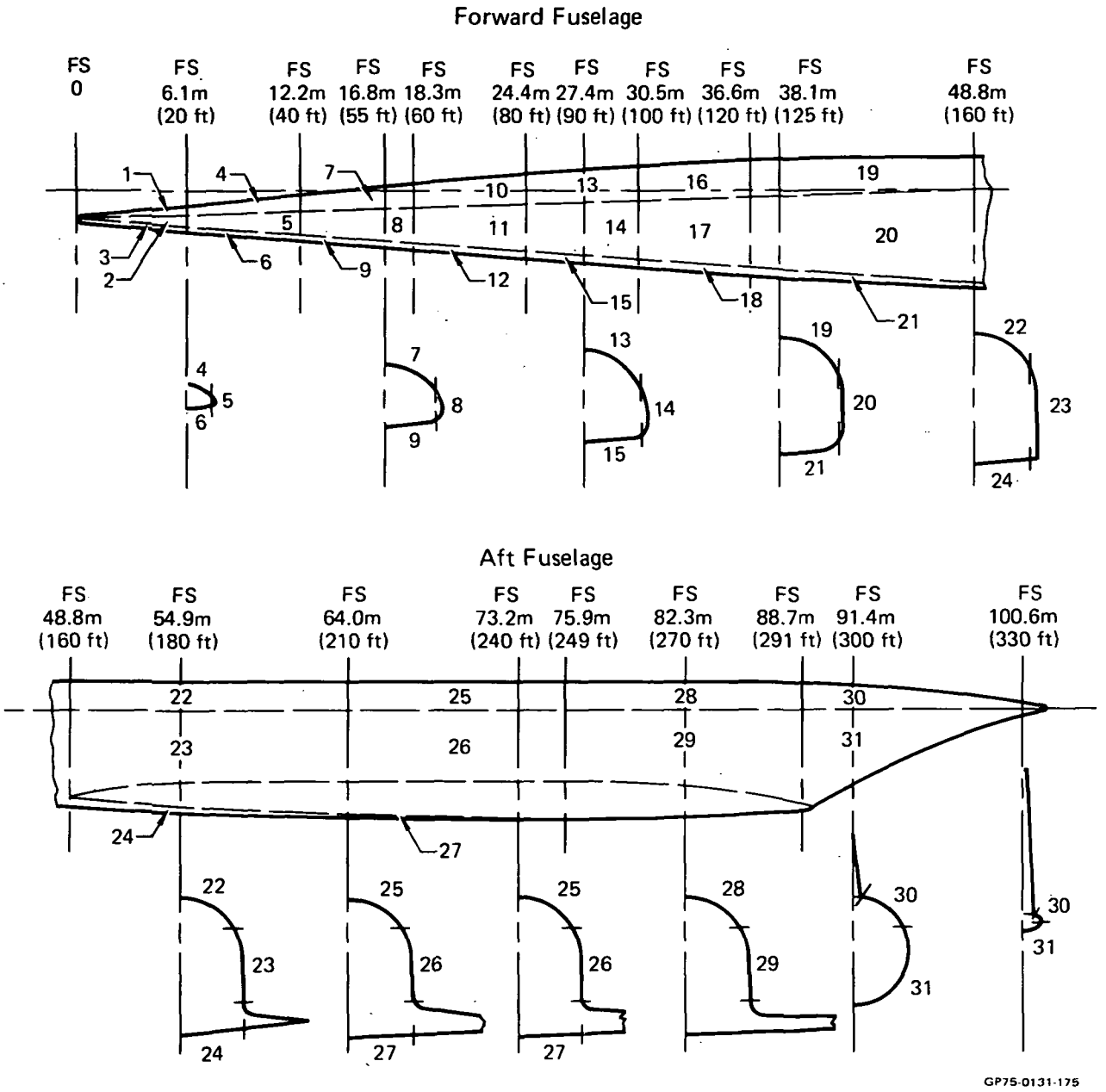

FIGURE 17
AIRCRAFT HEATING ZONES, CONCEPT 1

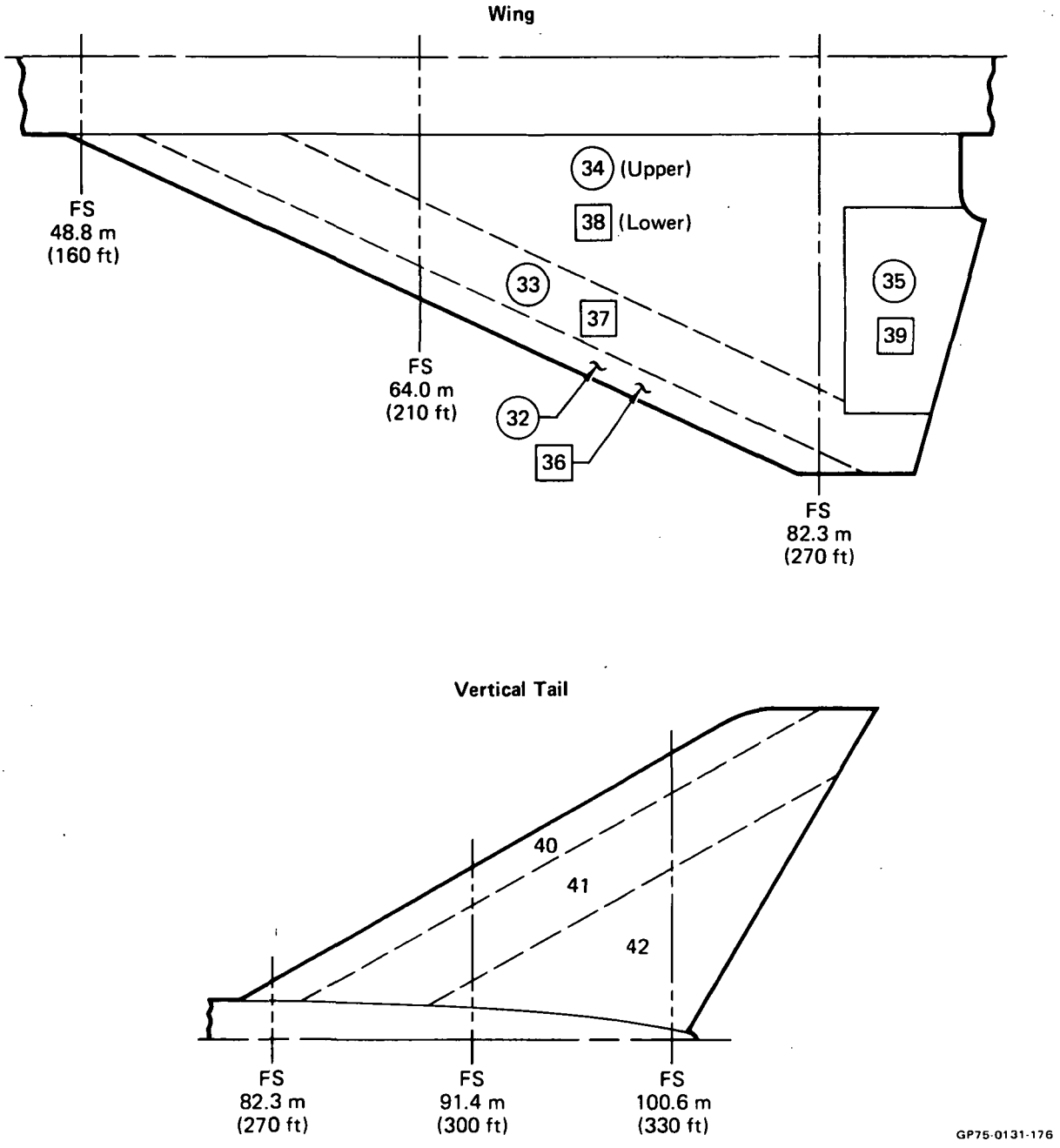

FIGURE 17 (Continued)
AIRCRAFT HEATING ZONES, CONCEPT 1

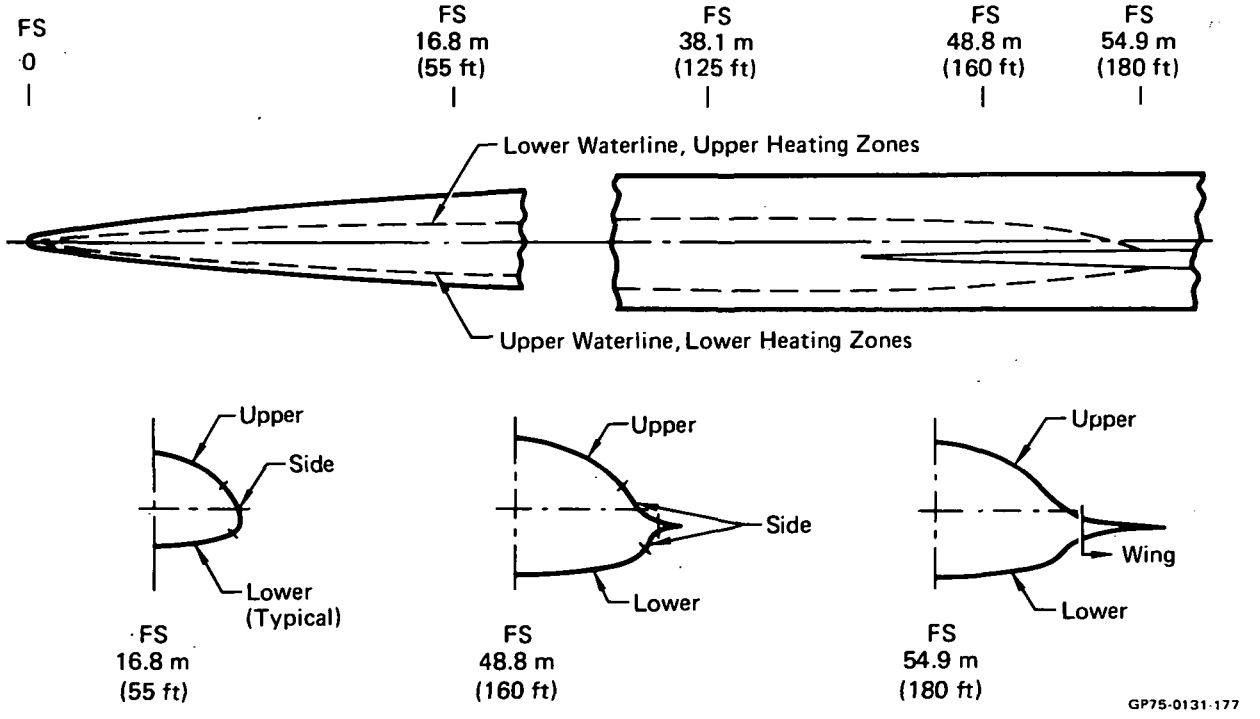

Note: Detailed zone definitions are presented in Figure 21.

FIGURE 18
TYPICAL FUSELAGE HEATING ZONES, CONCEPT 3

Zone	Fuselage Station		Fuselage Location	Total Area		Maximum Heating Rate, $\dot{q}$ max		Average Heating Rate, $\dot{q}$ avg		Zonal Heating Rate $\dot{Q}$	
	m	(ft)		m^2	(ft^2)	kW/m^2	(Btu/sec ft^2)	kW/m^2	(Btu/sec ft^2)	MW	(Btu/sec)
Fuselage:											
1	0-6.1	(0-20)	Upper	7.5	(81.2)	27	(2.4)	23	(2.0)	0.17	(162)
2	↓	(0-20)	Side	6.7	(72.4)	199	(17.5)	119	(10.5)	0.80	(760)
3	↓	(0-20)	Lower	9.4	(101.4)	104	(9.2)	82	(7.2)	0.77	(730)
4	6.1-12.2	(20-40)	Upper	20.2	(217.6)	23	(2.0)	22	(1.9)	0.44	(413)
5	↓	(20-40)	Side	16.9	(181.4)	71	(6.3)	64	(5.6)	1.07	(1,016)
6	↓	(20-40)	Lower	23.0	(248.0)	71	(6.3)	68	(6.0)	1.57	(1,488)
7	12.2-18.3	(40-60)	Upper	34.6	(372.0)	20	(1.8)	19	(1.7)	0.67	(632)
8	↓	(40-60)	Side	27.3	(294.0)	57	(5.0)	44	(3.9)	1.21	(1,147)
9	↓	(40-60)	Lower	34.8	(375.0)	66	(5.8)	65	(5.7)	2.25	(2,138)
10	18.3-24.4	(60-80)	Upper	43.6	(469.0)	19	(1.7)	18	(1.6)	0.79	(750)
11	↓	(60-80)	Side	31.3	(337.0)	34	(3.0)	26	(2.3)	0.82	(775)
12	↓	(60-80)	Lower	36.5	(393.0)	62	(5.5)	61	(5.4)	2.24	(2,122)
13	24.4-30.5	(80-100)	Upper	50.1	(550.0)	18	(1.6)	18	(1.6)	0.93	(880)
14	↓	(80-100)	Side	35.1	(378.0)	20	(1.8)	19	(1.7)	0.68	(643)
15	↓	(80-100)	Lower	38.5	(414.0)	59	(5.2)	58	(5.1)	2.23	(2,111)
16	30.5-36.6	(100-120)	Upper	54.3	(584.0)	17	(1.5)	17	(1.5)	0.92	(876)
17	↓	(100-120)	Side	38.1	(410.0)	19	(1.7)	19	(1.7)	0.73	(697)
18	↓	(100-120)	Lower	45.0	(484.0)	57	(5.0)	57	(5.0)	2.55	(2,420)
19	36.6-48.8	(120-160)	Upper	96.3	(1,036.0)	16	(1.4)	15	(1.3)	1.42	(1,347)
20	↓	(120-160	Side	106.1	(1,142.0)	19	(1.7)	18	(1.6)	1.93	(1,827)
21	↓	(120-160)	Lower	86.4	(930.0)	56	(4.9)	53	(4.7)	4.61	(4,371)
22	48.8-64.0	(160-210)	Upper	120.2	(1,294.0)	14	(1.2)	14	(1.2)	1.64	(1,553)
23	↓	(160-210)	Side	157.0	(1,690.0)	18	(1.6)	18	(1.6)	2.85	(2,704)
24	↓	(160-210)	Lower	112.8	(1,214.0)	48	(4.2)	43	(3.8)	4.86	(4,613)
25	64.0-75.9	(210-249)	Upper	99.8	(1,074.0)	12	(1.1)	12	(1.1)	1.25	(1,181)
26	↓	(210-249)	Side	107.0	(1,152.0)	18	(1.6)	17	(1.5)	1.82	(1,728)
27	↓	(210-249)	Lower	96.3	(1,036.0)	36	(3.2)	36	(3.2)	3.50	(3,315)
28	75.9-88.7	(249-291)	Upper	106.8	(1,150.0)	12	(1.1)	12	(1.1)	1.33	(1,265)
29	↓	(249-291)	Side	130.1	(1,400.0)	17	(1.5)	17	(1.5)	2.21	(2,100)
30	88.7-101.8	(291-334)	Upper	63.4	(682.0)	12	(1.1)	12	(1.1)	0.79	(750)
31	↓	(291-334)	Side/ Lower	77.9	(838.0)	17	(1.5)	17	(1.5)	1.33	(1,257)
Fuselage Totals:				1,913.8	(20,600.0)					50.37	(47,771)

GP75-0131-16

FIGURE 19
DESIGN HEATING RATES AND HEAT LOADS, CONCEPT 1

Zone	Location	Total Area		Maximum Heating Rate, $\dot{q}$ max		Average Heating Rate, $\dot{q}$ avg		Zonal Heating Rate $\dot{Q}$	
		m^2	(ft^2)	kW/m^2	(Btu/sec ft^2)	kW/m^2	(Btu/sec ft^2)	MW	(Btu/sec)
Wings:									
32	Upper Surface, Forward 3.05m (10 ft)	94.8	(1,020.0)	24	(2.1)	20	(1.8)	1.94	(1,836)
33	Upper Surface, 3.05-9.14m (10 - 30 ft) from LE	183.8	(1,978.0)	23	(2.0)	19	(1.7)	3.55	(3,363)
34	Upper Surface, 9.14+m (30 + ft) from LE	366.8	(3,948.0)	18	(1.6)	16	(1.4)	5.83	(5,527)
35	Upper Surface, Elevon	86.8	(934.0)	54	(4.8)	54	(4.8)	4.73	(4,483)
36	Lower Surface, Forward 3.05m (10 ft)	94.8	(1,020.0)	75	(6.6)	59	(5.2)	5.59	(5,304)
37	Lower Surface, 3.05-9.14m (10 - 30 ft) from LE	183.8	(1,978.0)	54	(4.8)	49	(4.3)	8.97	(8,505)
38	Lower Surface, 9.14+m (30+ ft) from LE	277.6	(2,988.0)	45	(4.0)	42	(3.7)	11.66	(11,056)
39	Lower Surface, Elevon	86.8	(934.0)	71	(6.3)	71	(6.3)	6.20	(5,884)
	Wing Totals:	1,375.0	(14,800.0)					48.46	(45,958)
Vertical Tail:									
40	Forward 3.05m (10 ft)	86.1	(926.0)	34	(3.0)	28	(2.5)	2.44	(2,315)
41	3.05-9.14m (10-30 ft) from LE	154.6	(1,664.0)	30	(2.6)	25	(2.2)	3.86	(3,661)
42	9.14+m (30+ft) from LE	144.9	(1,560.0)	22	(1.9)	20	(1.8)	2.96	(2,808)
	Vertical Tail Totals:	385.6	(4,150.0)					9.26	(8,784)
	Airframe Totals:	3,674.3	(39,550.0)					108.08	(102,513)

GP78-0131-17

FIGURE 19 (Continued)
DESIGN HEATING RATES AND HEAT LOADS, CONCEPT 1

Zone	Fuselage Station		Fuselage Location	Total Area		Maximum Heating Rate, $\dot{q}$ max		Average Heating Rate, $\dot{q}$ avg		Zonal Heating Rate $\dot{Q}$	
	m	(ft)		m^2	(ft^2)	kW/m^2	(Btu/sec ft^2)	kW/m^2	(Btu/sec ft^2)	MW	(Btu/sec)
Fuselage:											
1	0-6.1	(0-20)	Upper	7.5	(81.2)	27	(2.4)	23	(2.0)	0.17	(162)
2	↓	(0-20)	Side	6.7	(72.4)	199	(17.5)	119	(10.5)	0.80	(760)
3	↓	(0-20)	Lower	9.4	(101.4)	104	(9.2)	82	(7.2)	0.77	(730)
4	6.1-12.2	(20-40)	Upper	20.2	(217.6)	23	(2.0)	22	(1.9)	0.44	(413)
5	↓	(20-40)	Side	16.9	(181.4)	71	(6.3)	64	(5.6)	1.07	(1,016)
6	↓	(20-40)	Lower	23.0	(248.0)	71	(6.3)	68	(6.0)	1.57	(1,488)
7	12.2-18.3	(40-60)	Upper	34.6	(372.0)	20	(1.8)	19	(1.7)	0.67	(632)
8	↓	(40-60)	Side	27.3	(294.0)	57	(5.0)	44	(3.9)	1.21	(1,147)
9	↓	(40-60)	Lower	34.8	(375.0)	66	(5.8)	65	(5.7)	2.25	(2,138)
10	18.3-24.4	(60-80)	Upper	43.6	(469.0)	19	(1.7)	18	(1.6)	0.79	(750)
11	↓	(60-80)	Side	31.3	(337.0)	34	(3.0)	26	(2.3)	0.82	(775)
12	↓	(60-80)	Lower	36.5	(393.0)	62	(5.5)	61	(5.4)	2.24	(2,122)
13	24.4-30.5	(80-100)	Upper	50.1	(550.0)	18	(1.6)	18	(1.6)	0.93	(880)
14	↓	(80-100)	Side	33.6	(362.0)	20	(1.8)	19	(1.7)	0.65	(615)
15	↓	(80-100)	Lower	34.0	(398.0)	59	(5.2)	58	(5.1)	2.14	(2,030)
16	30.5-36.6	(100-120)	Upper	51.5	(554.0)	17	(1.5)	17	(1.5)	0.88	(831)
17	↓	(100-120)	Side	35.3	(380.0)	19	(1.7)	19	(1.7)	0.68	(646)
18	↓	(100-120)	Lower	42.2	(454.0)	57	(5.0)	57	(5.0)	2.39	(2,270)
19	36.6-48.8	(120-160)	Upper	88.8	(956.0)	16	(1.4)	15	(1.3)	1.31	(1,243)
20	↓	(120-160)	Side	100.5	(1,082.0)	19	(1.7)	18	(1.6)	1.83	(1,731)
21	↓	(120-160)	Lower	80.8	(870.0)	56	(4.9)	53	(4.7)	4.31	(4,089)
22	48.8-64.0	(160-210)	Upper	110.9	(1,194.0)	14	(1.2)	14	(1.2)	1.51	(1,433)
23	↓	(160-210)	Side	147.7	(1,590.0)	18	(1.6)	18	(1.6)	2.68	(2,544)
24	↓	(160-210)	Lower	103.5	(1,114.0)	48	(4.2)	43	(3.8)	4.46	(4,233)
25	64.0-75.9	(210-249)	Upper	93.3	(1,004.0)	12	(1.1)	12	(1.1)	1.16	(1,104)
26	↓	(210-249)	Side	100.5	(1,082.0)	18	(1.6)	17	(1.5)	1.71	(1,623)
27	↓	(210-249)	Lower	89.7	(966.0)	36	(3.2)	36	(3.2)	3.26	(3,091)
28	75.9-88.7	(249-291)	Upper	99.0	(1,066.0)	12	(1.1)	12	(1.1)	1.24	(1,173)
29	↓	(249-291)	Side	130.1	(1,316.0)	17	(1.5)	17	(1.5)	2.08	(1,974)
30	88.7-101.8	(291-334)	Upper	63.4	(682.0)	12	(1.1)	12	(1.1)	0.79	(750)
31	↓	(291-334)	Side/Lower	77.9	(838.0)	17	(1.5)	17	(1.5)	1.33	(1,257)
Fuselage Totals:				1,820.9	(19,600.0)					48.13	(45,650)

GP75-0131-19

FIGURE 20
DESIGN HEATING RATES AND HEAT LOADS, CONCEPT 2

Zone	Location	Total Area		Maximum Heating Rate, q max		Average Heating Rate, $\dot{q}$ avg		Zonal Heating Rate $\dot{Q}$	
		m^2	(ft^2)	kW/m^2	(Btu/sec ft^2)	kW/m^2	(Btu/sec ft^2)	MW	(Btu/sec)
Wings:									
32	Upper Surface, Forward 3.05m (10 ft)	96.6	(1,040.0)	24	(2.1)	20	(1.8)	1.97	(1,872)
33	Upper Surface, 3.05-9.14m (10-30 ft) from LE	189.3	(2,038.0)	23	(2.0)	19	(1.7)	3.65	(3,465)
34	Upper Surface, 9.14+m (30+ ft) from LE	385.4	(4,148.0)	18	(1.6)	16	(1.4)	6.12	(5,807)
35	Upper Surface, Elevon	86.8	(934.0)	54	(4.8)	54	(4.8)	4.73	(4,483)
36	Lower Surface, Forward 3.05m (10 ft)	96.6	(1,040.0)	75	(6.6)	59	(5.2)	5.70	(5,408)
37	Lower Surface, 3.05-9.14m (10-30 ft) from LE	189.3	(2,038.0)	54	(4.8)	49	(4.3)	9.24	(8,763)
38	Lower Surface, 9.14+m (30+ ft) from LE	310.3	(3,340.0)	45	(4.0)	42	(3.7)	13.03	(12,358)
39	Lower Surface, Elevon	86.8	(934.0)	71	(6.3)	71	(6.3)	6.20	(5,884)
	Wing Totals:	1,441.1	(15,512.0)					50.65	(48,040)
Vertical Tail:									
40	Forward 3.05m (10 ft)	86.1	(926.0)	34	(3.0)	28	(2.5)	2.44	(2,315)
41	3.05-9.14m (10-30 ft) from LE	154.6	(1,664.0)	30	(2.6)	25	(2.2)	3.86	(3,661)
42	9.14+m (30+ ft) from LE	144.9	(1,560.0)	22	(1.9)	20	(1.8)	2.96	(2,808)
	Vertical Tail Totals:	385.6	(4,150.0)					9.26	(8,784)
	Airframe Totals:	3,647.6	(39,262.0)					108.04	(102,474)

GP75-0131-20

FIGURE 20 (Continued)
DESIGN HEATING RATES AND HEAT LOADS, CONCEPT 2

Zone	Fuselage Station		Fuselage Location	Total Area		Maximum Heating Rate, $\dot{q}$ max		Average Heating Rate, $\dot{q}$ avg		Zonal Heating Rate $\dot{Q}$	
	m	(ft)		m^2	(ft^2)	kW/m^2	(Btu/sec ft^2)	kW/m^2	(Btu/sec ft^2)	MW	(Btu/sec)
Fuselage:											
1	0-6.1	(0-20)	Upper	10.7	(115)	36	(3.2)	28	(2.5)	0.30	(288)
2	↓	(0-20)	Side	4.2	(45)	176	(15.5)	108	(9.5)	0.45	(428)
3	↓	(0-20)	Lower	14.9	(160)	133	(11.7)	98	(8.6)	1.45	(1,376)
4	6.1-12.2	(20-40)	Upper	21.4	(230)	25	(2.2)	23	(2.0)	0.49	(460)
5	↓	(20-40)	Side	20.0	(215)	71	(6.3)	59	(5.2)	1.18	(1,118)
6	↓	(20-40)	Lower	27.4	(295)	83	(7.3)	73	(6.4)	1.99	(1,888)
7	12.2-18.3	(40-60)	Upper	27.9	(300)	20	(1.8)	18	(1.6)	0.51	(480)
8	↓	(40-60)	Side	31.1	(335)	49	(4.3)	43	(3.8)	1.34	(1,273)
9	↓	(40-60)	Lower	34.8	(375)	66	(5.8)	60	(5.3)	2.10	(1,988)
10	18.3-24.4	(60-80)	Upper	33.0	(355)	17	(1.5)	16	(1.4)	0.52	(497)
11	↓	(60-80)	Side	34.8	(375)	37	(3.3)	35	(3.1)	1.23	(1,163)
12	↓	(60-80)	Lower	41.8	(450)	54	(4.8)	51	(4.5)	2.14	(2,025)
13	24.4-30.5	(80-100)	Upper	43.2	(465)	16	(1.4)	15	(1.3)	0.64	(605)
14	↓	(80-100)	Side	38.6	(415)	33	(2.9)	31	(2.7)	1.18	(1,121)
15	↓	(80-100)	Lower	51.1	(550)	48	(4.2)	45	(4.0)	2.32	(2,200)
16	30.5-36.6	(100-120)	Upper	44.1	(475)	15	(1.3)	15	(1.3)	0.65	(618)
17	↓	(100-120)	Side	39.5	(425)	28	(2.5)	24	(2.1)	0.94	(893)
18	↓	(100-120)	Lower	53.4	(575)	42	(3.7)	40	(3.5)	2.12	(2,013)
19	36.6-42.7	(120-140)	Upper	48.8	(525)	14	(1.2)	14	(1.2)	0.66	(630)
20	↓	(120-140)	Side	42.3	(455)	20	(1.8)	19	(1.7)	0.82	(774)
21	↓	(120-140)	Lower	58.1	(625)	37	(3.3)	36	(3.2)	2.11	(2,000)
22	42.7-48.8	(140-160)	Upper	55.7	(600)	14	(1.2)	14	(1.2)	0.76	(720)
23	↓	(140-160)	Side	33.9	(365)	18	(1.6)	18	(1.6)	0.62	(584)
24	↓	(140-160)	Lower	60.4	(650)	36	(3.2)	36	(3.2)	2.19	(2,080)
25	48.8-54.9	(160-180)	Upper	65.0	(700)	14	(1.2)	14	(1.2)	0.89	(840)
26	↓	(160-180)	Side	15.3	(165)	18	(1.6)	18	(1.6)	0.28	(264)
27	↓	(160-180)	Lower	62.7	(675)	35	(3.1)	35	(3.1)	2.21	(2,093)
28	54.9-66.3	(180-217.6)	Upper	134.7	(1,450)	12	(1.1)	12	(1.1)	1.68	(1,595)
29	54.9-70.7	(180-232.1)	Lower	116.1	(1,250)	35	(3.1)	35	(3.1)	4.09	(3,875)
30	66.3-78.0	(217.6-255.8)	Upper	153.3	(1,650)	12	(1.1)	12	(1.1)	1.91	(1,815)
31	78.0-93.9	(255.8-308)	Upper	121.7	(1,310)	12	(1.1)	12	(1.1)	1.52	(1,441)
32	↓	(255.8-308)	Lower	95.2	(1,025)	17	(1.5)	17	(1.5)	1.62	(1,538)
Fuselage Totals:				1,635.1	(17,600)					42.89	(40,683)

GP75-0131-22

FIGURE 21
DESIGN HEATING RATES AND HEAT LOADS, CONCEPT 3

Zone	Location	Total Area		Maximum Heating Rate, $\dot{q}$ max		Average Heating Rate, $\dot{q}$ avg		Zonal Heating Rate $\dot{Q}$	
		m^2	(ft^2)	kW/m^2	(Btu/sec ft^2)	kW/m^2	(Btu/sec ft^2)	MW	(Btu/sec)
Wings:									
33	Upper Surface, Forward 3.05 m (10 ft)	79.1	(851)	24	(2.1)	20	(1.8)	1.62	(1,532)
34	Upper Surface, 3.05-9.14m (10-30 ft) from LE	151.8	(1,634)	23	(2.0)	19	(1.7)	2.93	(2,778)
35	Upper Surface, 9.14+m (30+ ft) from LE	232.4	(2,501)	18	(1.6)	17	(1.5)	3.96	(3,752)
36	Upper Surface, Elevon	78.1	(841)	54	(4.8)	54	(4.8)	4.26	(4,037)
37	Lower Surface, Forward 3.05m (10 ft)	79.1	(851)	75	(6.6)	59	(5.2)	4.67	(4,425)
38	Lower Surface, 3.05-9.14m (10-30 ft) from LE	151.8	(1,634)	54	(4.8)	49	(4.3)	7.41	(7,026)
39	Lower Surface, 9.14+m (30+ ft) from LE	214.7	(2,311)	45	(4.0)	43	(3.8)	9.26	(8,782)
40	Lower Surface, Elevon	78.1	(841)	71	(6.3)	71	(6.3)	5.59	(5,298)
	Wing Totals:	1,065.0	(11,464)					39.68	(37,630)
Vertical Tail:									
41	Forward 3.05m (10 ft)	72.8	(784)	42	(3.7)	33	(2.9)	2.40	(2,274)
42	3.05-9.14m (10-30 ft) from LE	131.0	(1,410)	31	(2.7)	27	(2.4)	2.57	(3,384)
43	9.14+m (30+ ft) from LE)	81.4	(876)	22	(1.9)	20	(1.8)	1.66	(1,577)
	Vertical Tail Totals:	285.2	(3,070)					7.63	(7,235)
	Airframe Totals:	2,985.4	(32,134)					90.20	(85,548)

GP75-0131-23

FIGURE 21 (Continued)
DESIGN HEATING RATES AND HEAT LOADS, CONCEPT 3

The maximum heating rate was used in sizing actively cooled panels for each zone while the average rate was significant in establishing cooling system requirements. In most heating zones, the maximum heating rate occurs at the most forward location, while the average is typical of the zone mid-point. Exceptions are heating zones that incorporate stagnation regions, which experience both very high local heating rates and a transition from laminar to turbulent flow. On Concept 1 these include zones 1, 2 and 3 on the fuselage, zones 32 and 36 on the wing, and zone 40 on the vertical tail. Sizing the panels in these zones to handle stagnation heating is unrealistic. Therefore, the maximum turbulent heating value was designated as the maximum heating rate. Special provisions, such as more closely spaced coolant passages or ablators, would be required locally at stagnation regions, but these should not greatly affect the overall system weight requirements. Average heating rates in these zones were determined by integrating beneath the curve of local heating rate versus distance from the leading edge and dividing by the zonal length. In this manner, the effects of stagnation, laminar and turbulent heating were considered for each area.

Elevon surface heating rates reflect the effects of control surface deflections during flight. It was estimated that maximum deflections of 15° up and 5° down would be required. The expression used to determine peak elevon heating rates, based on correlations of high speed test data on turbulent flow for wedge configurations related to local pressure, is as follows:

$$\frac{\dot{q}_{\text{elevon}}}{\dot{q}_{\text{hinge line}}} = \left(\frac{P_{\text{elevon}}}{P_{\text{hinge line}}} \right)^{0.85}$$

Whereas this relationship defines the peak heating along a specific locus across the elevon, available data indicate that most of the elevon surface would experience almost equally severe heating. The heating rates for elevon zones reflect only peak heating values which are assumed to be applicable over the entire elevon surface.

5. AIRFRAME COOLANT FLOWRATE REQUIREMENTS

Coolant flowrate requirements are dependent on various factors, such as local surface heating rates, panel skin thicknesses, maximum allowable skin temperature, allowable skin thermal gradient and coolant characteristics. To assist in determining these requirements, a thermal model of a typical section of an actively cooled panel was constructed and parametric data were generated. The method used to relate the parametric data to the study configuration is discussed in this section. The distribution of the design coolant flowrates established for the three concepts is also summarized.

5.1 ANALYTICAL TECHNIQUES

The thermal model used for these analyses represented a cooled panel one pitch (distance between tube centers) wide and 6.1 m (20 ft) long (the nominal panel length). The model, illustrated in Figure 22, consisted of 10 fluid thermal nodes and 54 structural nodes, to reflect both lengthwise and spanwise temperature gradients. Variations in unit surface heating rate, outer skin thickness, pitch and coolant flowrate are readily accommodated. Certain assumptions were made in order to minimize the number of variables in the analysis. These assumptions, discussed below, were based on the results of MCAIR work on actively cooled panels (Reference 6).

The coolant tubes were assumed to be "dee" shaped, 8.64 mm (0.34 in) in diameter, with 0.89 mm (0.035 in) thick tube walls. Tubes were considered to be bonded to the skin with an adhesive 0.13 mm (0.005 in) thick displaying a thermal conductivity of 5.77 W/m·K (40 Btu in/hr ft^2°F). A methanol/water solution (60% methanol by weight) was used as the coolant. Pumping power requirements associated with methanol/water solutions were shown in the Reference (6) study to be considerably lower than those for glycol/water solutions. Also, based on the Reference (6) study results, a coolant inlet temperature to the panels of 256 K (0°F) was assumed.

Heat transfer coefficients between the coolant and the tube wall were based on conventional laminar and turbulent flow expressions. Laminar flow was assumed to apply below Reynolds numbers of 2100 and a step change to turbulent flow was assumed at that Reynolds number. Based on these criteria, when flowrates are low, laminar flow can exist for a short distance down the coolant tubes. As a result, in rare instances, the peak temperatures existed

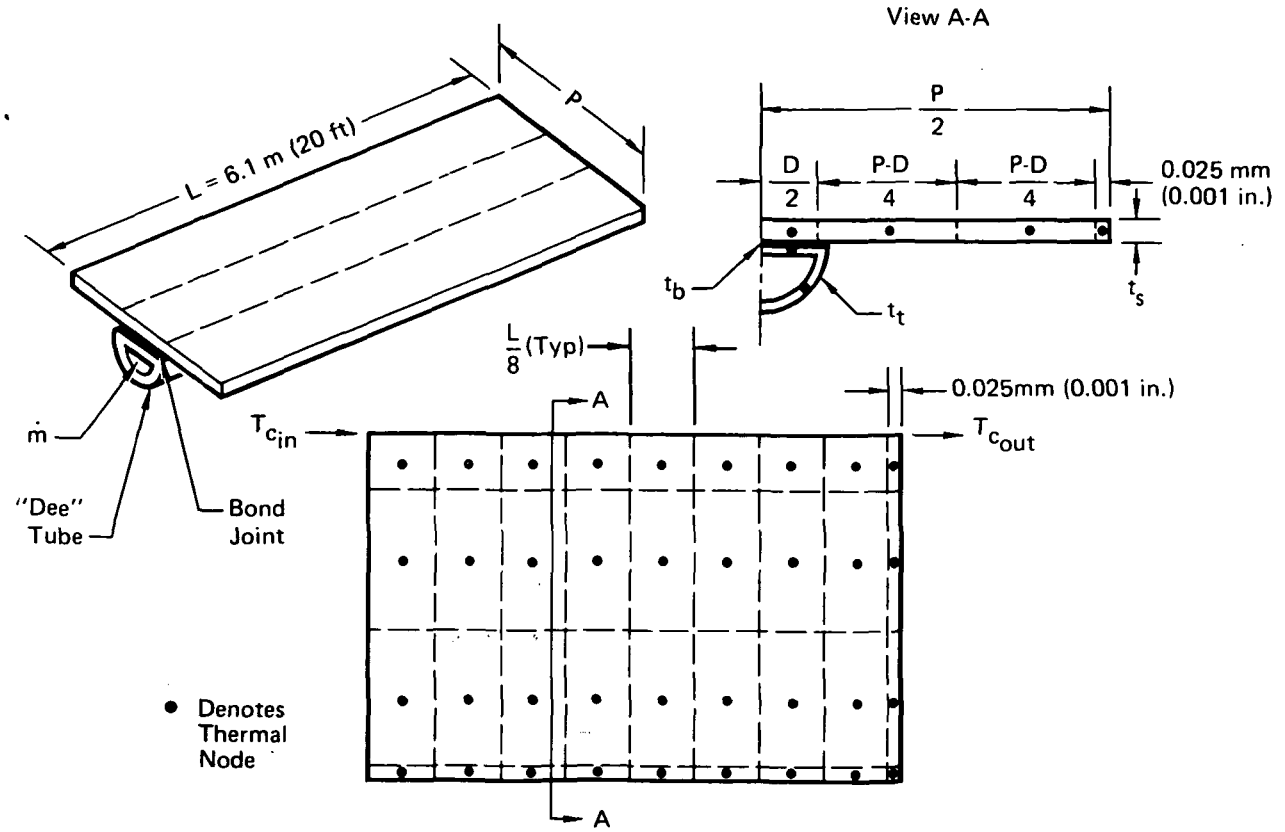

Constant Inputs:

- Material Properties vs Temperature, 60% Methanol/40% Water Solution 2219-T87 Aluminum
- Adhesive Bond Characteristics
- L = 6.1 m (20 ft)
- D = 8.64mm (0.34 in.)
- t_t = 0.89mm (0.035 in.)
- t_b = 0.13mm (0.005 in.)
- $T_{c_{in}}$ = 256K (0°F)

Variable Inputs:

- Surface Heating Rate ($\dot{q}$)
- Outer Skin Thickness (t_s)
- Pitch (P)
- Coolant Flowrate ($\dot{m}$)

Output:

- 10 Fluid Node Temperatures
- 54 Structural Node Temperatures
- Coolant Pressure Drop

GP75-0131-151

FIGURE 22
COOLED PANEL THERMAL MODEL

near the coolant inlet end of the panel. However, in nearly all cases, turbulent flow dominated and the maximum panel temperature occurred at the coolant outlet end. Pressure drops in the tubes were determined using conventional relationships.

Calculations were made for surface heating rates of 23, 45, 68, and 136 kW/M^2 (2, 4, 6, and 12 Btu/sec ft^2) to determine the panel temperatures associated with various skin thicknesses and tube spacings. Figure 23 illustrates the use of these data for a typical heating rate of 23 kW/m^2 (2 Btu/sec ft^2). An additional plot, Figure 24, was then constructed to show the coolant flowrate required to maintain 394 K (250°F), as a function of tube spacing for various skin thicknesses and heating rates.

In addition, coolant pressure drop characteristics were determined and summarized in Figure 25. Pressure drop is primarily a function of coolant

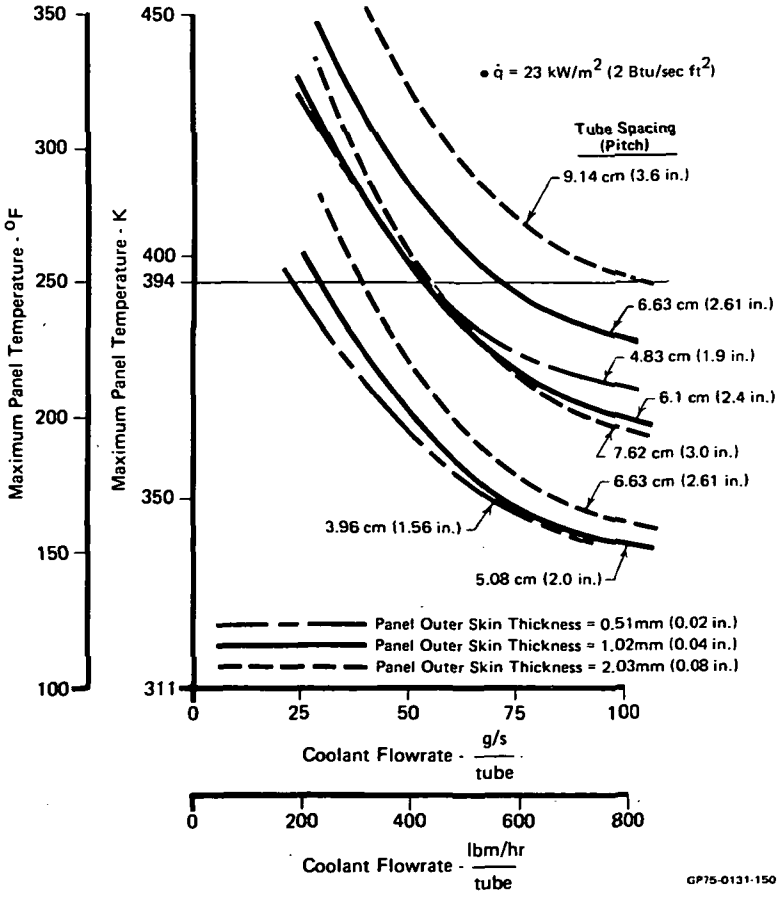

FIGURE 23
COOLED PANEL MAXIMUM TEMPERATURES

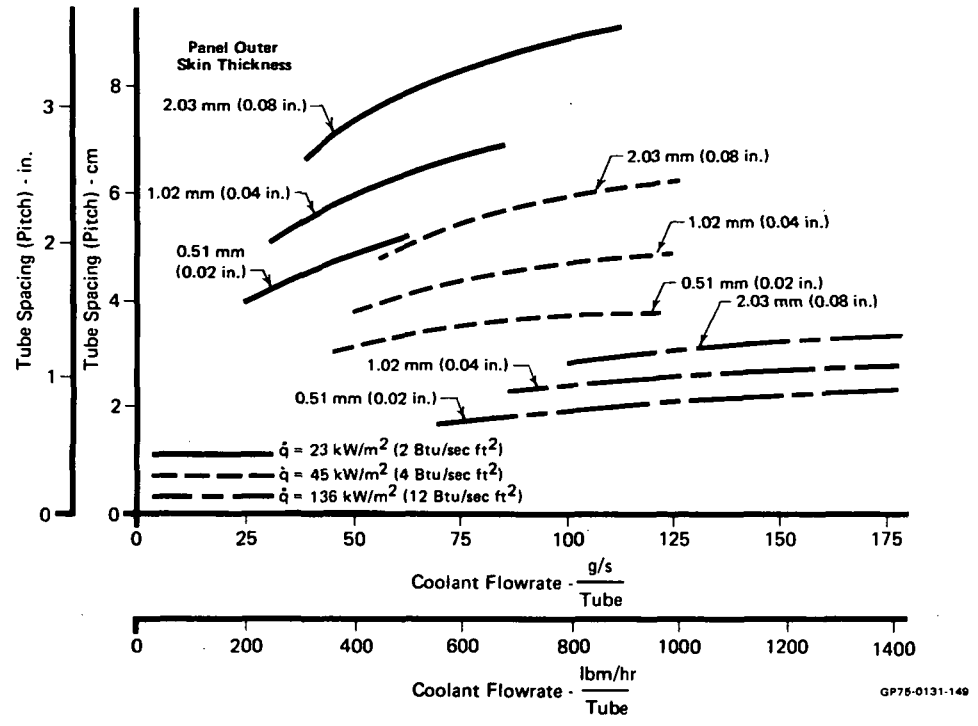

FIGURE 24
PANEL CONFIGURATIONS RESULTING IN MAXIMUM PANEL TEMPERATURES OF 394K (250°F)

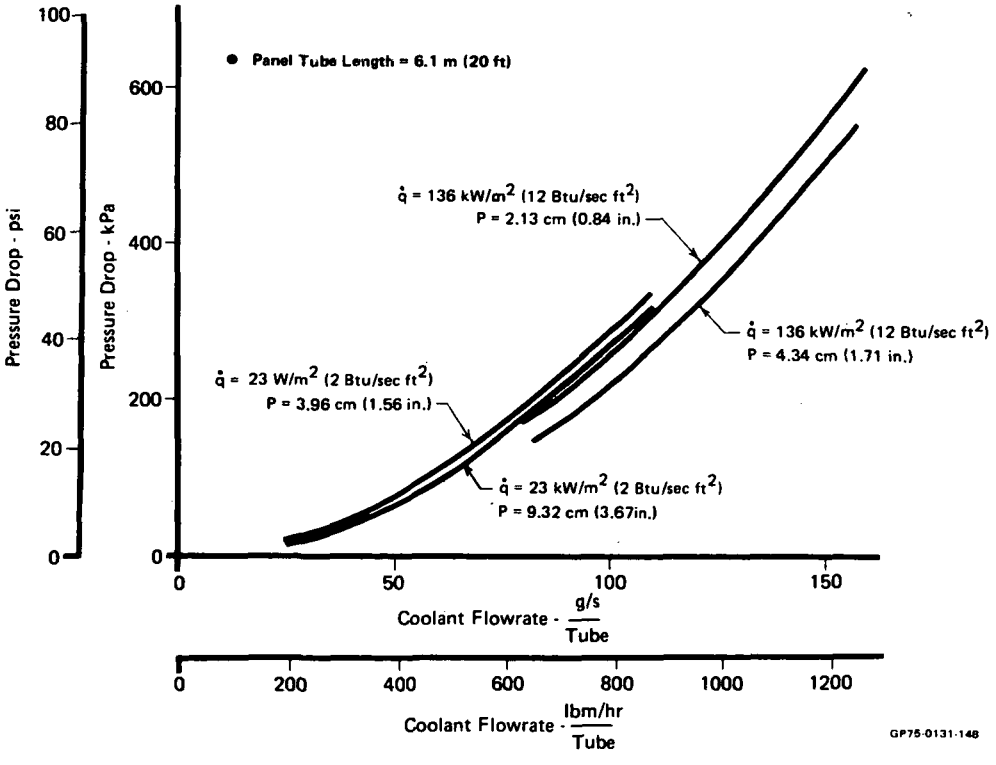

FIGURE 25
COOLED PANEL PRESSURE DROP

flowrate, but both the heating rate and tube spacing influenced the results since variations in these parameters affect the total heat absorbed by the coolant. Skin thickness effects are reflected in the resultant tube spacing. The total heat absorbed determined the coolant temperature which in turn affected fluid properties.

Coolant flowrates to each of the heating zones, as defined in Figures 19, 20, and 21, were determined as follows. Using the zonal maximum heating rate and the required panel outer skin thickness (as defined to withstand local loading conditions), the pitch (distance between coolant tubes) was determined. Applicable parametric tube spacing data were developed using the fin heat transfer relationship from Reference (5). This relationship can be reduced to the following simplified expression:

$$(P-D) = \sqrt{\frac{8k\ t_s\ \Delta T_s}{\dot{q}}}$$

where:

(P-D) = distance between tubes

k = thermal conductivity of skin material

t_s = thickness of skin material

ΔT_s = temperature difference between a point midway between tubes and a point immediately above the tubes

$\dot{q}$ = surface heating rate

The panel skin material was assumed to be 2219-T87 aluminum alloy with a thermal conductivity of 138 W/m·K (80 Btu/hr ft°F). Based on an allowable skin thermal gradient of 56 K (100°F), data were generated to reflect variations in skin thickness and heating rate, and plotted as Figure 26. As indicated by Figure 26, for "dee" shaped tubes, the skin region above the tube was assumed to be isothermal for the width D, with the temperature difference applicable to the edge of the tube I.D. Although no consideration was given to a skin backside material (such as the proposed honeycomb core) MCAIR work on actively cooled panels, Reference (6), has indicated that those effects are quite small and the assumed configuration was considered adequate.

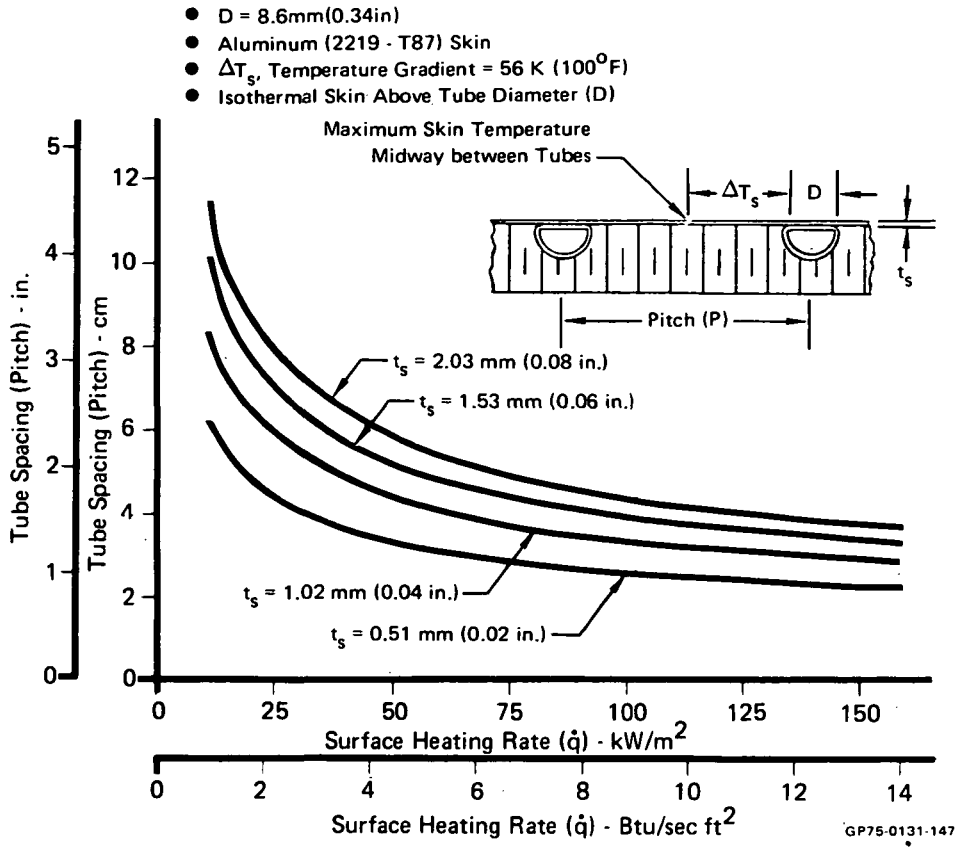

FIGURE 26
ACTIVELY COOLED STRUCTURE TUBE SPACING

With the pitch defined, the coolant flowrate per tube required to maintain maximum surface temperatures at 394 K (250°F) was obtained from Figure 24. With the pitch and zonal surface area known, the number of coolant tubes per panel, hence the total coolant flowrate per zone was determined.

5.2 DESIGN COOLANT FLOWRATES - CONCEPTS 1, 2, AND 3

Using the parametric data and techniques discussed above, the total design coolant flowrates required for airframe cooling for each of the study configurations were established. These results are presented in Figures 27, 28, and 29 for Concepts 1, 2, and 3 respectively. Skin thicknesses shown in these figures represent zonal average values. Thicknesses of 1.02 mm (0.040 in) were predominant over the airframe surfaces, but variations from 0.64 mm (0.025 in) to 1.6 mm (0.063 in) were considered.

Zone (Reference Fig 19)	Skin Thickness		Tube Spacing		Tubes/ Zone	Flowrate/Tube		Flowrate/Zone	
	mm	(in)	cm	(in)		g/s	(lbm/hr)	kg/s	(lbm/hr x 10^{-3})
1	1.016	(0.040)	5.66	(2.23)	21.85	60.5	(480)	1.32	(10.49)
2	1.016	(0.040)	2.64	(1.04)	41.77	298.4	(2,368)	12.46	(98.89)
3	1.016	(0.040)	3.30	(1.30)	46.80	167.6	(1,330)	7.84	(62.24)
4	1.016	(0.040)	6.12	(2.41)	54.17	54.2	(430)	2.93	(23.29)
5	1.016	(0.040)	3.81	(1.50)	72.56	122.0	(968)	8.85	(70.20)
6	1.016	(0.040)	3.81	(1.50)	99.20	122.0	(968)	12.09	(95.98)
7	1.016	(0.040)	6.40	(2.52)	88.57	51.0	(405)	4.52	(35.87)
8	1.016	(0.040)	4.19	(1.65)	106.91	101.4	(805)	10.84	(86.06)
9	1.016	(0.040)	3.94	(1.55)	145.16	114.0	(905)	16.55	(131.37)
10	1.016	(0.040)	6.55	(2.58)	109.07	49.5	(393)	5.39	(42.81)
11	1.016	(0.040)	5.16	(2.03)	99.61	69.9	(555)	6.97	(55.28)
12	1.016	(0.040)	4.04	(1.59)	148.30	109.4	(868)	16.21	(128.65)
13	1.600	(0.063)	8.23	(3.24)	101.85	59.7	(474)	6.08	(48.28)
14	1.600	(0.063)	7.80	(3.07)	73.88	64.5	(512)	4.77	(37.83)
15	1.600	(0.063)	4.95	(1.95)	127.38	145.9	(1,158)	18.59	(147.51)
16	1.600	(0.063)	8.46	(3.33)	105.23	57.3	(455)	6.03	(47.88)
17	1.600	(0.063)	8.00	(3.15)	78.10	62.1	(493)	4.85	(38.50)
18	1.600	(0.063)	5.03	(1.98)	146.67	141.1	(1,120)	20.70	(164.27)
19	0.889	(0.035)	6.73	(2.65)	234.57	44.7	(355)	10.49	(83.27)
20	0.711	(0.028)	5.61	(2.21)	310.05	49.5	(393)	15.33	(121.69)
21	0.660	(0.026)	3.56	(1.40)	398.57	99.9	(793)	39.80	(315.87)
22	0.737	(0.029)	6.63	(2.61)	297.47	41.6	(330)	12.37	(98.17)
23	0.635	(0.025)	5.51	(2.17)	467.28	47.9	(380)	22.37	(177.57)
24	0.787	(0.031)	4.04	(1.59)	458.11	88.8	(705)	40.69	(322.97)
25	0.864	(0.034)	7.39	(2.91)	221.44	40.1	(318)	8.87	(70.42)
26	0.838	(0.033)	6.20	(2.44)	283.28	47.9	(380)	13.56	(107.65)
27	0.686	(0.027)	4.27	(1.68)	370.00	73.1	(580)	27.04	(214.60)
28	0.686	(0.027)	6.68	(2.63)	262.36	40.1	(318)	10.50	(83.30)
29	0.762	(0.030)	6.12	(2.41)	348.55	46.4	(368)	16.14	(128.09)
30	0.635	(0.025)	6.45	(2.54)	161.10	40.1	(318)	6.44	(51.15)
31	0.635	(0.025)	5.66	(2.23)	225.47	46.4	(368)	10.44	(82.86)
32	1.016	(0.040)	5.99	(2.36)	259.32	55.8	(443)	14.46	(114.75)
33	1.016	(0.040)	6.12	(2.41)	492.45	54.2	(430)	26.68	(211.75)
34	1.600	(0.063)	8.23	(3.24)	731.11	59.7	(474)	43.66	(346.55)
35	1.016	(0.040)	4.24	(1.67)	335.57	98.3	(780)	32.98	(261.74)
36	1.016	(0.040)	3.76	(1.48)	413.51	126.6	(1,005)	52.36	(415.58)
37	1.016	(0.040)	4.24	(1.67)	710.66	98.3	(780)	69.84	(554.31)
38	1.600	(0.063)	5.51	(2.17)	826.18	117.2	(930)	96.81	(768.35)
39	1.016	(0.040)	3.81	(1.50)	373.60	122.0	(968)	45.54	(361.46)
40	1.016	(0.040)	5.16	(2.03)	273.69	69.9	(555)	19.14	(151.90)
41	1.270	(0.050)	6.02	(2.37)	421.27	63.6	(505)	26.80	(212.74)
42	1.270	(0.050)	6.88	(2.71)	345.39	52.7	(418)	18.17	(144.20)
Total					10,888.00			847.50	(6,726.34)

GP75-0131-26

FIGURE 27
DESIGN COOLANT FLOWRATES FOR AIRFRAME COOLING, CONCEPT 1

Zone (Reference Fig 20)	Skin Thickness		Tube Spacing		Tubes/ Zone	Flowrate/Tube		Flowrate/Zone	
	mm	(in.)	cm	(in.)		g/s	(lbm/hr)	kg/s	(lbm/hr x 10^{-3})
1	1.016	(0.040)	5.66	(2.23)	21.85	60.5	(480)	1.32	(10.49)
2	1.016	(0.040)	2.64	(1.04)	41.77	298.4	(2,368)	12.46	(98.89)
3	1.016	(0.040)	3.30	(1.30)	46.80	167.6	(1,330)	7.84	(62.24)
4	1.016	(0.040)	6.12	(2.41)	54.17	54.2	(430)	2.93	(23.29)
5	1.016	(0.040)	3.81	(1.50)	72.56	122.0	(968)	8.85	(70.20)
6	1.016	(0.040)	3.81	(1.50)	99.20	122.0	(968)	12.09	(95.98)
7	1.016	(0.040)	6.40	(2.52)	88.57	51.0	(405)	4.52	(35.87)
8	1.016	(0.040)	4.19	(1.65)	106.91	101.4	(805)	10.84	(86.06)
9	1.016	(0.040)	3.94	(1.55)	145.16	114.0	(905)	16.55	(131.37)
10	1.016	(0.040)	6.55	(2.58)	109.07	49.5	(393)	5.39	(42.81)
11	1.016	(0.040)	5.16	(2.03)	99.61	69.9	(555)	6.97	(55.28)
12	1.016	(0.040)	4.04	(1.59)	148.30	109.4	(868)	16.21	(128.65)
13	1.600	(0.063)	8.23	(3.24)	101.85	59.7	(474)	6.08	(48.28)
14	1.600	(0.063)	7.80	(3.07)	70.75	64.5	(512)	4.56	(36.22)
15	1.600	(0.063)	4.95	(1.95)	122.46	145.9	(1,158)	17.87	(141.81)
16	1.600	(0.063)	8.46	(3.33)	99.82	57.3	(455)	5.72	(45.42)
17	1.600	(0.063)	8.00	(3.15)	72.38	62.1	(493)	4.50	(35.68)
18	1.600	(0.063)	5.03	(1.98)	137.58	141.1	(1,120)	19.41	(154.08)
19	0.635	(0.025)	5.82	(2.29)	250.48	44.7	(355)	11.20	(88.92)
20	0.635	(0.025)	5.36	(2.11)	307.68	49.5	(393)	15.24	(120.92)
21	0.635	(0.025)	3.51	(1.38)	378.26	99.9	(793)	37.79	(299.96)
22	0.635	(0.025)	6.22	(2.45)	292.41	41.6	(330)	12.16	(96.49)
23	0.635	(0.025)	5.51	(2.17)	439.63	47.9	(380)	21.05	(167.06)
24	0.787	(0.031)	4.04	(1.59)	420.38	88.8	(705)	37.34	(296.37)
25	0.635	(0.025)	6.45	(2.54)	237.17	40.1	(318)	9.50	(75.42)
26	0.635	(0.025)	5.51	(2.17)	299.17	47.9	(380)	14.32	(113.68)
27	0.686	(0.027)	4.27	(1.68)	345.00	73.1	(580)	25.21	(200.10)
28	0.635	(0.025)	6.45	(2.54)	251.82	40.1	(318)	10.09	(80.08)
29	0.635	(0.025)	5.64	(2.22)	355.68	46.4	(368)	16.49	(130.89)
30	0.635	(0.025)	6.45	(2.54)	161.10	40.1	(318)	6.44	(51.15)
31	0.635	(0.025)	5.66	(2.23)	225.47	46.4	(368)	10.44	(82.86)
32	1.016	(0.040)	5.99	(2.36)	265.93	55.8	(443)	14.84	(117.81)
33	1.016	(0.040)	6.12	(2.41)	507.39	54.2	(430)	27.49	(218.18)
34	1.600	(0.063)	8.23	(3.24)	768.15	59.7	(474)	45.88	(364.10)
35	1.016	(0.040)	4.24	(1.67)	335.57	98.3	(780)	32.98	(261.74)
36	1.016	(0.040)	3.76	(1.48)	421.62	126.6	(1,005)	53.39	(423.73)
37	1.016	(0.040)	4.24	(1.67)	732.21	98.3	(780)	71.96	(571.13)
38	1.600	(0.063)	5.51	(2.17)	923.50	117.2	(930)	108.21	(858.86)
39	1.016	(0.040)	3.81	(1.50)	373.60	122.0	(968)	45.54	(361.46)
40	1.016	(0.040)	5.16	(2.03)	273.69	69.9	(555)	19.14	(151.90)
41	1.270	(0.050)	6.02	(2.37)	421.27	63.6	(505)	26.80	(212.74)
42	1.270	(0.050)	6.88	(2.71)	345.39	52.7	(418)	18.17	(144.20)
Total					10,971.00			855.82	(6,792.37)

GP75-0131-28

FIGURE 28
DESIGN COOLANT FLOWRATES FOR AIRFRAME COOLING, CONCEPT 2

Zone (Reference Fig 21)	Skin Thickness		Tube Spacing		Tubes/ Zone	Flowrate/Tube		Flowrate/Zone	
	mm	(in.)	cm	(in.)		g/s	(lbm/hr)	kg/s	(lbm/hr x 10^{-3})
1	1.016	(0.040)	5.03	(1.98)	34.85	73.1	(580)	2.55	(20.21)
2	1.016	(0.040)	2.74	(1.08)	25.00	266.9	(2,118)	6.67	(52.94)
3	1.016	(0.040)	3.02	(1.19)	80.67	207.0	(1,643)	16.69	(132.50)
4	1.016	(0.040)	5.87	(2.31)	59.74	57.3	(455)	3.42	(27.18)
5	1.016	(0.040)	3.81	(1.50)	86.00	122.0	(968)	10.48	(83.21)
6	1.016	(0.040)	3.61	(1.42)	124.65	137.8	(1,093)	17.16	(136.18)
7	1.016	(0.040)	6.40	(2.52)	71.43	51.0	(405)	3.65	(28.93)
8	1.016	(0.040)	4.45	(1.75)	114.86	90.5	(718)	10.38	(82.41)
9	1.016	(0.040)	3.94	(1.55)	145.16	114.0	(905)	16.55	(131.37)
10	1.016	(0.040)	6.93	(2.73)	78.02	46.4	(368)	3.61	(28.67)
11	1.016	(0.040)	4.95	(1.95)	115.38	74.7	(593)	8.61	(68.36)
12	1.016	(0.040)	4.24	(1.67)	161.68	98.1	(780)	15.89	(126.11)
13	1.600	(0.063)	8.74	(3.44)	81.10	55.0	(436)	4.46	(35.36)
14	1.600	(0.063)	6.32	(2.49)	100.00	90.8	(721)	9.08	(72.10)
15	1.600	(0.063)	5.41	(2.13)	154.93	122.0	(968)	18.90	(149.97)
16	1.600	(0.063)	9.04	(3.56)	80.06	53.0	(417)	4.21	(33.39)
17	1.600	(0.063)	6.76	(2.66)	95.86	81.3	(645)	7.79	(61.83)
18	1.600	(0.063)	5.72	(2.25)	153.33	110.0	(873)	16.87	(133.86)
19	0.635	(0.025)	6.22	(2.45)	128.57	41.6	(330)	5.35	(42.43)
20	0.635	(0.025)	5.23	(2.06)	132.52	51.0	(405)	6.76	(53.67)
21	0.635	(0.025)	4.09	(1.61)	232.92	75.0	(593)	17.39	(138.01)
22	0.635	(0.025)	6.22	(2.45)	146.94	41.6	(330)	6.11	(48.49)
23	0.635	(0.025)	5.51	(2.17)	100.92	47.9	(380)	4.83	(38.35)
24	0.635	(0.025)	4.14	(1.63)	239.26	73.1	(580)	17.48	(138.77)
25	0.635	(0.025)	6.22	(2.45)	171.43	41.6	(330)	7.13	(56.57)
26	0.635	(0.025)	5.51	(2.17)	45.62	47.9	(380)	2.18	(17.34)
27	0.635	(0.025)	4.19	(1.65)	245.45	71.6	(568)	17.55	(139.29)
28	0.635	(0.025)	6.45	(2.54)	342.52	40.1	(318)	13.70	(108.75)
29	0.635	(0.025)	4.19	(1.65)	454.55	71.6	(568)	32.50	(257.96)
30	0.635	(0.025)	6.45	(2.54)	389.76	40.1	(318)	15.59	(123.75)
31	0.635	(0.025)	6.45	(2.54)	309.45	40.1	(318)	12.38	(98.25)
32	0.635	(0.025)	5.66	(2.23)	275.78	46.4	(368)	12.77	(101.35)
33	1.016	(0.040)	5.99	(2.36)	216.36	55.8	(443)	12.06	(95.74)
34	1.016	(0.040)	6.12	(2.41)	406.80	54.2	(430)	22.04	(174.92)
35	1.600	(0.063)	8.23	(3.24)	463.15	59.7	(474)	27.66	(219.53)
36	1.016	(0.040)	4.24	(1.67)	302.16	98.3	(780)	29.70	(235.69)
37	1.016	(0.040)	3.76	(1.48)	345.00	126.6	(1,005)	43.69	(346.73)
38	1.016	(0.040)	4.24	(1.67)	587.07	98.3	(780)	57.70	(457.92)
39	1.600	(0.063)	5.51	(2.17)	638.99	117.2	(930)	74.88	(594.26)
40	1.016	(0.040)	3.81	(1.50)	336.40	122.0	(968)	41.01	(325.47)
41	1.016	(0.040)	4.72	(1.86)	252.90	81.0	(643)	20.47	(162.49)
42	1.270	(0.050)	5.92	(2.33)	363.09	65.3	(518)	23.68	(187.90)
43	1.270	(0.050)	6.88	(2.71)	193.95	52.7	(418)	10.20	(80.97)
Total					9,084.00			711.78	(5,649.16)

GP75-0131-30

FIGURE 29
DESIGN COOLANT FLOWRATES FOR AIRFRAME COOLING, CONCEPT 3

6. SUBSYSTEM THERMAL REQUIREMENTS

To provide realistic assessments of aircraft performance, size and weight, consideration was given to the requirements of primary subsystems. These subsystems were defined as those required to provide environmental control for the crew station and passenger compartment and supply the aircraft with hydraulic and electrical power. These analyses were only exploratory as the intent was merely to obtain reasonable estimates of the weight, volume, and power requirements associated with each subsystem. It was assumed that these requirements have a minimal impact on the structural design aspects of the study. The analyses were conducted specifically for the Concept 1 configuration and the results were applied to all three concepts. It was assumed that the hydrogen fuel would provide the heat sink for these subsystems. Therefore, consideration was given to integrating these subsystems with the aircraft active cooling system.

6.1 ENVIRONMENTAL CONTROL SYSTEM

The environmental control system (ECS) must provide suitable temperature, pressure, and humidity environments for the crew, passengers, and various equipment throughout all modes of flight and ground operation. For this study, it was assumed that ground support equipment would be used for ground operation requirements and the ECS was sized for flight requirements only. Mach 6 cruise was selected as the ECS design condition.

ECS weight, volume, and power requirements are dependent on the total design heat load. This was assumed to comprise four basic constituents:

a. Heating from crew and passenger compartment walls.

b. Metabolic heat load attributable to crew and passengers.

c. Crew station avionics heat load.

d. Heat load resulting from necessity to cool air from available sources for makeup of air leaked from pressurized compartment.

Heat loads were determined using the following ground rules:

a. Crew and passenger compartment internal wall surface area of 465 m^2 (5000 ft^2).

b. An average compartment air temperature of 297 K (75°F).

c. A minimum compartment pressurization of 75.2 kPa (10.91 psi) absolute or the equivalent of a 2.44 km (8000 ft) altitude.

d. An average ventilation air velocity of 1.02 m/s (200 ft/min).

e. An internal compartment wall surface temperature of 308 K (95°F).

f. A supply of 4.72×10^{-3} m^3/s (10 cfm) fresh air ventilation for each crew member.

g. A crew of 10 and 200 passengers, with an average metabolic heat load of 117 W/person (400 Btu/hr/person).

h. An effective pressurized compartment leakage area of 0.63 mm^2/m^2 of surface area (9.04×10^{-5} in^2/ft^2 of surface area).

i. An average external surface panel temperature (cooled structure) of 366 K (200°F).

These ground rules satisfy Reference (9) requirements and reflect current fabrication technology capabilities.

To minimize the effect of heating from the compartment walls, it was assumed that a low density glass fiber insulation would be installed between the cooled surface panels and the pressurized compartment walls. A side benefit of the actively cooled surface panel design is that the heat transfer through the passenger compartment walls is small (compared to hot structure configurations) and temperatures are low enough to permit the use of efficient, lightweight insulation materials. The use of a 2.54 cm (1 in) layer of 9.6 kg/m^3 (0.6 lbm/ft^3) density glass fiber insulation would produce average compartment wall temperatures of 305 K (90°F). However, considering heat shorts at structural attachments, maximum wall temperatures on the order of 308 K (95°F) can be expected. An allowance of 113 kg (250 lbm) was included in group weight statements to account for compartment insulation. Acoustic considerations may dictate additional insulation, but this aspect was not included in the study. As a result of the assumed ground rules, which result in an average compartment wall-to-air convective heat transfer coefficient of 10.8 $W/m^2 \cdot K$ (1.9 Btu/hr ft^2°F) the heating from the compartment walls was determined to be 55.7 kW (1.9×10^5 Btu/hr).

The metabolic heat load attributable to the 210 occupants (crew and passengers) was determined to be 24.6 kW (8.4×10^4 Btu/hr). A crew station

avionics heat load of 3.81 kW (1.3×10^4 Btu/hr) consistent with current C-5A aircraft system requirements was assumed.

A cursory examination of the Mach 6 transport requirements for fresh air ventilation and leakage air makeup revealed that a conventional open loop ECS would result in large weight penalties. At Mach 6, ram air must be cooled from a total temperature of about 1700 K (2600°F) for use as a source of makeup air. Therefore, the selected ECS configuration is semi-closed and processes only enough ram air to make up for leakage losses. The bulk of the cabin airflow is continuously recirculated, being purified by filtering and odor removal in the recirculation loop.

Based on the assumed pressurization and leakage area, a makeup flowrate requirement of 51.7 g/s (6.84 lbm/min) was determined. Cooling this amount of ram air directly to 294 K (70°F) would result in a heat load of 75.9 kW (2.59×10^5 Btu/hr). However, the assumed ECS configuration afforded a means of minimizing this penalty concurrent with supplying the required system power.

A ram air turbine is used to supply ECS power at high speed flight conditions. A flowrate of 287 g/s (38 lbm/min) through a turbine with an expansion ratio of 4.6 can provide the 139 kW (187 HP) power required to circulate compartment airflow and pump coolant in associated heat transport loops. Turbine discharge flow at 103 kPa (15 psi) absolute and 1279 K (1842°F) is then available to provide leakage makeup air. Cooling this air to 294 K (70°F) results in a heat load of 55.4 kW (1.89×10^5 Btu/hr) a 27% reduction compared to cooling the ram air directly. Designing a ram air turbine for use in this temperature environment would pose difficulties that were not examined in this study.

Figure 30 summarizes the ECS design heat loads which total 139.4 kW (4.76×10^5 Btu/hr). A schematic of the assumed ECS configuration is presented in Figure 31. The semi-closed system uses the hydrogen fuel directly as a heat sink, eliminating the necessity for mechanical refrigeration. Weight trends as a function of design heat load are shown in Figure 32. Based on the design heat load of 139.4 kW (4.76×10^5 Btu/hr) an ECS installed weight allowance of 454 kg (1000 lbm) appeared reasonable and was reflected in the aircraft weight statements.

HEAT SOURCE	HEAT LOAD kW	(Btu/hr)
1. Environmental Control System:		
a. Crew and Passenger Compartment Walls	55.6	(1.9×10^5)
b. Crew and Passenger Metabolic	24.6	(8.4×10^4)
c. Crew Station Avionics	3.8	(1.3×10^4)
d. Cooled Air for Pressurized Compartment Leakage Make-up	55.4	(1.89×10^5)
Total, ECS	139.4	(4.76×10^5)
2. Hydraulic System	56.6	(1.932×10^5)
3. Electrical Power Generation System	87.0	(2.97×10^5)
Total, Subsystems	283.0	(9.662×10^5)

FIGURE 30
SUBSYSTEM DESIGN HEAT LOAD SUMMARY

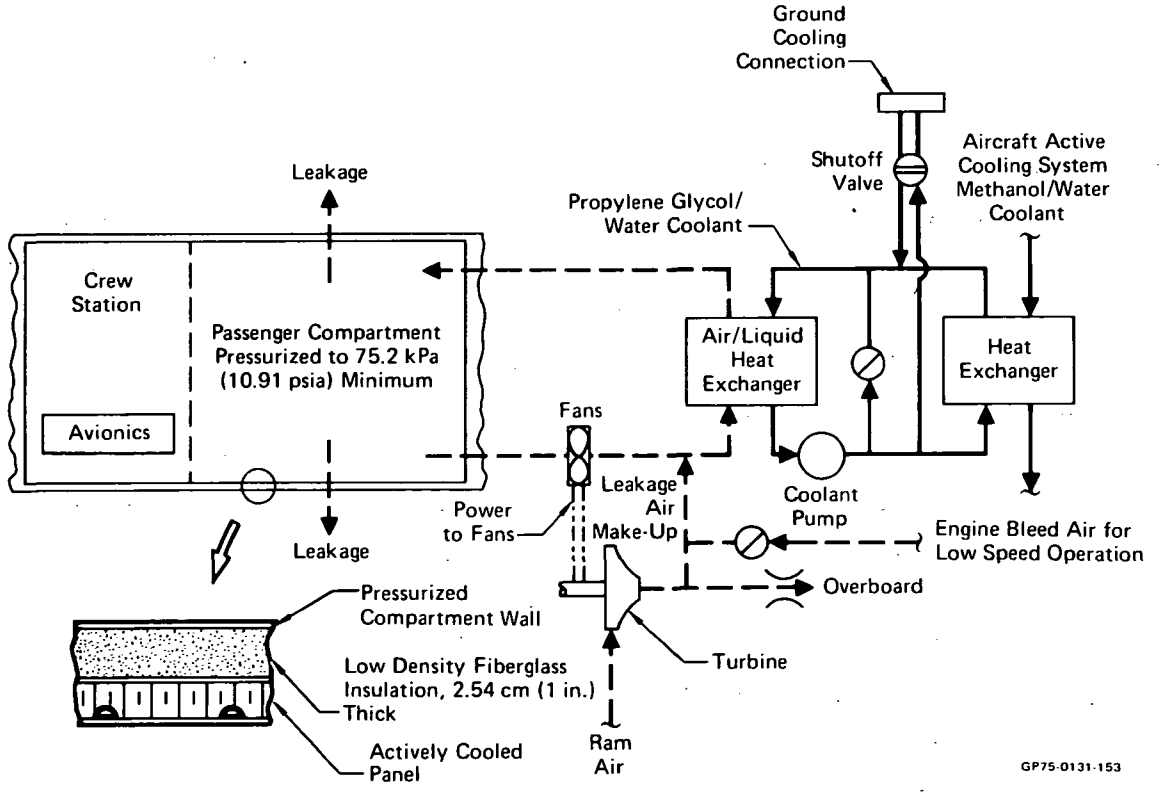

FIGURE 31
ENVIRONMENTAL CONTROL SYSTEM SCHEMATIC

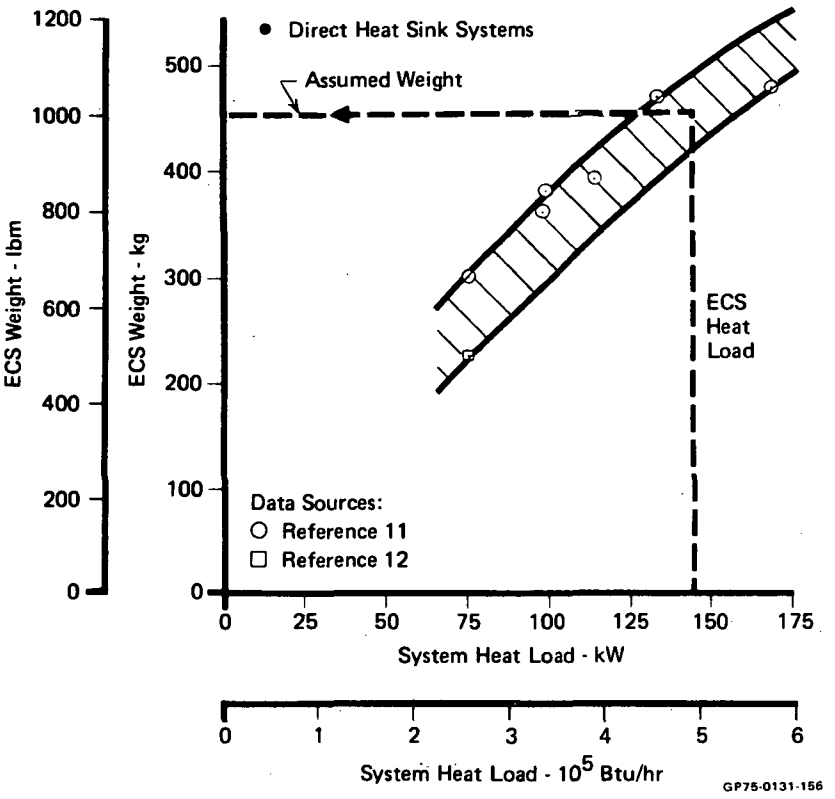

FIGURE 32
ENVIRONMENTAL CONTROL SYSTEM WEIGHT TRENDS

6.2 HYDRAULIC AND ELECTRICAL POWER GENERATION SYSTEMS

Requirements for the hydraulic and electrical power generation systems were estimated by extrapolating available commercial airliner requirements on a weight basis. It was assumed that a 27.6 MPa (4000 psi) absolute hydraulic system will be used. A hydraulic fluid flowrate of 1.03×10^{-2} m^3/s (163 gal/min) was established, which requires an input power of 283 kW (380 HP). System heat rejection was based on a 20% capacity heat rejection ratio; 15% for case drain and 5% system leakage. The resultant hydraulic system design heat load was established as 56.6 kW (1.932×10^5 Btu/hr).

It was estimated that an input power of 582 kW (780 HP) is required to generate sufficient electrical power for the study aircraft. The resultant system heat rejection, based on 85% efficiency, was established as 87 kW (2.97×10^5 Btu/hr).

6.3 INTEGRATION OF SUBSYSTEM COOLING WITH STRUCTURAL COOLING SYSTEM

Figure 30 summarizes the subsystem heat loads which total 283 kW (9.66×10^5 Btu/hr). The impact of subsystem heat loads on active cooling system requirements is small as can be noted in Section 7.

To simplify the transfer of rejected subsystem heat to the hydrogen fuel heat sink, these systems were integrated with the primary active cooling system as indicated in Figure 33. Each subsystem uses an intermediate liquid heat transport loop between the heat source and the primary cooling system fluid. In the case of the ECS, a propylene glycol/water mixture was assumed. This coolant was selected to interface with the air loop because of its nonflammable, nontoxic, and relatively nonvolatile characteristics. Coolants in the hydraulic and electrical power generation systems loops would be selected primarily on temperature compatibility.

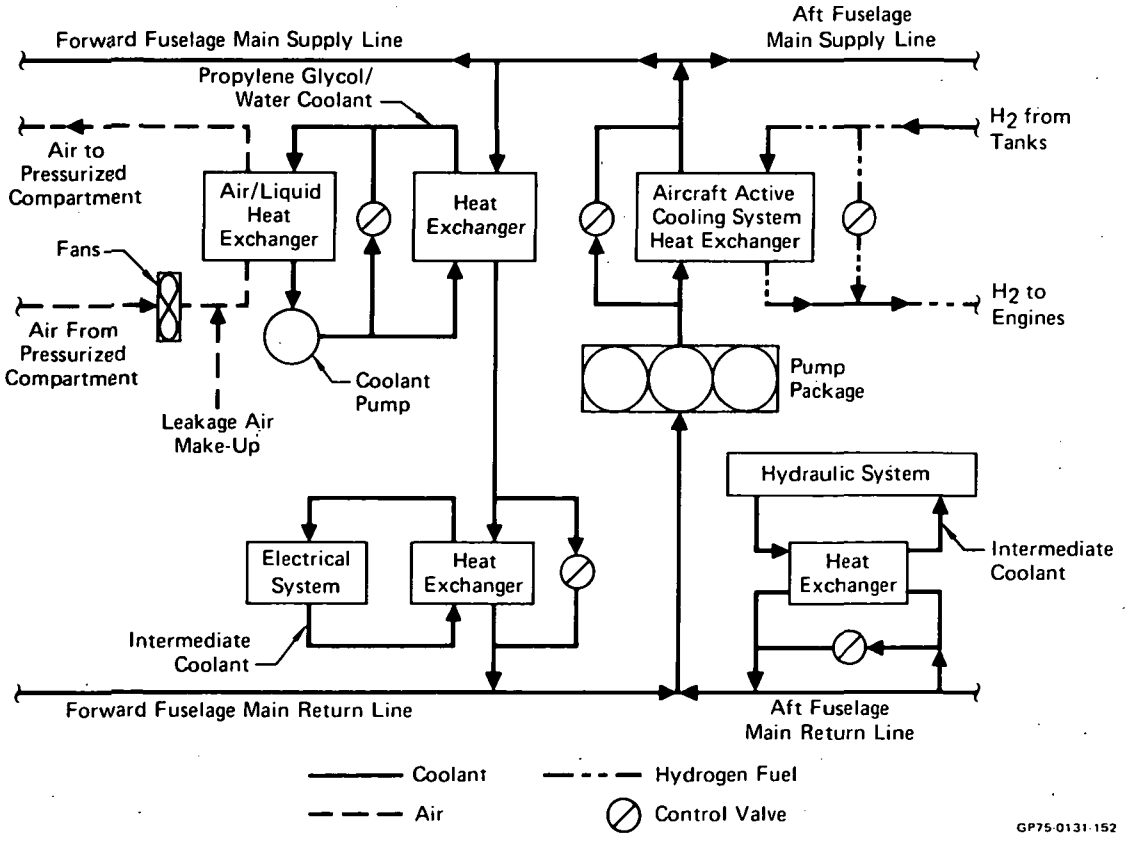

FIGURE 33
INTEGRATION OF SUBSYSTEMS WITH ACTIVE COOLING SYSTEM

7. ACTIVE COOLING SYSTEM SIZING

The weight and volume requirements of cooling system components such as the heat exchanger and pumps are primarily dependent on the total design heat loads and coolant flowrates. Figures 34 and 35 present the total design heat loads and coolant flowrate requirements, respectively. The total heat loads reflect the airframe heat loads (Figures 19, 20, and 21), the subsystem heat load (Figure 30), and a coolant pump heat load which is discussed in Section 7.2. The total coolant flowrates reflect the airframe requirements (Figures 27, 28, and 29) with a nominal additional allowance for the subsystems.

	CONCEPT 1		CONCEPT 2		CONCEPT 3	
	MW	(Btu/sec)	MW	(Btu/sec)	MW	(Btu/sec)
AIRFRAME HEAT LOADS:						
FUSELAGE	50.4	(47,771)	48.1	(45,650)	42.9	(40,683)
WINGS	48.5	(45,958)	50.7	(48,040)	39.7	(37,630)
VERTICAL TAIL	9.3	(8,784)	9.3	(8,784)	7.6	(7,235)
SUBSYSTEM HEAT LOADS	0.3	(283)	0.3	(283)	0.3	(283)
COOLANT PUMP HEAT LOADS	0.2	(143)	0.2	(143)	0.1	(127)
TOTAL	108.5	(102,939)	108.5	(102,900)	90.6	(85,958)

FIGURE 34
TOTAL DESIGN HEAT LOADS

	CONCEPT 1		CONCEPT 2		CONCEPT 3	
	kg/s	(lbm/hr)	kg/s	(lbm/hr)	kg/s	(lbm/hr)
AIRFRAME FLOWRATES:						
FUSELAGE	401	(3.18×10^6)	392	(3.11×10^6)	349	(2.77×10^6)
WINGS	382	(3.03×10^6)	401	(3.18×10^6)	310	(2.45×10^6)
VERTICAL TAIL	64	(0.51×10^6)	64	(0.51×10^6)	54	(0.43×10^6)
SUBSYSTEM FLOWRATES:	1	(1×10^4)	1	(1×10^4)	1	(1×10^4)
TOTAL	848	(6.73×10^6)	858	(6.81×10^6)	714	(5.66×10^6)

FIGURE 35
TOTAL COOLANT FLOWRATE REQUIREMENTS

However, to completely define the cooling system size, the weight of the coolant distribution lines and residual coolant within these lines must be determined. It was therefore necessary to establish a realistic coolant distribution system routing scheme and define locations for major system components. Section 7.1 describes the assumed coolant distribution system and denotes some of the more significant considerations. Section 7.2 discusses the procedures used to calculate component weights and summarizes the weights for each concept.

7.1 DESCRIPTION OF COOLANT SYSTEM ROUTING AND COMPONENT LOCATION

As discussed in Reference (5), for an aircraft the size of the hypersonic transport, many different line routing arrangements are possible. The routing scheme used was based on engineering logic and influenced by results from Reference (5). Tradeoffs to minimize weight were not considered for this study.

For these analyses, the nominal panel size was assumed to be 1.22 m (4 ft) by 6.1 m (20 ft), with the length oriented parallel to freestream flow. Fuselage panels were assumed to be staggered, while wing and vertical tail panels were assumed to remain in alignment.

System routings for the Concept 1 and 2 configurations are nearly identical. Basically, the routing is parallel, with sets of main supply and return lines for major structural sections located on each side of the aircraft, as illustrated in Figure 36. The basic system components (heat exchanger and pumps) are centrally located in the lower fuselage. In Concept 1, the heat exchanger is located on the fuselage centerline between fuel tanks normal to the aircraft centerline. However, due to the improved fuel volume utilization, this location is unavailable in Concept 2. For this aircraft, the heat exchanger was reoriented and moved to a slightly outboard location parallel to the aircraft centerline, where volume was available. This change in location did not affect cooling system size significantly.

Main distribution lines (both supply and return) were arranged as follows and reflected in Figure 36:

a. Forward Fuselage - a set of lines on either side of the fuselage from FS 64 m (210 ft) forward

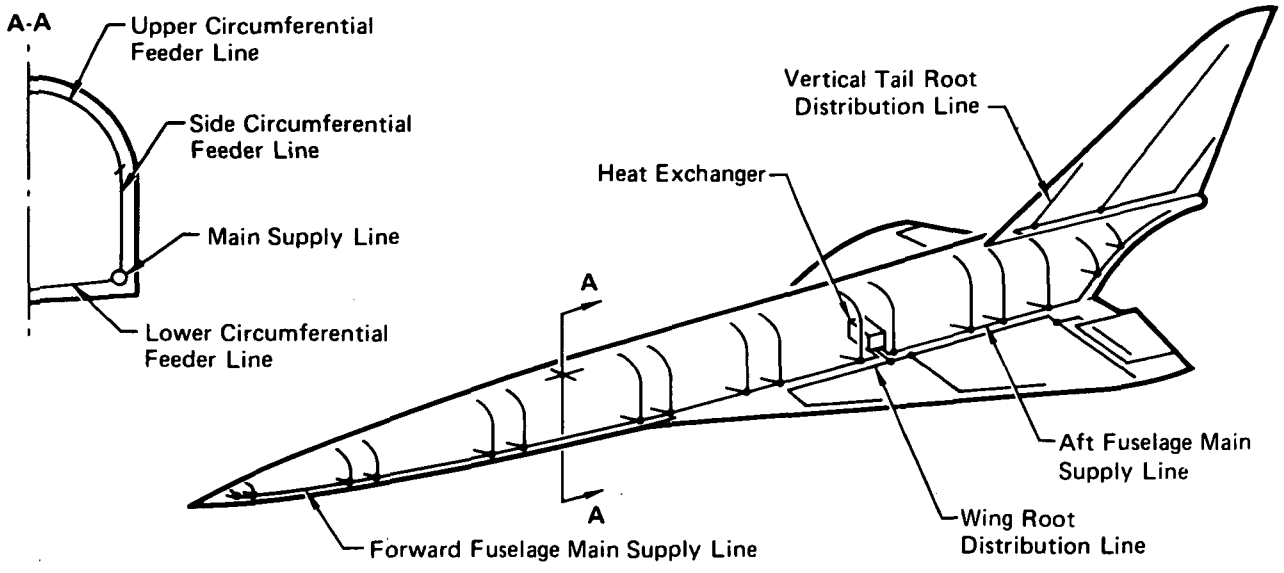

- Supply Lines only are Shown, Return Lines Spaced Similarly
- Lines Represent Those on One Side of Aircraft only, Except for Vertical Tail Lines

GP75-0131-172

FIGURE 36
SIMPLIFIED DISTRIBUTION SYSTEM SCHEMATIC, CONCEPTS 1 AND 2

b. Aft Fuselage - a set of lines on either side of the fuselage from FS 64 m (210 ft) aft

c. Wings - a set of lines toward each wing, branching out along the wing roots

d. Vertical Tail - a set of lines branching out of the aft fuselage ducting up to the tail root, then branching out.

Feeder lines to the manifold region of each panel were also included. In the fuselage region, this resulted in feeder lines (either supply or return) every 3.05 m (10 ft) based on 6.1 m (20 ft) long panels in a staggered arrangement. Each feeder line services two adjacent panels such that flow in adjacent panels is in opposite directions.

Routing typical of the distribution system at the major component location is illustrated in Figure 37. This figure also shows the manner in which adjacent panels would be supplied with coolant from the feeder lines.

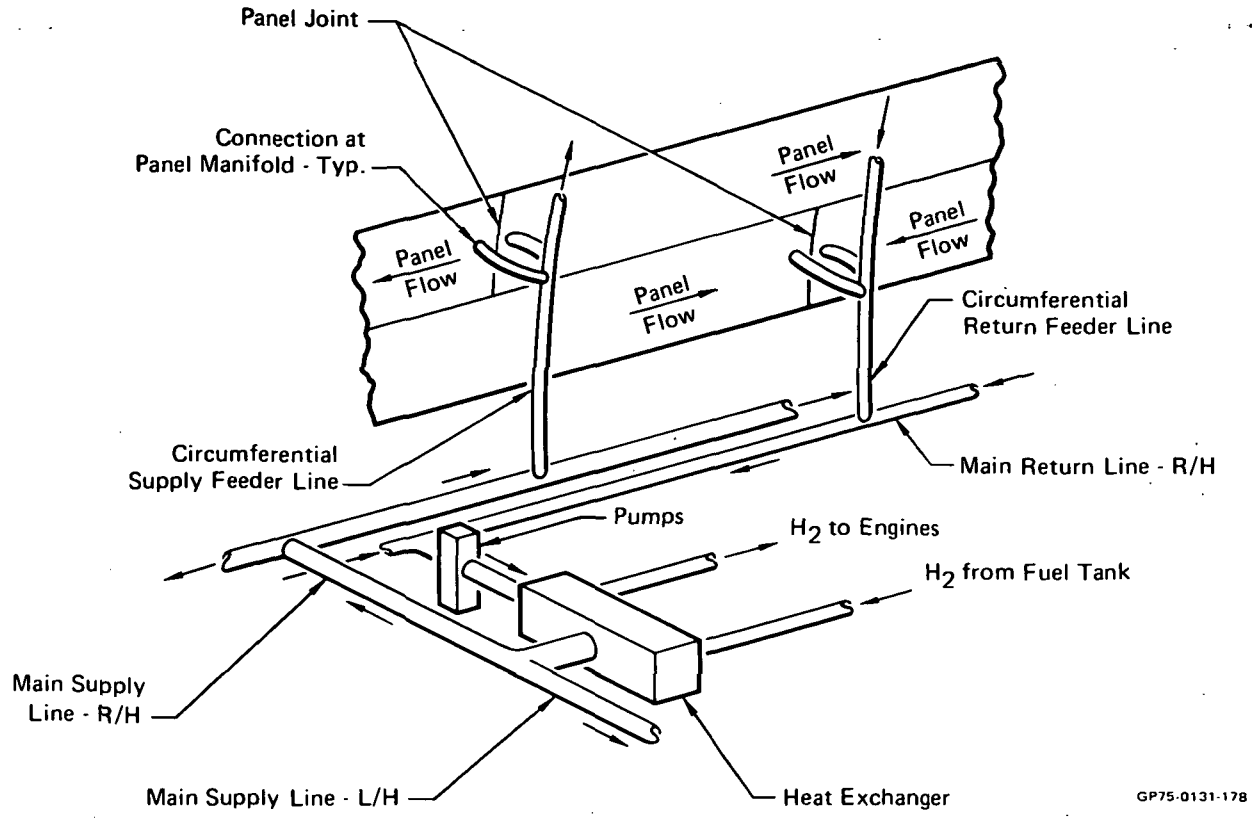

FIGURE 37
TYPICAL COOLANT DISTRIBUTION ROUTING AT MAJOR COMPONENT LOCATION

It was necessary to define a different coolant distribution system routing scheme for Concept 3. The centralized location for the heat exchanger was not available, since the fuel tank fills more than 90% of the fuselage volume and is continuous over its full length. Three potential locations were examined.

a. In the wing root outboard of the fuel tanks at approximately FS 64 m (210 ft).

b. In the fuselage aft of the fuel tanks.

c. In the fuselage forward of the fuel tanks and behind the passenger compartment bulkhead.

The first location retained a high degree of commonality with the routing scheme used in Concepts 1 and 2, providing a high degree of consistency in comparisons. Adequate volume exists in this wing root location. However, the heat exchanger shape would have to be changed, which would result in fabri-

cation and assembly difficulties. In addition, numerous interference problems with primary wing and support structure and the line routings for subsystems (hydraulics, etc.) would create additional complexity. Finally, this location would result in an unbalance problem, with the heavy heat exchanger located 4.6 to 6.1 m (15 to 20 ft) outboard of the line of symmetry. The disadvantages associated with this location were considered significant enough that alternate locations were examined.

Locating the heat exchanger in the aft fuselage would produce significant system weight penalties. Since the coolant would have to be pumped the entire length of the fuselage, considerable pumping power and pump weight penalties would be incurred. In addition, main supply and return coolant lines would have to be quite large, increasing the weight of residual coolant. The aft fuselage location was considered to be the least desirable of the proposed locations.

The heat exchanger location finally selected for Concept 3 was the area forward of the fuel tanks and behind the passenger compartment. Adequate volume exists at this location and no major design interference problems are encountered. Subsequent weight analyses, discussed in Section 7.2, indicate that this location did result in a significant weight penalty compared to a centralized location. However, further attempts to find a more suitable location for the heat exchanger were not made.

Basically, the distribution system for Concept 3 is similar to that of Concepts 1 and 2. One basic difference resulting from the different heat exchanger location is that coolant to the wings is routed through the aft fuselage ducting, rather then having separate main supply and return lines. Figure 38 illustrates the Concept 3 distribution system.

7.2 COOLING SYSTEM WEIGHTS - CONCEPTS 1, 2 AND 3

Active cooling system weight consists of seven components. These components, along with an explanation for the weight bases for each are as follows:

a. Residual coolant in the actively cooled panels - These weights were based on the summation of tubes listed in Figures 27, 28, and 29. Tube geometry was defined in Section 5.1. An allowance was made for coolant in the manifolds of each panel, based on Reference (6).

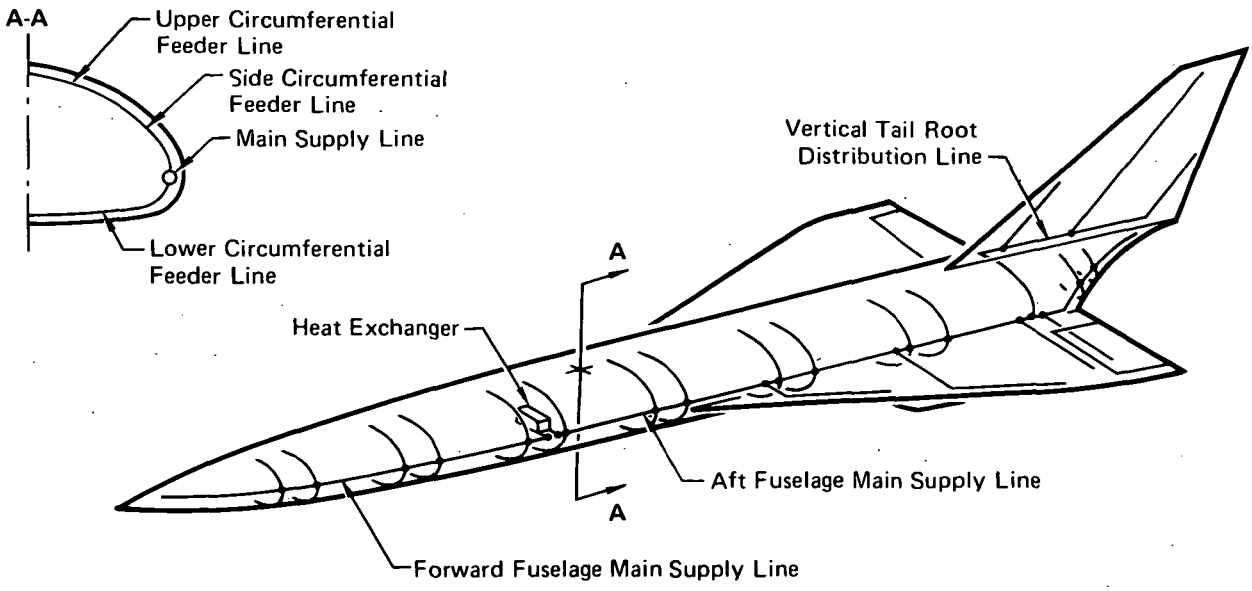

- Supply Lines only are Shown, Return Lines Spaced Similarly
- Lines Represent Those on One Side of Aircraft only, Except for Vertical Tail Lines

GP75-0131-173

FIGURE 38
SIMPLIFIED DISTRIBUTION SYSTEM SCHEMATIC, CONCEPT 3

b. Residual coolant in the distribution lines - Distribution line sizes were established per the routing indicated in Figures 36 and 38. All lines (including feeder lines) were sized based on an allowable pressure drop of 2.26 kPa/m (0.1 psi/ft). An allowance for the differences in coolant density between supply and return lines was included.

c. Distribution lines - Line sizing was established as discussed above. Design pressures and minimum gage requirements were used.

d. Connectors and miscellaneous - These weights were estimated based on the number of connections indicated by the distribution routing in Figures 36 and 38. An allowance for miscellaneous items including hangers, valves, controls and sensors was also included, based on previous studies.

e. Heat exchanger - Although this study assumed a methanol/water coolant rather than a glycol/water solution, it was felt that the heat exchanger design results from Reference (5) were valid for first order weight and volume approximations. The coolant, after absorbing the total heat load, returns to the heat exchanger at approximately 294 K (70°F) and is cooled to

256 K (0°F) by the hydrogen fuel. This requires a heat exchanger effectiveness of approximately 0.84, which is considered acceptable. The Reference (5) heat exchanger weight of 726 kg (1600 lbm) required for a heat load of 69 MW (236×10^6 Btu/hr) was used as a basis for weight estimates. Weights for the heat exchangers in all three concepts were determined on linear extrapolations of the basic weight, using the ratio of the applicable total heat load to the Reference (5) heat load.

f. Pumps - Total coolant flowrate requirements dictated the pump sizes, which were estimated using the information in Figures 30 (pump weight) and 31 (pump capacity) of Reference (5). For Concept 1 and 2, three pumps (plus one pump for redundancy) sized to deliver 290 kg/s (2.3×10^6 lbm/hr) at a 1.03 MPa (150 psi) absolute head, were assumed. At 85% efficiency a power requirement of 336 kW (450 HP) was determined. For Concept 3, three pumps (plus one pump for redundancy) sized to deliver 239 kg/s (1.9×10^6 lbm/hr) at a 1.03 MPa (150 psi) absolute head, were assumed. The power requirements for these pumps were determined to be 298 kW (400 HP). Pump heat rejection to the coolant was determined based on three pumps operating at peak capacity with at 85% efficiency. These heat loads are reflected in Figure 34.

g. Fuel required to drive the coolant pumps - The assumption was used, from Reference (5), that a hydrogen fuel weight penalty of 0.845 g/kW·s (5 lbm/HP hr) is required to provide coolant pump power. Variations in flowrate requirements throughout the mission were assumed. The design flowrates listed in Figures 27, 28, and 29 are representative of requirements at the start of cruise. At the end of cruise these requirements are significantly reduced due to the lower aerodynamic heating at the higher altitude. It was assumed that flow is modulated to meet the required flowrate plus a factor to permit small deviations in heat load. In addition, during the takeoff and loiter phases of the trajectory, it was assumed that flowrate requirements were only one half the cruise value. Flowrate requirements during climb and descent were linearly interpolated between these values. While this is an approximation it is still preferable to assuming that the design flowrate is required throughout the mission. A cursory examination of nonmodulated flow design revealed that the penalty in coolant pump fuel requirements could be quite large.

Cooling system weights are summarized in Figure 39. Final weights for Concepts 1, 2, and 3 are presented in addition to the preliminary weights for Concept 1 before the trajectory and nacelle cooling requirements were firmly established as discussed in Sections 4.2 and 4.3.

	Concept 1						Concept 2		Concept 3	
	(Original Trajectory, Cooled Nacelle) Preliminary		(Final Trajectory, Cooled Nacelle) Preliminary		(Final Trajectory, "Hot" Nacelle) Final		Final		Final	
	Mg	(lbm)	Mg	(lbm)	Mg	(lbm)	Mg	(lbm)	Mg	(lbm)
Coolant In Panels	2.70	(5,950)	2.42	(5,345)	2.10	(4,625)	2.12	(4,662)	1.75	(3,860)
Coolant in Lines	13.88	(30,600)	9.53	(21,005)	7.49	(16,505)	7.49	(16,520)	7.17	(15,807)
Distribution Lines	2.11	(4,655)	1.45	(3,195)	1.14	(2,520)	1.14	(2,522)	1.08	(2,370)
Connectors + Misc	0.54	(1,195)	0.37	(820)	0.31	(690)	0.31	(690)	0.27	(597)
Heat Exchanger	2.16	(4,750)	1.49	(3,290)	1.13	(2,500)	1.13	(2,501)	0.95	(2,088)
Pumps	0.64	(1,400)	0.49	(1,080)	0.32	(700)	0.32	(700)	0.26	(580)
Fuel to Drive Pumps	3.01	(6,625)	2.93	(6,450)	2.67	(5,895)	2.68	(5,913)	2.25	(4,958)
Total	25.03	(55,175)	18.68	(41,185)	15.17	(33,435)	15.20	(33,508)	13.73	(30,260)

GP75-0131-31

FIGURE 39
ACTIVE COOLING SYSTEM WEIGHTS

The final Concept 1 and 2 system weights are nearly equal. This resulted from the similarity in design heat loads (Figures 19 and 20) and coolant flowrate requirements (Figures 27 and 28) attributable to the minor differences in moldline contours between the aircraft. The Concept 3 active cooling system weight is considerably smaller than those for Concepts 1 and 2 but heavier on a wetted area basis primarily because of the change in distribution system as discussed in Section 7.1.

As discussed in Section 7.1, a location forward of the fuel tanks and behind the passenger compartment was selected for the Concept 3 heat exchanger. While some weight penalty was anticipated, it was determined that this penalty is quite significant. The weights of some components are directly related to system heat load such that Concept 3 weights are in the order of 83% of the Concept 1 weights. However, the weight of the primary distribution system for Concept 3 (lines, connectors and residual coolant) is more than 95% of the comparable Concept 1 weight.

A cursory examination of potential distribution system routing plans was conducted to confirm that a penalty in the order of 1.07 Mg (2360 lbm)

could result from differences in the assumed routing. It is obvious that to reach the forward heat exchanger location, coolant must be transported an additional 18.3 m (60 ft). Compared to a mid-tank location, distribution system weight for the Concept 3 wings alone was determined to be over 1.91 Mg (4200 lbm) higher. By combining the flow for the wings with that for the aft fuselage and vertical tail, this penalty was significantly reduced. Still a penalty of 1.07 Mg (2360 lbm) was incurred, translating to an approximate range loss of 103 km (55.5 NM).

These results emphasize the importance of centralizing the location of the cooling system heat exchanger so that wing distribution line sizes are minimized. A trade between the weight penalty associated with the forward heat exchanger location versus the cost and complexity involved with a mid-tank wing root heat exchanger location as described in Section 7.1, would be in order to optimize the Concept 3 aircraft. Such a trade study, however, was felt to be beyond the scope of this program.

The effect of the forward heat exchanger location on system pumping power penalty was also examined. In Concepts 1 and 2, the maximum system pressure drop is experienced in the circuit supplying the forward fuselage panels. On Concept 3 the maximum pressure drop is encountered in the vertical tail circuit. Coincidentally, the magnitudes of these pressure drops were approximately the same and the pumping power requirement was affected only by the difference in flowrates.

8. FUSELAGE/TANK THERMAL PROTECTION SYSTEM DESIGN

Thermal protection systems (TPS) for the fuselage hydrogen tankage configurations designed for non-integral tankage (Concept 1) and integral tankage (Concepts 2 and 3) were selected. This was accomplished by sizing the TPS such that the combined TPS/fuel boiloff penalties to the aircraft resulted in maximum aircraft range.

The TPS for the non-integral tankage (Concept 1) was specified by Reference (4) as consisting of insulation applied to the external tankage surfaces. The trade of insulation weight versus fuel boiloff related to this configuration is discussed in Section 8.2.

Eight candidate tankage TPS concepts compatible with integral tank structure (Concepts 2 and 3) and with the overall airframe surface active cooling system were studied. These candidate concepts were sized and compared in terms of aircraft range penalties and other factors. The selected concept is thermodynamically and structurally similar to the non-integral tankage TPS.

The sizing of the tankage area purge system is discussed in Section 8.4.

8.1 ANALYTICAL TECHNIQUES

Definition of time related flight requirements was basic to analyses of both non-integral and integral hydrogen tankage TPS concepts and sizing of the associated purge systems. Figure 40 illustrates the assumed requirements for fuel boiloff calculations, which include an initial one hour ground hold followed by the nominal Mach 6 hypersonic transport 9.26 Mm (5000 NM) flight and 20 minutes of Mach 0.8 loiter at 12.2 km (40,000 ft) prior to final descent. A panel temperature of 366 K (200°F) was assumed typical during the climb, cruise, and descent to loiter phases of the flight. An average temperature of 242 K (-25°F) was used during the loiter and subsequent descent flight phase. During ground hold, a hot day ambient temperature of 313 K (103°F) was assumed.

A closed cell freon-blown, fiberglass reinforced, polyurethane foam material with a density of 64.1 kg/m^3 (4 lbm/ft^3) was specified for external cryogenic insulation application by Reference (1). Figure 41 presents the value of thermal conductivity used for this material, which is denoted as non-permeated. Certain integral tankage candidate TPS concepts also incorporated

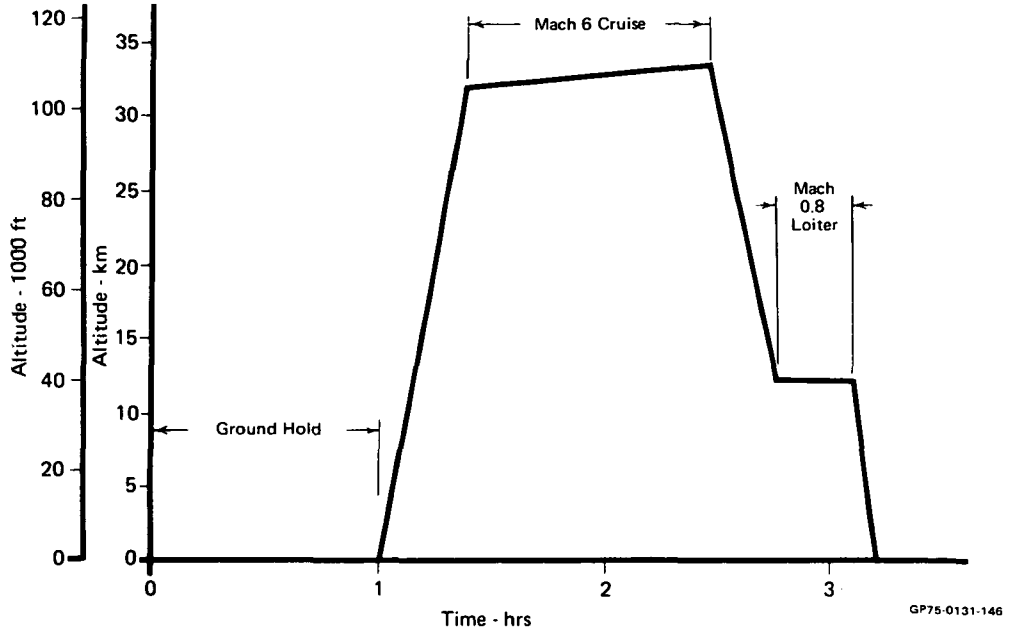

FIGURE 40
TIME RELATED FLIGHT REQUIREMENTS FOR SIZING HYDROGEN TANKAGE THERMAL PROTECTION AND PURGE SYSTEMS

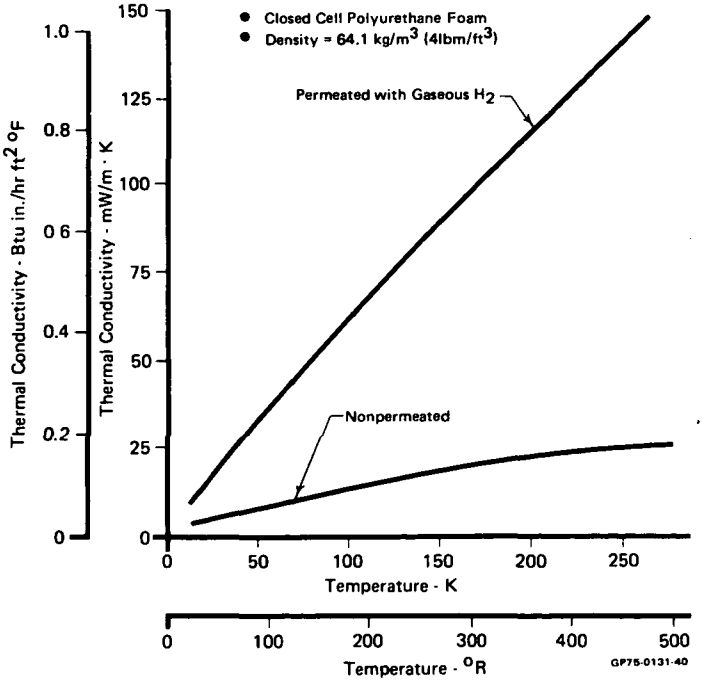

FIGURE 41
CRYOGENIC INSULATION THERMAL CONDUCTIVITIES

internal insulation. Reference 1 specified that the same type of material be used, but that the analysis be modified to reflect the effect of gaseous hydrogen permeation on its thermal conductivity. Figure 41 also presents these values, based on the assumption that complete permeation would produce a conductivity approximately equal to 90% of the conductivity of gaseous hydrogen.

Assumptions used to determine hydrogen fuel boiloff rates were as follows:

a. The liquid hydrogen sensible temperature rise is negligible relative to the latent heat of vaporization, h_v = 452 J/g (194 Btu/lbm).

b. The liquid hydrogen temperature is 20.3 K (-423°F) and tank pressures are constant.

c. Heat transfer between the tank wall and ullage gas as well as between the liquid surface and ullage gas is negligible.

d. The entire internal tankage surface area is wetted with liquid hydrogen.

e. A factor of 1.1 was applied to the heat transferred through the TPS to account for heat leaks due to structural penetrations through the insulation, etc.

The convective heat transfer effects of the purge gas on the adjacent surfaces was considered where appropriate. Radiation heat transfer between surfaces across purge gaps was also considered.

Additional considerations used for these analyses were:

a. Tankage insulation was sized to prevent condensation of nitrogen purge gas. The design goal was to insure that the surfaces adjacent to purge spaces were maintained at temperatures above the N_2 gas critical temperature of 78 K (-320°F).

b. External moldline temperatures must be held above 273 K (32°F) during ground hold to prevent frost buildup. The design goal was based on standard day conditions, ambient temperature = 289 K (60°F), with a 2.24 m/s (5 mph) wind, ignoring any solar heat input.

c. Tankage thermal protection systems must provide sufficient protection to prevent freezing of the coolant in the panel feeder lines. Individual analyses were conducted, when necessary, to confirm that feeder line coolant temperatures remain above 211 K (-80°F).

Purge system sizing was based on maintaining a positive gage pressure of 3.45 kPa (0.5 lbf/in^2) in the void spaces between the panels and the tank walls/ insulation. Reference 1 specified that dry nitrogen gas be used for purging. The amount of purge gas was defined as that required to replace gas leaked during the ground hold and flight times specified in Figure 40. Leakage area was defined as 0.63 mm^2/m^2 of surface area (9.04×10^{-5} in^2/ft^2 of surface area) based on current transport fabrication technology for pressurized structure. The surface area used was the moldline area in the tankage region. The effects of temperature on purge gas density were accounted for. A thin layer of aluminized mylar was assumed to cover the insulation. This cover would prevent N_2 purge gas leakage to the tank wall and at the same time exhibits a desirable low surface emissivity.

8.2 NON-INTEGRAL TANKAGE TRADE-OFF STUDY - CONCEPT 1

A steady-state one-dimensional heat transfer analysis was conducted on a typical non-integral tankage section to establish the relationship between insulation thickness and hydrogen fuel boiloff. Figure 42 illustrates the thermal model used and summarizes pertinent considerations. A 3.81 cm (1.5 in) cooled honeycomb surface panel was selected for the Concept 1 aircraft, based on a trade study discussed in Section 7 of Reference (2). The structural depth required for panel support frames resulted in a gap of approximately 12.7 cm (5 in) between the panels and the tank wall. Based on the techniques and assumptions discussed in Section 8.1, the results summarized in Figure 43 were obtained. These data indicate that the minimum combined insulation and fuel boiloff weight is realized when the insulation thickness is between 2.54 and 3.18 cm (1.0 and 1.25 inches).

Still, this did not establish the TPS configuration that results in maximum aircraft range. Originally, it was assumed that trends developed in previous hypersonic aircraft studies would be applicable. These studies indicated that aircraft range would be maximized by decreasing fixed insulation weight and increasing expendable weight (LH_2 boiloff), if the total weight remains near the minimum. This is because the aircraft must carry the fixed weight (insulation) throughout the mission, whereas the average fuel weight carried over the total flight time is only about 50 percent of the initial value. This resulted in the selection of an insulation thickness of 2.03 cm (0.8 in) for preliminary studies.

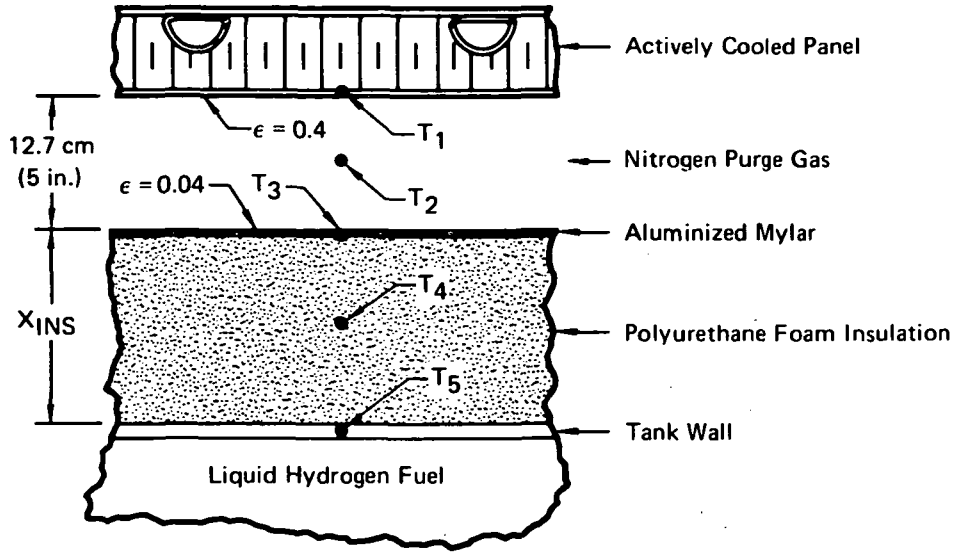

T_1 = 313K (103°F) = 366K (200°F) = 242K (−25°F)
Ground Hold Mach 6 Cruise Mach 0.8 Loiter

$$T_2 = \frac{T_1 + T_3}{2} \quad , \quad T_3 = f(X_{INS}) \quad , \quad T_4 = \frac{T_3 + T_5}{2} \quad , \quad T_5 = 20.3K\ (-423^{\circ}F)$$

Heat Transfer Considerations:

- Natural Convection between Purge Gas and Adjacent Surfaces,

  $h_{1\text{-}2}$ Based on GN_2 Properties at $\left(\frac{T_1 + T_2}{2}\right)$

  $h_{2\text{-}3}$ Based on GN_2 Properties at $\left(\frac{T_2 + T_3}{2}\right)$

- Radiation Across Gap
- Conduction Through Insulation, Thermal Conductivity (k) Evaluated at T_4

GP75-0131-164

FIGURE 42
NON-INTEGRAL TANKAGE TPS THERMAL MODEL

However, these previous trends had been developed on a basis of fixed range, with aircraft weight as the variable. When range sensitivities for the Concept 1 aircraft became available, this decision was re-evaluated. Based on the Figure 14 data, it was established that, in terms of range, every kilogram (lbm) gain in usable fuel is equivalent to a 1.61 kilogram (lbm) savings in empty weight. In other words, additional fuel is more valuable than lighter insulation weight, by a ratio of 1.61 to 1. This greatly increases

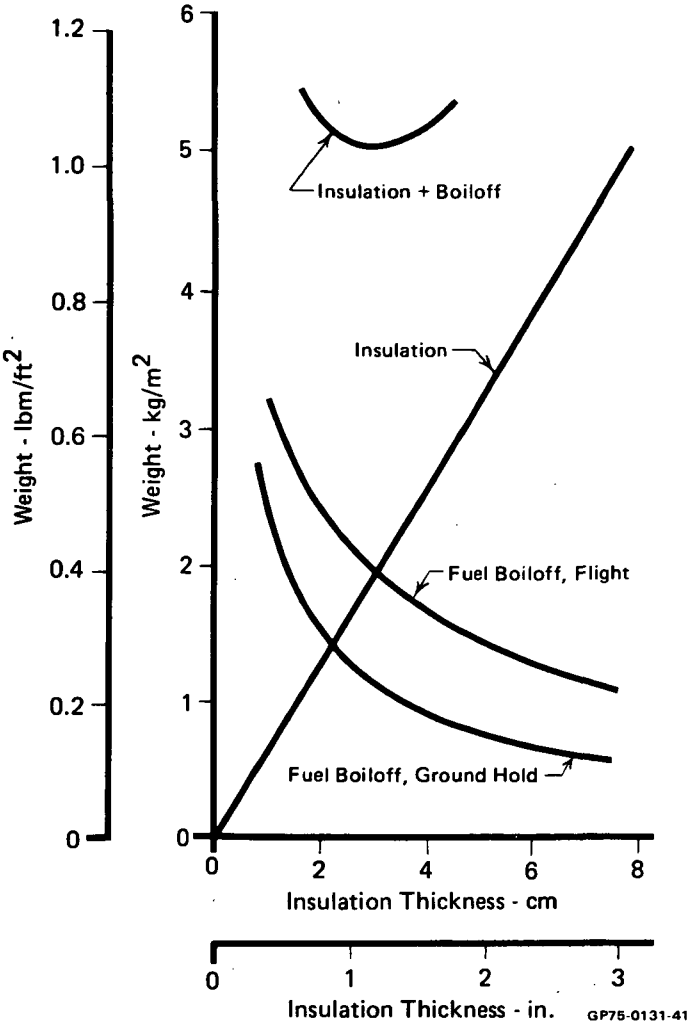

FIGURE 43
NON-INTEGRAL TANKAGE TPS CHARACTERISTICS

the insulation thickness, as shown in Figure 44. By plotting the unit insulation weight versus the unit hydrogen fuel boiloff weight and determining the tangency of a line with a 1.61 slope, a 4.27 cm (1.68 in) insulation thickness was determined to yield the maximum range. This is more than twice the previous value. The net result was an effective range gain of 72 km (39 NM).

To verify that this thickness and the associated fuel boiloff maximized aircraft range, other acceptable combinations of insulation and fuel boiloff weights were considered. These results, presented in Figure 45, verify the selection of 4.27 cm (1.68 in) of insulation, with an associated fuel boiloff of 2.54 kg/m^2 (0.52 lbm/ft^2). Based on a total tankage surface area of 1022 m^2 (11,000 ft^2), the total insulation weight was found to be 2.79 Mg (6160 lbm) and the total fuel boiloff to be 2.60 Mg (5720 lbm).

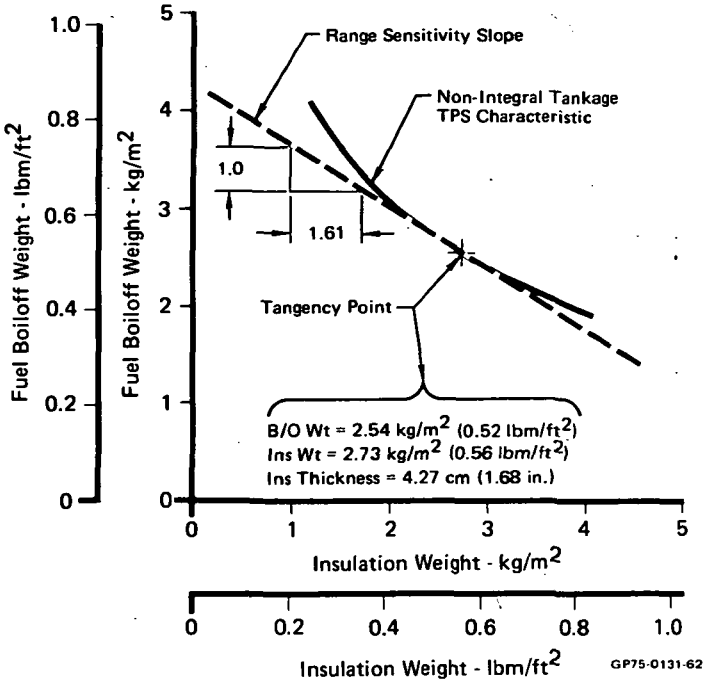

FIGURE 44
NON-INTEGRAL TANKAGE TPS SIZING

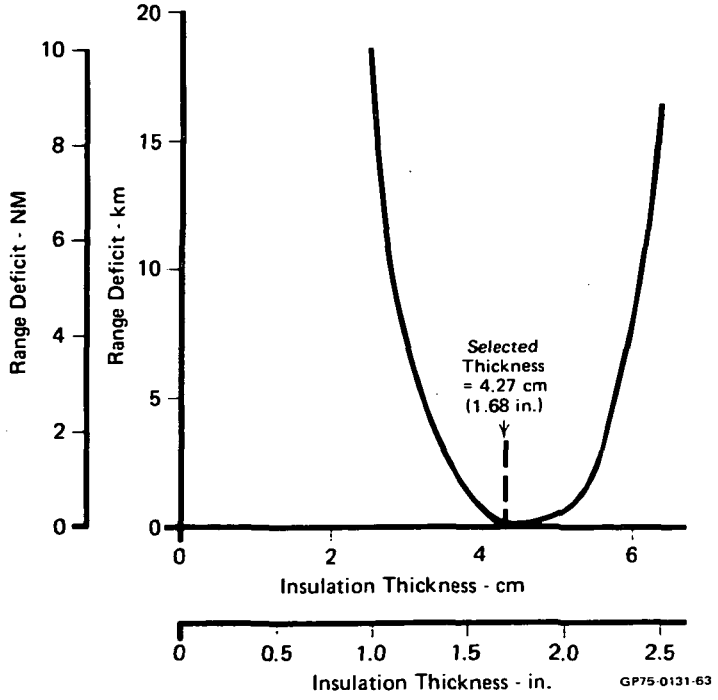

FIGURE 45
RANGE PENALTY ASSOCIATED WITH ALTERNATE NON-INTEGRAL TANKAGE TPS CONFIGURATIONS

Interface temperatures between the insulation and N_2 purge gas were investigated. This temperature had to be held above the N_2 condensation temperature of 78 K (-320°F). Figure 46 illustrates the insulation/N_2 interface temperatures for the ground hold, Mach 6 cruise, and Mach 0.8 loiter conditions. The interface temperatures for these three conditions were well above the critical temperature level at the selected insulation thickness.

Another consideration investigated was the effect on moldline surface temperatures of heat transfer to the cryogenic fuel during ground hold. These temperatures had to be held above 273 K (32°F) to prevent frost buildup on the aircraft skin. Minimum external surface temperatures were found to be approximately 283 K (50°F) with the selected tank insulation thickness. As discussed in Section 8.1, this analysis was based on standard day ambient conditions. For lower temperature ambients, it is likely that some type of ground support provisions would be required to prevent frost buildup. Possibly heating the coolant and circulating it through the panels during ground hold would be an acceptable solution. This consideration was not addressed during this study.

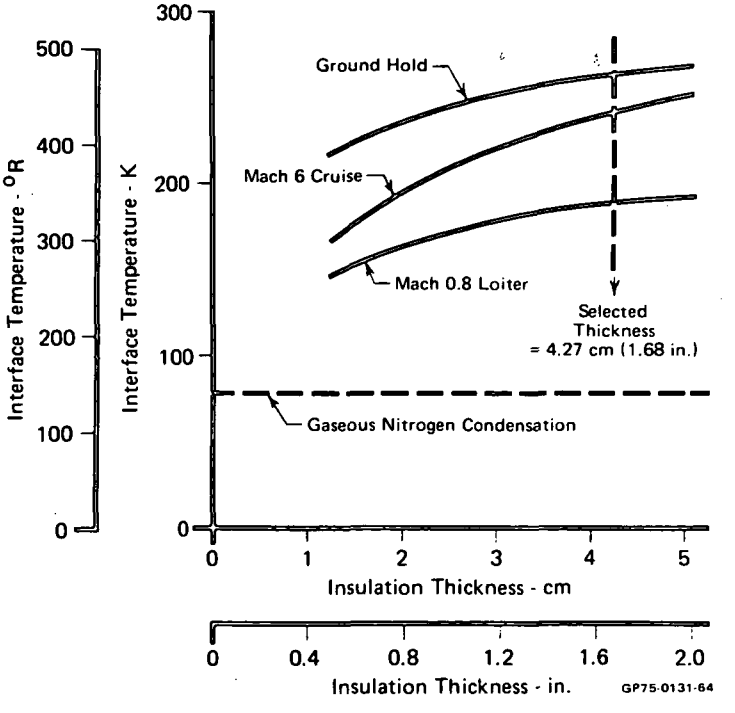

FIGURE 46
HYDROGEN TANKAGE INSULATION/PURGE GAS INTERFACE TEMPERATURES

8.3 INTEGRAL TANKAGE TRADE-OFF STUDY - CONCEPTS 2 AND 3

Eight candidate TPS concepts compatible with the integral tank structure and the cooling system were evaluated. The TPS weight and volume requirements and the resultant fuel boiloff were established for each concept, recognizing the differences in the thermodynamic aspects of each configuration. Parametric data were used to derive the combination of insulation and fuel boiloff resulting in maximizing aircraft range for each concept. The TPS requirements were then evaluated, along with structural, maintainability, and producibility considerations, to select a recommended concept for integral tankage design studies. NASA approval of the recommended concept was obtained before Concept 2 and 3 system design studies were undertaken.

8.3.1 Candidate Design Concepts - The eight candidate TPS concepts, designated as concepts (a) through (h), are indicated in Figure 47. This figure also defines pertinent configuration characteristics, such as whether or not:

a. the surface panels are primary structure,

b. the surface panels are cooled by the primary cooling system coolant or by hydrogen fuel directly,

c. the insulation material is assumed to be permeated with gaseous hydrogen and

d. a gap requiring purge is involved.

Evaluation of concepts (a), (b), and (c) was specified by Reference (4). Concept (a) is attractive due to its simplicity. Concept (b) was included to establish any benefits that would be derived by direct hydrogen cooled panels in the tankage area. Concept (c) was both thermodynamically and structurally similar to the non-integral tankage (Concept 1) configuration.

Concepts (d) through (h) were evaluated to insure that alternate concepts with unique advantages were not overlooked. Concept (d) reflected the effect of incorporating a gap in a configuration using permeated insulation. Concept (e) considered combining both non-permeated and permeated insulations. Concept (f) was included to determine if a payoff results from using the inherent hydrogen fuel boiloff to advantage as part of the overall TPS. Concept (g) provided an insight into any advantages to be gained by preventing GH_2 permeation of the insulation while maintaining utilization of the surface

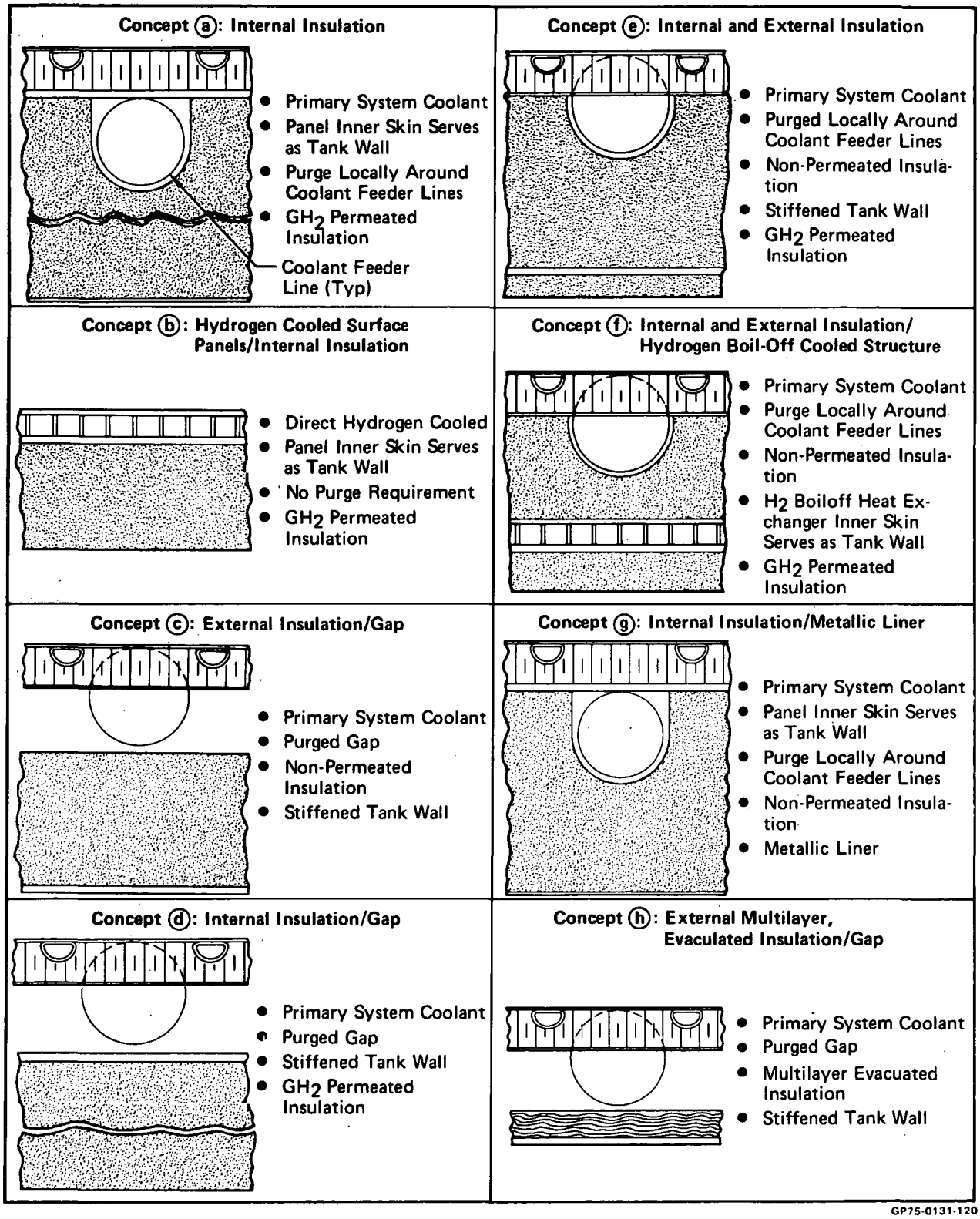

FIGURE 47
CANDIDATE INTEGRAL TANKAGE TPS CONCEPTS

panel as the primary structure. Concept (h) was included to establish if development of a multilayer, evacuated (super) insulation would pay significant dividends for this application.

8.3.2 Sizing Studies - Parametric data on TPS characteristics were generated for subsequent optimization study. These data were based on techniques and assumptions described in Section 8.1. Heat transfer characteristics of these concepts were primarily dependent on two factors - whether or not the cryogenic insulation was permeated with GH_2 and whether or not a purged gap was incorporated in the design. Figures 48 through 51 present TPS characteristics reflecting combinations of these two factors. Figure 48 contains data used in the evaluation of concepts (a) and (b) . Figure 49 (which is comparable to Figure 43) data pertain to concept (c) . Concept (d) sizing was based on Figure 50. Figure 51 data were used in sizing concept (g) and, ultimately, concept (e) .

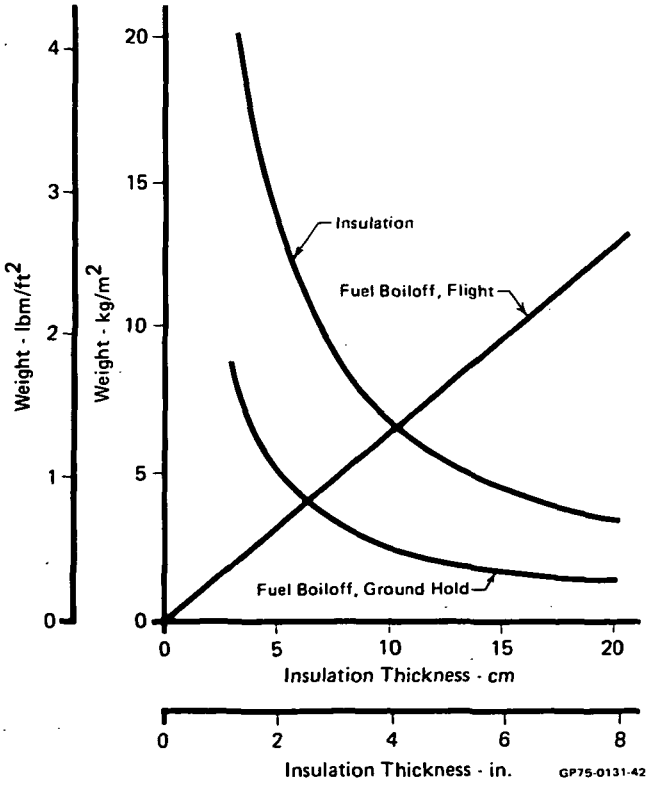

FIGURE 48
INTEGRAL TANKAGE TPS CHARACTERISTICS, INSULATION PERMEATED WITH GH_2, NO GAP

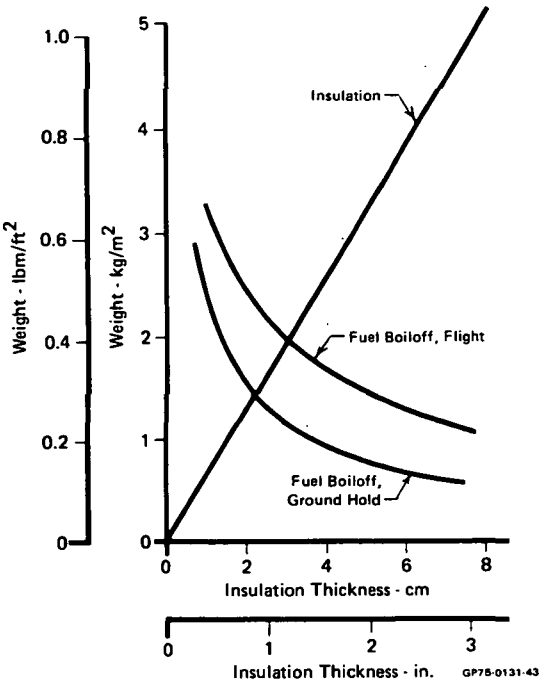

FIGURE 49
INTEGRAL TANKAGE TPS CHARACTERISTICS, NONPERMEATED INSULATION, GAP

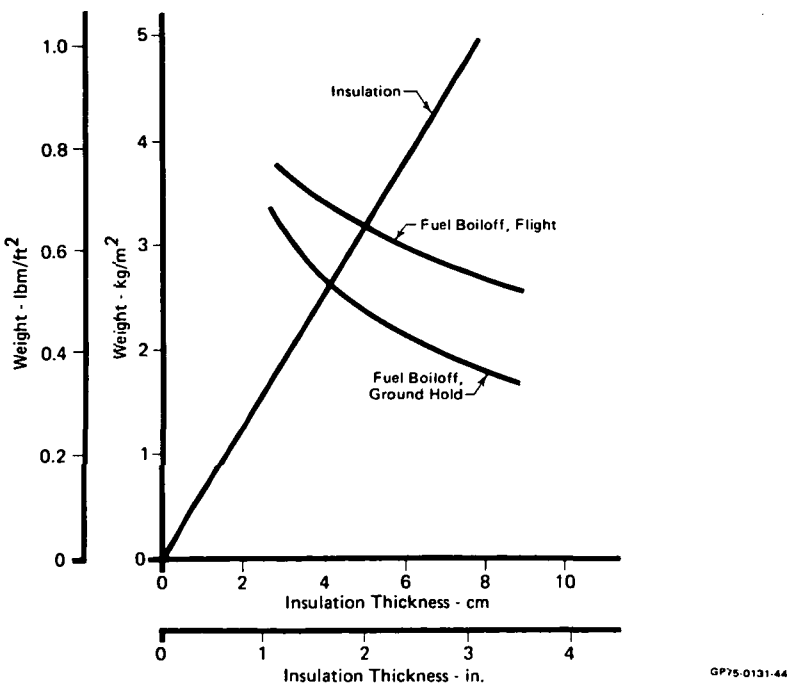

FIGURE 50
INTEGRAL TANKAGE TPS CHARACTERISTICS, INSULATION PERMEATED WITH GH_2, GAP

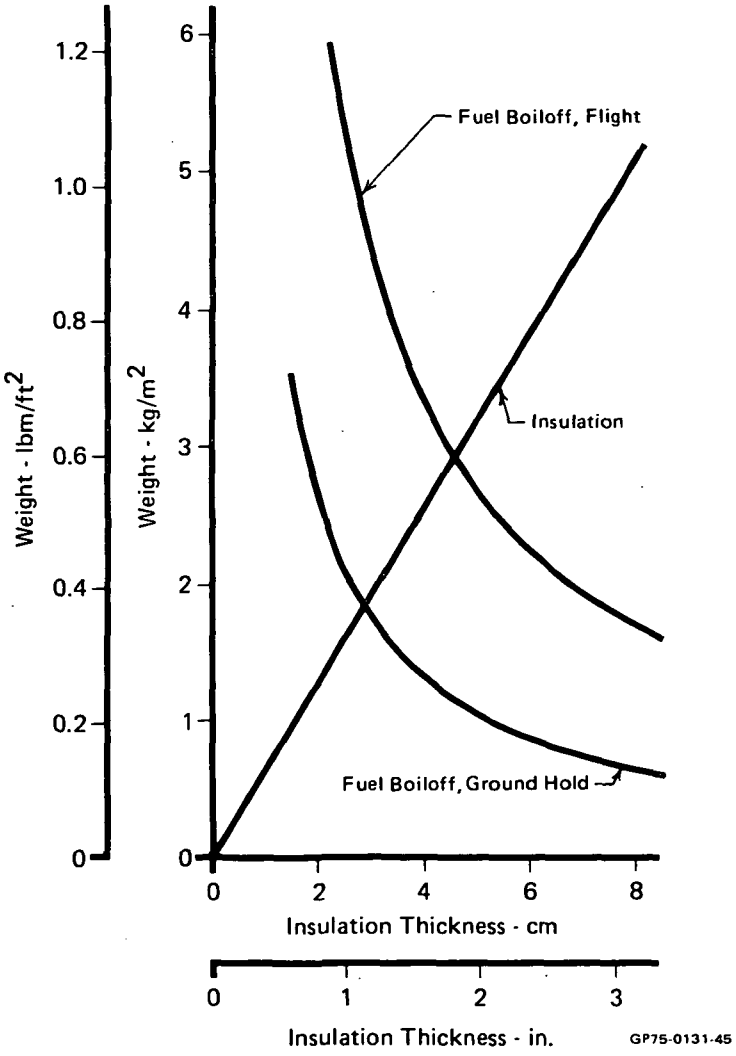

FIGURE 51
INTEGRAL TANKAGE TPS CHARACTERISTICS, NONPERMEATED INSULATION, NO GAP

Figure 52 shows the characteristics of concept (h), which has a multilayer, evacuated insulation and a purge gap. A cursory study was conducted to determine realistic values of density and thermal conductivity. These insulations, as a rule, are not considered as load bearing insulations. However, data indicate that, for densities of 320 kg/m^3 (20 lbm/ft^3) and greater, loads of 14-276 kPa (2-40 psi) can be considered. Thus, a density of 320 kg/m^3 (20 lbm/ft^3) was assumed, along with an optimistic average thermal conductivity of 2.88 mW/m·K (0.02 Btu in/hr ft^2°R).

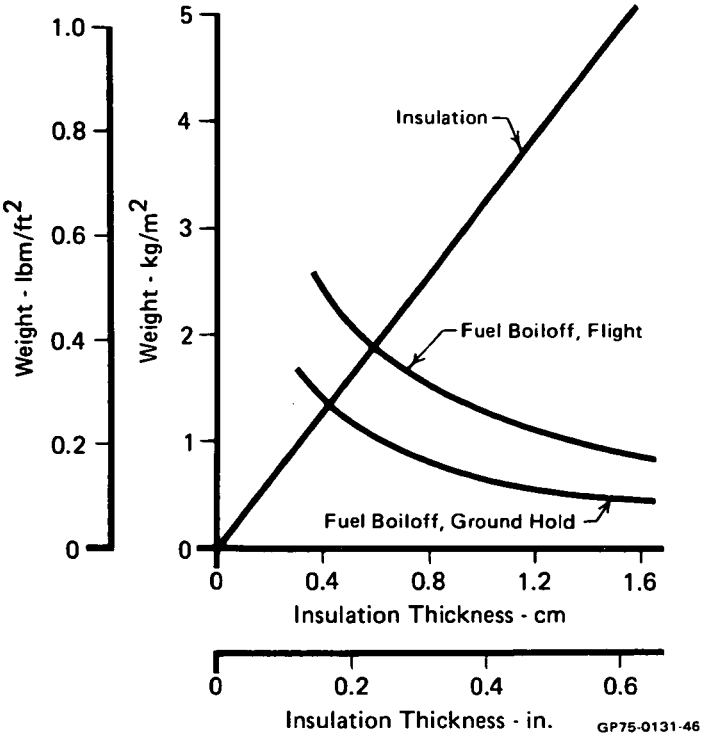

FIGURE 52
INTEGRAL TANKAGE TPS CHARACTERISTICS; MULTILAYER, EVACUATED INSULATION; GAP

Sizing concept (f) required a more detailed analysis. The analysis involved balancing the heat transferred through the external insulation with the heat transferred to the boiloff H_2 passing through the heat exchanger and the heat transferred to the fuel. This latter term was transformed into a boiloff rate which must balance with the flowrate through the heat exchanger. Various combinations of external (non-permeated) and internal (permeated) insulation were considered.

System weights were consistently minimized with approximately 1.27 cm (0.5 in) internal insulation. Figure 53 presents the characteristics for concept (f) with the internal insulation thickness fixed at 1.27 cm (0.5 in) and the external insulation thickness as a variable.

While Figures 48 through 53 characterize the various TPS concepts, a criterion was required to find the combination of insulation thickness and

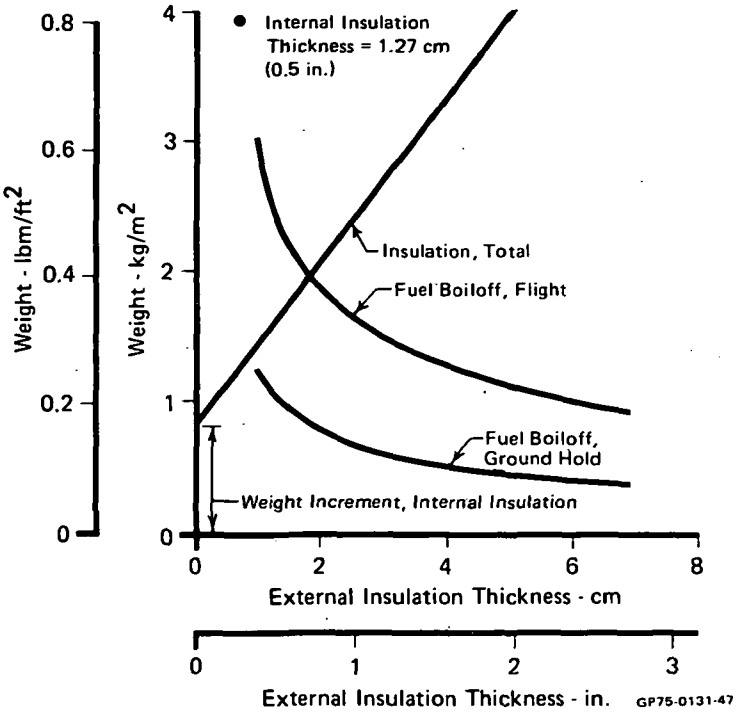

FIGURE 53
INTEGRAL TANKAGE TPS CHARACTERISTICS, INTERNAL (PERMEATED WITH GH_2) AND EXTERNAL (NONPERMEATED) INSULATIONS, H_2 BOILOFF COOLED STRUCTURE

fuel boiloff that resulted in a minimum penalty to the aircraft. The sensitivity data generated for Concept 1 (Figure 14) revealed that, for small variations around the baseline values, the following relationships hold:

$$\text{Effect of Empty Weight on Range} = 57.6 \text{ m/kg } \left(0.0141 \frac{\text{NM}}{\text{lbm}}\right)$$

$$\text{Effect of Fuel (Usable) Weight on Range} = 92.7 \text{ m/kg } \left(0.0227 \frac{\text{NM}}{\text{lbm}}\right)$$

These relationships indicate that a 1 kg (2.2 lbm) gain in usable fuel is equivalent to a 1.61 kg (3.55 lbm) savings in empty weight. The TPS configurations were then defined (as discussed in Section 8.2 for Concept 1) by plotting H_2 boiloff unit weight versus insulation unit weights and finding the tangency of a line with a 1.61 slope, as discussed earlier. The results are presented as Figure 54. To verify the adequacy of this approach, a few of

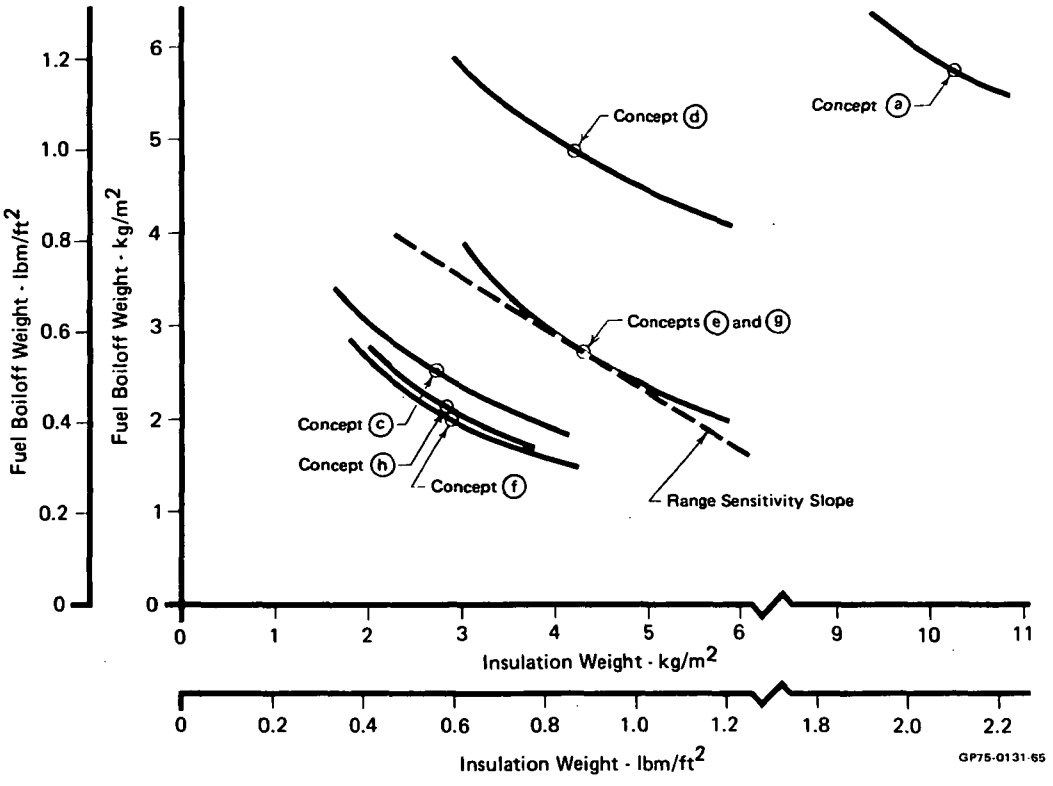

FIGURE 54
INTEGRAL TANKAGE TPS SIZING CURVES

the concepts were evaluated in detail (considering numerous combinations of boiloff and insulation weights), to insure that the selected TPS configurations maximized aircraft range.

From Figure 54, the selected TPS configurations for seven of the eight proposed concepts (all except concept ⓑ) are summarized in Figure 55.

Concept	Insulation Thickness		Insulation Weight		Fuel Boiloff Weight	
	cm	(in)	kg/m^2	(lbm/ft^2)	kg/m^2	(lbm/ft^2)
ⓐ	16.00	(6.3)	10.25	(2.1)	5.76	(1.18)
ⓒ	4.27	(1.68)	2.73	(0.56)	2.54	(0.52)
ⓓ	6.55	(2.58)	4.20	(0.86)	4.88	(1.00)
ⓔ	6.71	(2.64)	4.30	(0.88)	2.73	(0.56)
ⓕ (Ext)	3.23	(1.27)	2.88	(0.59)	2.00	(0.41)
(Int)	1.27	(0.50)				
ⓖ	6.71	(2.64)	4.30	(0.88)	2.73	(0.56)
ⓗ	0.89	(0.35)	2.83	(0.58)	2.15	(0.44)

FIGURE 55
SELECTED TPS CONFIGURATIONS

As shown, the TPS requirements for concepts ⓔ and ⓖ were the same. In concept ⓔ both permeated and non-permeated insulations were initially considered. However the minimum aircraft range penalties were realized when the thickness of the permeated insulation approached zero. Therefore, the selected concept ⓔ configuration did not reflect permeated insulation and concepts ⓔ and ⓖ became thermally identical.

Concept ⓑ required a unique thermal analysis since it was the only concept involving a change to the basic active cooling system. Cooling the surface directly with gaseous hydrogen deleted the requirement for an intermediate coolant system, with its associated penalties. To evaluate the weight savings, the cooling system weights directly attributable to cooling the upper surface of the fuselage in the tankage region, an area of approximately 511 m^2 (5500 ft^2), were determined. Using the Concept 1 active cooling system weight breakdown, the weight reduction potentials determined for concept ⓑ are summarized in Figure 56.

	kg	(lbm)
Coolant in Panels	274.4	(605)
Coolant in Lines	127.9	(282)
Distribution Lines	24.5	(54)
Connectors + Misc	6.8	(15)
Heat Exchanger	83.0	(183)
Pumps	25.9	(57)
Fuel to Drive Pumps	219.1	(483)
Total Potential Weight Savings =	761.6	(1679)

FIGURE 56
POTENTIAL WEIGHT SAVINGS IN ACTIVE COOLING SYSTEM WITH TPS CONCEPT ⓑ

Estimating the amount of hydrogen required to maintain the surface panels in the tankage region to a 367 K (200°F) average temperature was necessary to complete the evaluation of concept ⓑ . Based on an average heating rate of 15.7 kW/m^2 (1.38 Btu/ft^2 sec), typical of the tankage region, and an allowable temperature rise in the hydrogen of 291 K (523°F), a requirement for 13 Mg (28,765 lbm) of hydrogen during cruise was determined. Selecting the

insulation thickness and determining the associated fuel boiloff for concept ⓑ also involved unique considerations. These considerations are discussed in Section 8.3.4.

8.3.3 Structural, Maintainability, and Producibility Considerations - The structural components of each of the TPS concepts were sized to permit their weight and volume to be factors in the selection process. Actively cooled panels were considered non-structural when they were separated from the tank structure, and were sized to carry only their own pressure loading. When the panels were adjacent to the tank wall, they were considered to be bonded to the wall to provide stability.

The non-structural panels were considered to be supported by longitudinal stiffeners to prevent buckling. These stiffeners were assumed to be 3.8 cm (1.5 in) by 0.13 cm (0.05 in) with 12.2 cm (4.8 in) spacing. While some circumferential stiffening would be required, no weight allowance was introduced in the TPS comparisons, since the requirements would be common to all concepts.

Tank shell analyses were conducted using the same structural design criteria that were used for the non-integral tanks of Concept 1. Tank structure was designed to withstand ultimate burst pressure (factor of safety = 2.0) at room temperature. The tank structure for TPS concepts ⓑ and ⓕ also serves as a heat exchanger, with the internal pressures assumed to be variable between 0 and 138 kPa (20 psi) gage pressure. For these concepts, the tank walls were designed to withstand the internal pressure. However, sufficient redundancy exists so that the outer shell factor of safety was reduced to 1.5.

The candidate TPS concepts (Figure 47) could be classified into two structural arrangements. Concepts ⓐ, ⓑ, and ⓖ represent single structural wall arrangements. Concepts ⓒ, ⓓ, ⓔ, ⓕ, and ⓗ are arranged with actively cooled panels separated from the primary aircraft structure, the tank wall.

The single structural wall arrangements are efficient from a weight standpoint. However, the necessity to bond actively cooled panels to an all welded tank was considered to present significant fabrication problems. In addition, field inspection and repair procedures would be difficult and expensive. From the standpoints of maintainability and producibility, the

use of separate, non-structural panels was considered to be more attractive, despite their higher fixed weight. These panels could be readily removed for inspection, replacement, or repair, and fuel tanks could be replaced without full removal of the surface panels. In addition, the non-structural panel arrangements require only "state-of-the-art" techniques for fabrication and assembly.

The tank wall/heat exchanger structural requirements for TPS concepts ⓑ and ⓕ present an additional consideration. It was concluded that the structure would require diffusion bonding to insure against hydrogen leakage and to remain competitive on a weight basis. Development of this bonding process would significantly increase the initial cost investment, and the resultant structure would be extremely difficult to inspect and repair. Based on these considerations, concepts ⓑ and ⓕ were considered uncompetitive.

Concept ⓗ was included only for comparative purposes, since multilayer, evacuated insulation material was not felt to be sufficiently developed for this application.

In summary, the selection of one of the concepts ⓒ , ⓓ , or ⓔ was recommended in recognition of structural, maintainability, and producibility considerations.

8.3.4 Configuration Selection - After the concepts had been sized thermodynamically, the TPS requirements were combined with structural weight and volume requirements to define a tradeoff study. An additional factor was the possibility of coolant freezing, particularly in feeder lines to the panels. To protect these lines with insulation alone would result in an unacceptable weight penalty. The solution, in part, was to provide a gap of at least 2.54 mm (0.10 in) between the feeder line and any adjacent insulation. When the gap is purged with N_2, an efficient thermal barrier results. This solution also places all of the concepts on a more or less equal basis regarding the freezing potential. While additional provisions to prevent freezing may be necessary, the penalty involved was considered to be comparable for all of the concepts.

The size of the feeder lines directly influenced the overall thickness requirement for some of the concepts. While this consideration was taken into account, its effect was minimized to avoid any unfair penalties. In the

analyses conducted for Concept 1, the feeder lines had been sized for an allowable pressure drop of 2.26 kPa/m (0.1 psi/ft). However, in the tankage region, the design pressure drop can be increased to take advantage of the pressure drop between the main supply and return lines. Instead of incorporating flow restrictions to balance pressures, feeder line size was reduced from approximately 5.08 cm (2.0 in) I.D. to 3.00 cm (1.18 in) I.D. Space provisions were made for a feeder line of this size in each of the active cooling system concepts.

Figures 57 through 64 summarize the resultant candidate integral tankage TPS definitions. Concept weight and volume requirements are indicated, along with pertinent ambient temperatures. Notes are provided indicating relative fabricability, inspectability, maintainability, and cost characteristics.

Range calculations were conducted for system comparisons using concept (c) as the tradeoff baseline. Weight changes and the effects of fuel boiloff on usable fuel were reflected by using the sensitivity relationships discussed in Section 8.3.2. A sensitivity of 3.72 km/cm (5.1 NM/in.) in tankage region diameter was developed to reflect the effect of variations in volume requirements. Total weight and usable fuel changes were based on an assumed area of 511 m^2 (5500 ft^2), corresponding to the upper fuselage/tank area of Concept 1.

Only the upper half of the tankage area was used during the trade study to assess TPS concept (b) as fairly as possible. Since on this concept there are no surface panels directly below the circular fuselage tankage, properly evaluating the reduced effectiveness on the tankage lower half would have been complicated. It was decided to avoid this evaluation unless preliminary screening proved concept (b) to be a leading candidate. As a result of this provision, the aircraft ranges derived in the TPS trade study were only one half of those based on actual tankage area. The resultant half-range changes, relative to the baseline concept (c), are shown in Figures 57 through 64.

Concept (b) received additional attention. Originally, the analysis was conducted using the internal insulation thickness of 16 cm (6.3 in) determined for concept (a). As indicated in Figure 58, where this concept, (b_1), is compared to the baseline concept (c), the TPS weight increase of 1.35 Mg (2970 lbm) was only partially offset by the reduction in active cooling

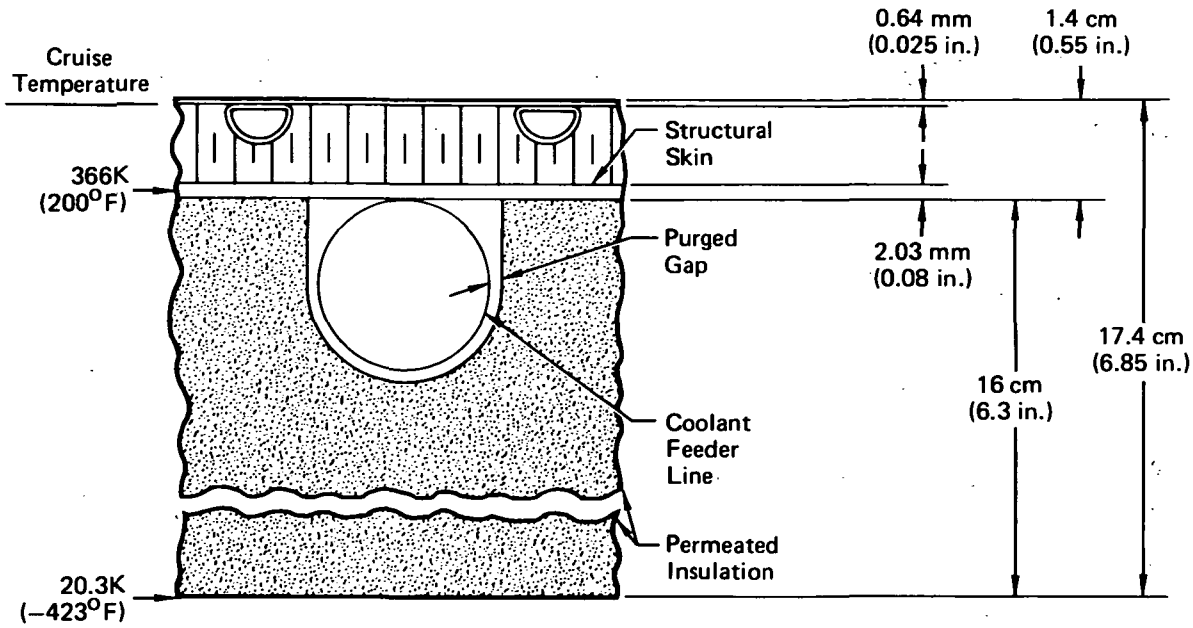

Unit Weights:	kg/m^2	(lbm/ft^2)	Difference from Concept Ⓒ	1/2 Range Change from Concept Ⓒ km (NM)
Actively Cooled Panel	13.4	(2.75)		
Insulation	10.3	(2.10)	Aircraft Weight = +4.3 kg/m^2 (0.88 lbm/ft^2) →	− 130 (70)
Purge System	0.1	(0.01)		
Fuel Boiloff	5.76	(1.18) →	Usable Fuel = − 3.22 kg/m^2 (0.66 lbm/ft^2) →	− 154 (83)
			Fuselage Diameter = +19 cm (7.48 in.) →	− 69 (37)
			Total =	− 352(190)

Notes:
1. Fabrication difficult, panels must be bonded to all welded tank
2. Poor inspectability and maintainability characteristics
3. High cost
4. Residual coolant weight not included.

GP75-0131-48

FIGURE 57
INTEGRAL TANKAGE TPS, CONCEPT (a)

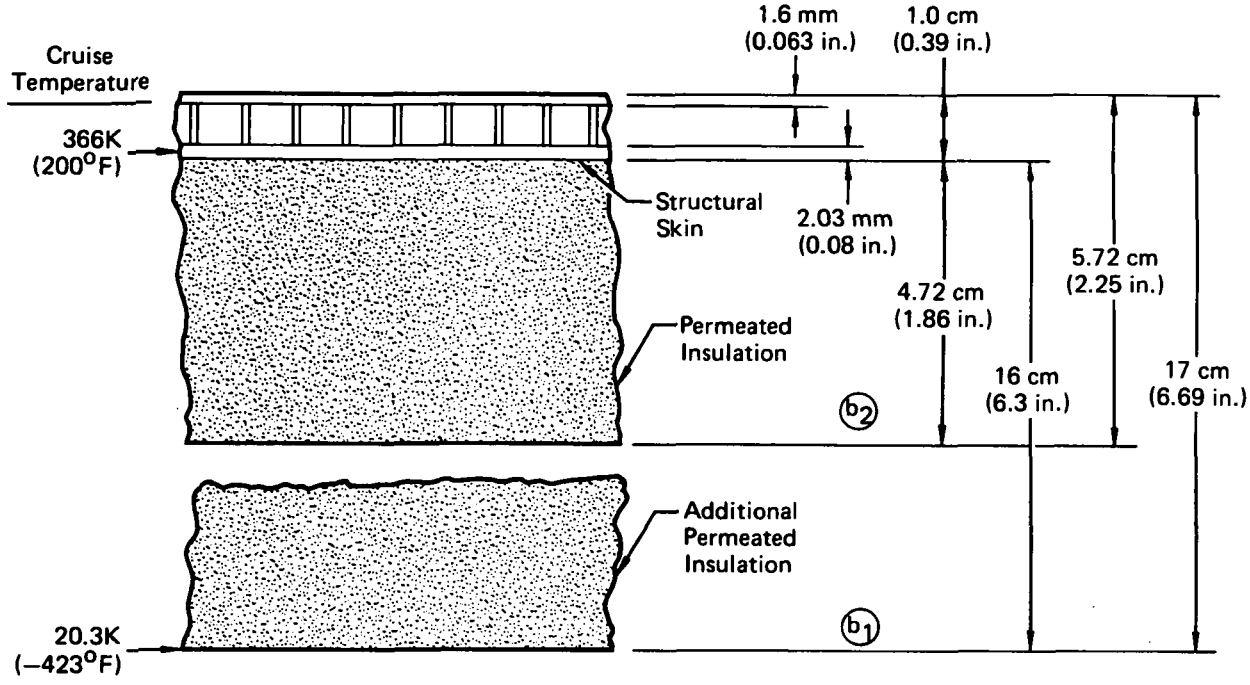

Unit Weights:	kg/m^2	(lbm/ft^2)	Difference from Concept (c)	1/2 Range Change from Concept (c) km (NM)
Hydrogen Cooled Panel	11.7	(2.39)		
Insulation, (b1)	10.3	(2.10)	Aircraft Weight	(b1) = +586 kg (1291 lbm) → − 33 (18)
(b2)	3.0	(0.62)		(b2) = −3110 kg (6949 lbm) → +178 (96)
Purge System	0.1	(0.01)	Usable Fuel	(b1) = +984 kg (2170 lbm) → + 91 (49)
				(b2) = −2900 kg (6390 lbm) → −269 (145)
			Fuselage Diameter	(b1) = +18.2 cm (7.16 in.) → − 67 (36)
				(b2) = −4.4 cm (1.72 in.) → + 17 (9)
				Total (b1) = − 9 (5)
				(b2) = − 74 (40)

Notes:
1. Aircraft weight differences reflect reduced active cooling system requirements
2. Fabrication difficult, cooled panel must be diffusion bonded
3. Poor inspectability and maintainability characteristics
4. High cost
5. Additional penalties for distribution system requirements are not reflected
6. Residual coolant weight not included.

GP75-0131-49

FIGURE 58
INTEGRAL TANKAGE TPS, CONCEPT (b)

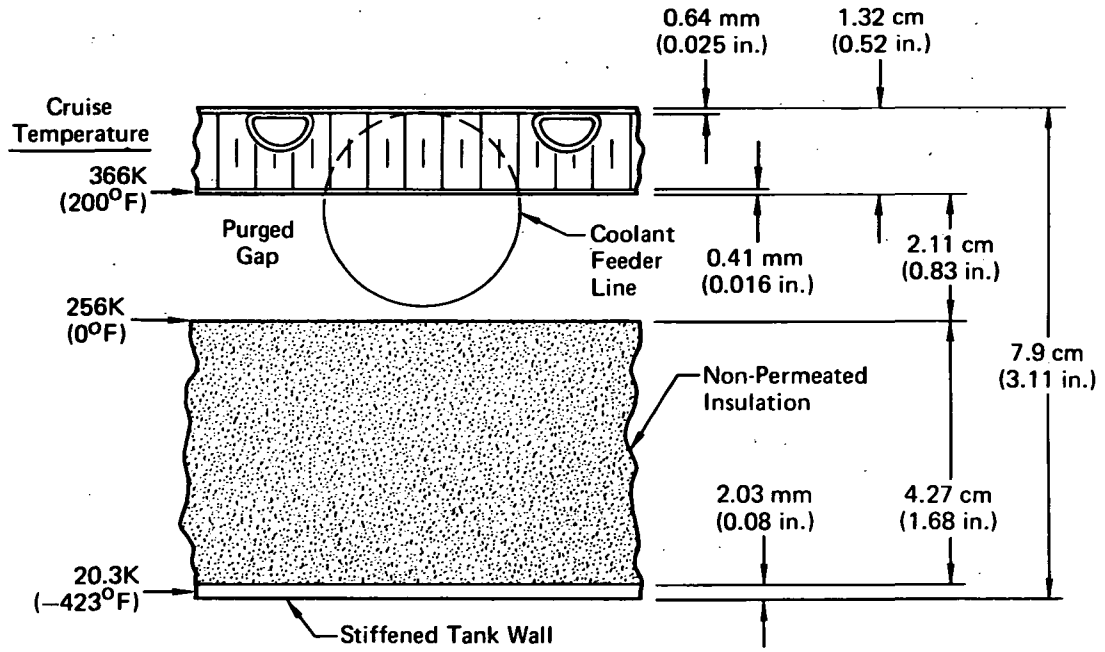

Unit Weights:	kg/m^2	(lbm/ft^2)		
Actively Cooled Panel	8.9	(1.82)	19.4 kg/m^2 (3.98 lbm/ft^2)	Baseline Concept
Panel Supports	0.5	(0.10)		
Insulation	2.7	(0.56)		
Tank Wall	6.7	(1.38)		
Purge System	0.6	(0.12)		
Fuel Boiloff	2.53	(0.52)		

Notes:
1. Current fabrication techniques are adequate
2. Good inspectability and maintainability characteristics
3. Residual coolant weight not included

GP75-0131-50

FIGURE 59
INTEGRAL TANKAGE TPS, CONCEPT (c)

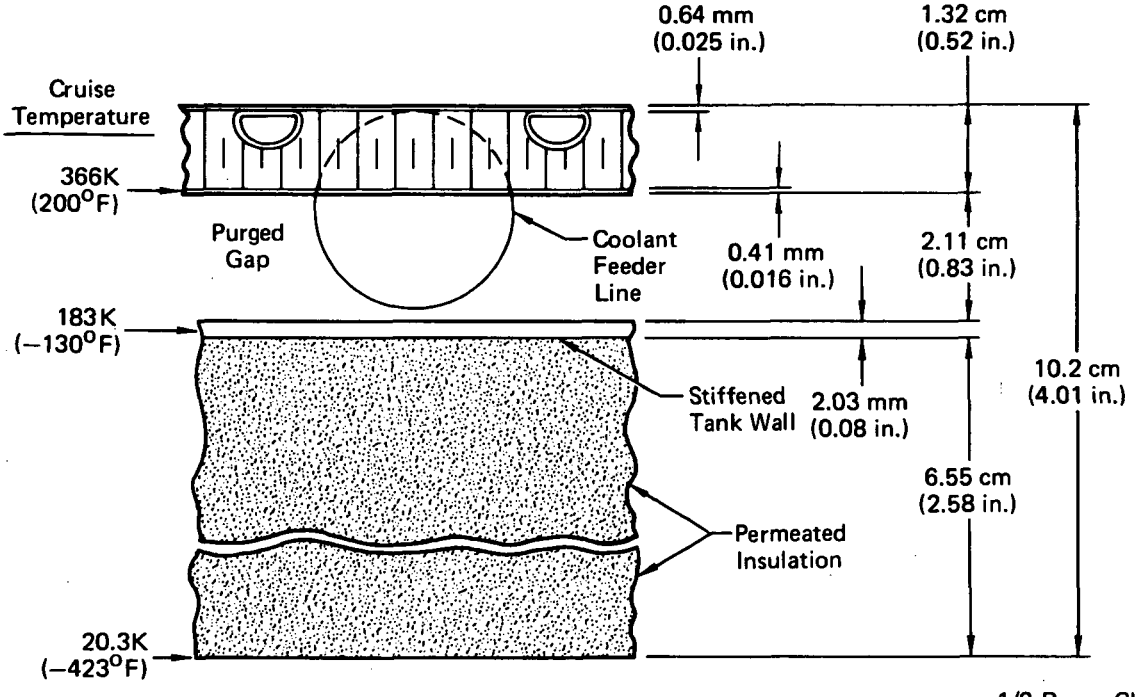

Unit Weights:	kg/m^2	(lbm/ft^2)	Difference from Concept (c)	1/2 Range Change from Concept (c) km (NM)
Actively Cooled Panel	8.9	(1.82)		
Panel Supports	0.5	(0.10)		
Tank Wall	6.7	(1.38)	Aircraft Weight = + 1.46 kg/m^2 (0.3 lbm/ft^2) →	− 46 (25)
Insulation	4.2	(0.86)		
Purge System	0.6	(0.12)		
Fuel Boiloff	5.18	(1.06)	→ Usable Fuel = −2.34 kg/m^2 (0.48 lbm/ft^2) →	−111 (60)
			Fuselage Diameter = + 4.6 cm (1.8 in.) →	− 17 (9)
			Total =	−174 (94)

Notes:
1. Current fabrication techniques are adequate
2. Good inspectability and maintainability characteristics
3. Residual coolant weight not included

GP75-0131-51

FIGURE 60
INTEGRAL TANKAGE TPS, CONCEPT (d)

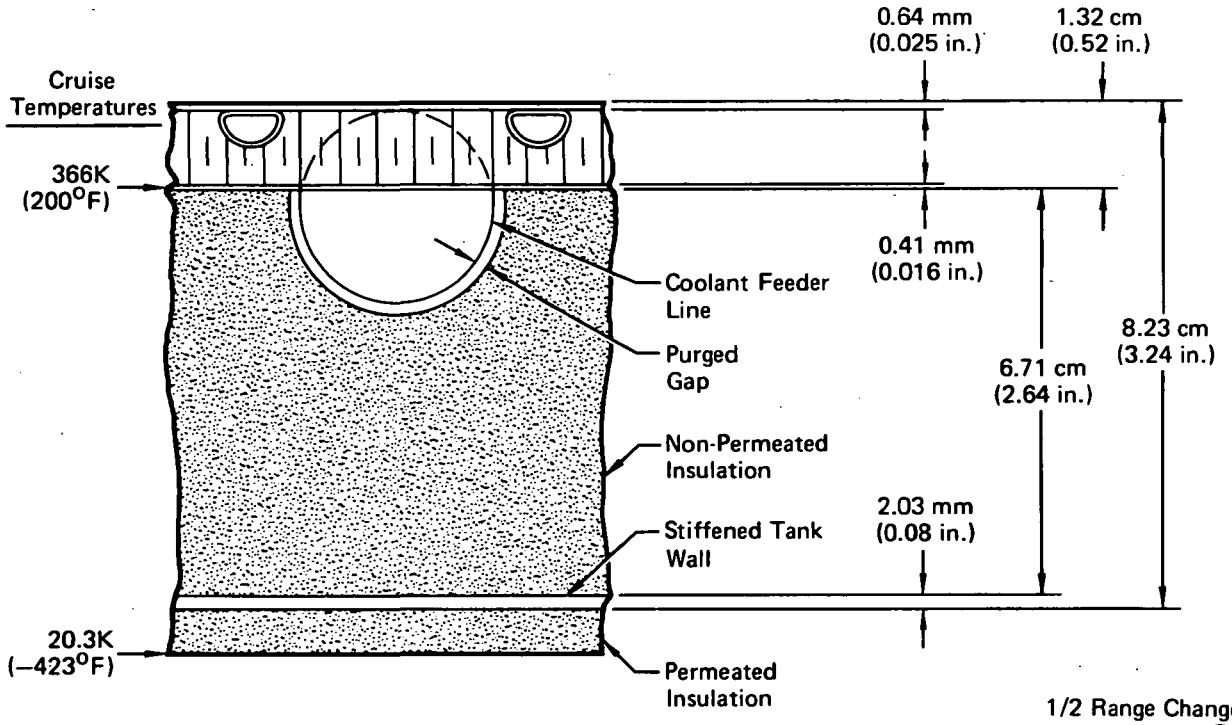

Unit Weights	kg/m^2	(lbm/ft^2)	Difference from Concept (c)	1/2 Range Change from Concept (c) km (NM)
Actively Cooled Panel	8.9	(1.82)		
Panel Supports	0.5	(0.10)		
Insulation	4.3	(0.88)	Aircraft Weight = + 1.03 kg/m^2 (0.21 lbm/ft^2)	→ −33 (18)
Tank Wall	6.7	(1.38)		
Purge System	0.1	(0.01)		
Fuel Boiloff	2.73	(0.56) →	Usable Fuel = −0.20 kg/m^2 (0.04 lbm/ft^2)	→ − 9 (5)
			Fuselage Diameter = + 0.7 cm (0.26 in.)	→ − 2 (1)
				Total = −44 (24)

Notes:
1. Current fabrication techniques are adequate
2. Good inspectability and maintainability characteristics
3. Residual coolant weight not included

GP75-0131-52

FIGURE 61
INTEGRAL TANKAGE TPS, CONCEPT (e)

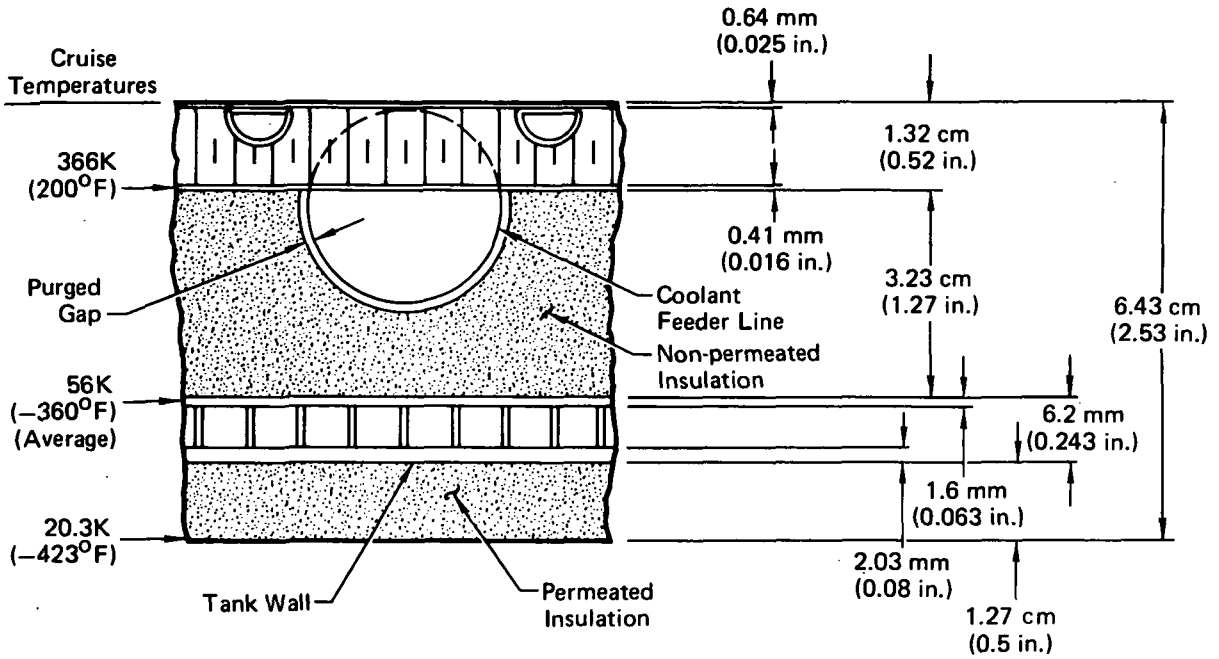

Unit Weights:	kg/m^2	(lbm/ft^2)	Difference from Concept Ⓒ	1/2 Range Change from Concept Ⓒ km (NM)
Actively Cooled Panel	8.9	(1.82)		
Panel Supports	0.5	(0.10)		
Insulation	2.9	(0.59)	Aircraft Weight = +4.54 kg/m^2 (0.93 lbm/ft^2) →	− 135 (73)
Structural Heat Exchanger	11.7	(2.39)		
Purge System	0.1	(0.01)		
Fuel Boiloff	2.00	(0.41)	→Usable Fuel = +0.54 kg/m^2 (0.11 lbm/ft^2) →	+ 26 (14)
			Fuselage Diameter = −2.9 cm (1.16 in.) →	+ 11 (6)
			Total =	− 98 (53)

Notes:
1. Fabrication difficult, structural heat exchanger must be diffusion bonded.
2. Poor inspectability and maintainability characteristics.
3. High cost.
4. Complex construction (internal manifolds, etc.)
5. Residual coolant weight not included

GP75-0131-53

FIGURE 62
INTEGRAL TANKAGE TPS, CONCEPT Ⓕ

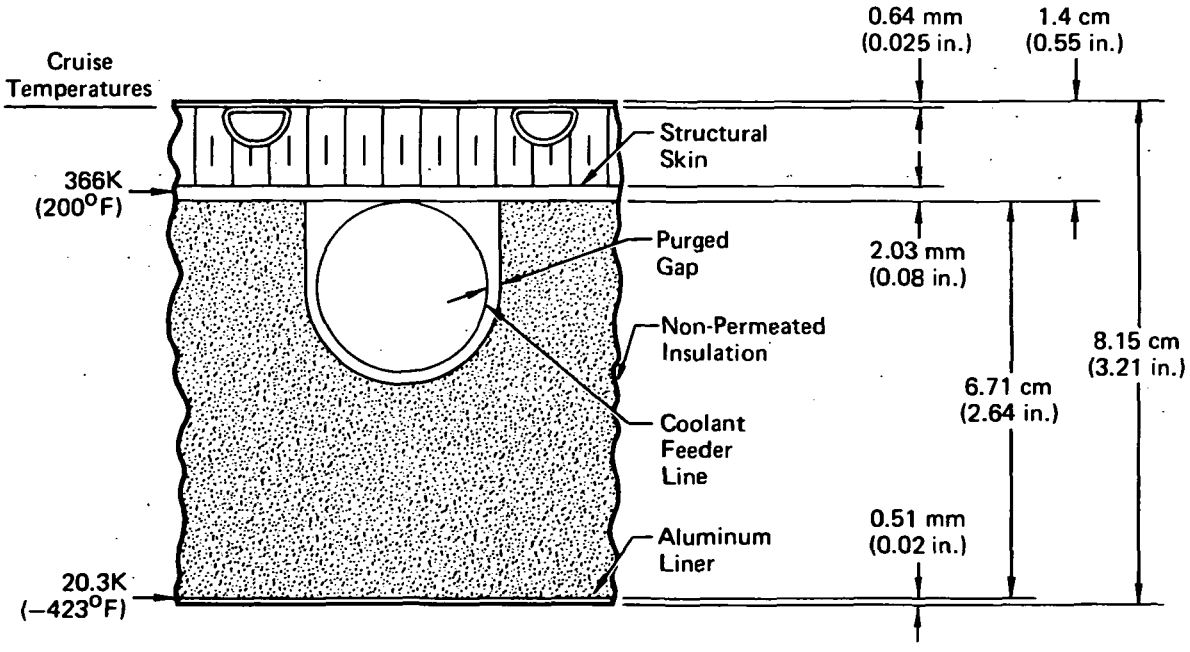

Unit Weights:	kg/m^2	(lbm/ft^2)	Difference from Concept (c)	1/2 Range Change from Concept (c) km (NM)
Actively Cooled Panel	13.4	(2.75)	Aircraft Weight = $-0.10\ kg/m^2$ $(0.02\ lbm/ft^2)$	→ +4 (2)
Insulation	4.3	(0.88)		
Tank Liner	1.6	(0.32)		
Purge System	0.1	(0.01)		
Fuel Boiloff	2.73	(0.56) →	Usable Fuel = $-0.20\ kg/m^2$ $(0.04\ lbm/ft^2)$	→ −9 (5)
			Fuselage Diameter = + 0.5 cm (0.21 in.)	→ −2 (1)
				Total −7 (4)

Notes:
1. Fabrication difficult, panels must be bonded to all-welded tank
2. Poor inspectability and maintainability characteristics
3. High cost
4. Residual coolant weight not included

GP75-0131-54

FIGURE 63
INTEGRAL TANKAGE TPS, CONCEPT (g)

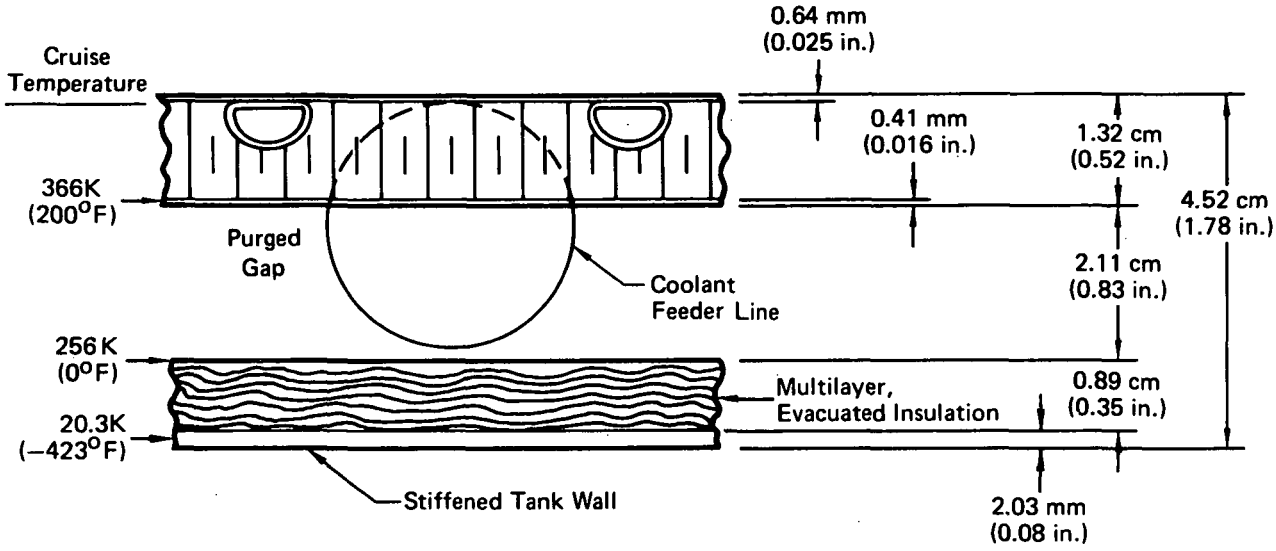

Unit Weights:	kg/m^2	(lbm/ft^2)	Difference from Concept (c)	1/2 Range Change from Concept (c) km (NM)
Actively Cooled Panel	8.9	(1.82)		
Panel Supports	0.5	(0.10)		
Insulation	2.8	(0.58)	Aircraft Weight = +0.10 kg/m^2 (0.02 lbm/ft^2)	→ − 4 (2)
Tank Wall	6.7	(1.38)		
Purge System	0.6	(0.12)		
Fuel Boiloff	2.15	(0.44) →	Usable Fuel = +0.39 kg/m^2 (0.08 lbm/ft^2)	→ + 19(10)
			Fuselage Diameter = −6.8 cm (2.66 in)	→ + 24(13)
				Total = + 39(21)

Notes:
1. Multilayer, evacuated insulation considered to be insufficiently developed
2. Good inspectability and maintainability characteristics
3. Residual coolant weight not included

GP75-0131-55

FIGURE 64
INTEGRAL TANKAGE TPS, CONCEPT (h)

system requirements. A net weight increase of 586 kg (1291 lbm) resulted. However, a gain in usable fuel was realized, since only 1.61 Mg (3540 lbm) are boiled off during ground hold, compared to 2.59 Mg (5710 lbm) in concept (c), a gain of 984 kg (2170 lbm). TPS height was increased 8.74 cm (3.44 in), however.

Considering each of these changes, a net range loss of 9.26 km (5 NM) was associated with concept (b_1) relative to concept (c). Additional requirements associated with concept (b) but not taken into account in this comparison were:

a. Provisions to route the H_2 to the external panels and then collect the H_2 and return it to the engines.

b. Provisions to boiloff sufficient H_2 during cruise to provide adequate surface cooling. With the assumed TPS configuration, only 3.84 Mg (8470 lbm) of H_2 would boiloff during cruise, compared to the required 13 Mg (28,765 lbm), due to the system heat leak.

Both of these considerations would substantially add to the weight of concept (b_1) and make it even less competitive.

An additional analysis was conducted on concept (b_2) by sizing the insulation to provide adequate surface cooling during cruise. The resultant insulation thickness was 4.72 cm (1.86 in). This approach saved 2.35 Mg (5170 lbm) (compared to concept (c)) and when added to the weight savings realized by deleting the active cooling system provisions, a net weight savings of 3.11 Mg (6849 lbm) resulted. In addition, TPS thickness was reduced 2.54 cm (1.0 in). Both of these changes resulted in benefits to aircraft range.

However, with this small amount of insulation, 5.49 Mg (12,100 lbm) of fuel would be lost as boiloff during ground hold. The net usable fuel loss of 2.9 Mg (6390 lbm) produced a loss in range potential that offset the aforementioned gains by 74.1 km (40 NM). Again, additional concept (b) requirements make the concept even less competitive.

Figure 65 summarizes the information contained in Figures 57 through 64. Concept (c) was selected for the Concept 2 and 3 aircraft, and was approved by NASA. This concept is thermodynamically and structurally similar to the one used on the Concept 1 (non-integral tankage) aircraft.

CONCEPT	1/2 RANGE CHANGE FROM BASELINE CONCEPT (c) km(NM)	DIFFERENCES FROM SELECTED CONCEPT (c)					TPS UNIT FIXED WEIGHT kg/m^2(lbm/ft^2)
		RANGE	FABRICATION	INSPECTABILITY/ MAINTAINABILITY	COST	DEVELOPMENT	
(a) STRUCTURAL COOLED PANEL, PERMEATED INSULATION	-352(190)	SIGNIFICANT LOSS	DIFFICULT	POOR	HIGH	-----	23.7 (4.86)
(b) STRUCTURAL H_2 COOLED PANEL, PERMEATED INSULATION	-9(5), (b_1) -74(40), (b_2)	---- LOSS	DIFFICULT DIFFICULT	POOR POOR	HIGH HIGH	REQ'D REQ'D	22.0 (4.50) 14.7 (3.02)
(c) STRUCTURAL TANK WALL, NON-PERMEATED INSULATION, GAP		BASELINE AND SELECTED CONCEPT					19.4 (3.98)
(d) STRUCTURAL TANK WALL, PERMEATED INSULATION, GAP	-174(94)	SIGNIFICANT LOSS	----	----	----	----	20.9 (4.28)
(e) STRUCTURAL TANK WALL, NON-PERMEATED INSULATION	-44(24)	LOSS	----	----	----	----	20.5 (4.19)
(f) STRUCTURAL BOILOFF H_2 COOLED TANK WALL, PERMEATED/NON-PERMEATED INSULATION	-98(53)	LOSS	DIFFICULT	POOR	HIGH	REQ'D	24.0 (4.91)
(g) STRUCTURAL COOLED PANEL, NON-PERMEATED INSULATION, METALLIC LINER	-7(4)	----	DIFFICULT	POOR	HIGH	REQ'D	19.3 (3.96)
(h) STRUCTURAL TANK WALL, MULTILAYER, EVACUATED INSULATION, GAP	+39(21)	INCREASE	----	----	----	REQ'D	19.5 (4.00)

FIGURE 65
INTEGRAL TANK TPS SELECTION

Originally, the selection was to be based solely on aircraft range. Figure 65, however, shows that most of the TPS concepts analyzed fall within a range band of one percent. This band was not felt to be wide enough for a clear decision. Thus, other factors were used in the selection of Concept ⓒ including fabricability, inspectability, and maintainability, as discussed in Section 8.3.3.

An insulation thickness of 4.27 cm (1.68 in) with an associated fuel boiloff of 2.54 kg/m^2 (0.52 lbm/ft^2), derived from the previously described tradeoff, were applied directly to the Concept 2 aircraft. This was justified when the Concept 2 range sensitivities were determined to be the same as those for Concept 1, Figure 14. For the Concept 2 tankage surface area of 1008 m^2 (10,850 ft^2), this resulted in a total insulation weight of 2.76 Mg (6076 lbm) and a fuel boiloff weight of 2.56 Mg (5642 lbm).

The Concept 3 aircraft was assumed to also have an integral tankage TPS similar to concept ⓒ . However, the TPS characteristics were modified to reflect range sensitivities determined specifically for Concept 3 (Figure 66). The following relationships were used:

Effect of Empty Weight on Range = 51.4 m/kg (0.0126 NM/lbm)

Effect of Fuel (Usable) Weight on Range = 95.9 m/kg (0.0235 NM/lbm)

Concept 3 TPS characteristics were defined by finding the tangency of a line with a 1.87 slope (0.0235/0.0126) with the plot of concept ⓒ insulation versus fuel boiloff weight shown in Figure 54. The resultant characteristics were established as an insulation thickness of 4.57 cm (1.8 in) with an associated fuel boiloff of 2.44 kg/m^2 (0.50 lbm/ft^2). For the Concept 3 tankage surface area of 1061 m^2 (11,425 ft^2), a total insulation weight of 3.11 Mg (6855 lbm) and a fuel boiloff weight of 2.59 Mg (5713 lbm) were determined.

8.4 PURGE SYSTEM SIZING - CONCEPTS 1, 2, AND 3

Purge system requirements were established using the techniques and assumptions discussed in Section 8.1. Due to the similarity of tankage TPS concepts, purge requirements were nearly the same for Concepts 1, 2, and 3. Leakage of the purge gas through the moldline panels was based on a leakage area relationship developed from available, current transport (specifically, the DC-10) characteristics. The extremely small leakage area was felt to be reasonable for the tankage region, due to the thermal design requirements of

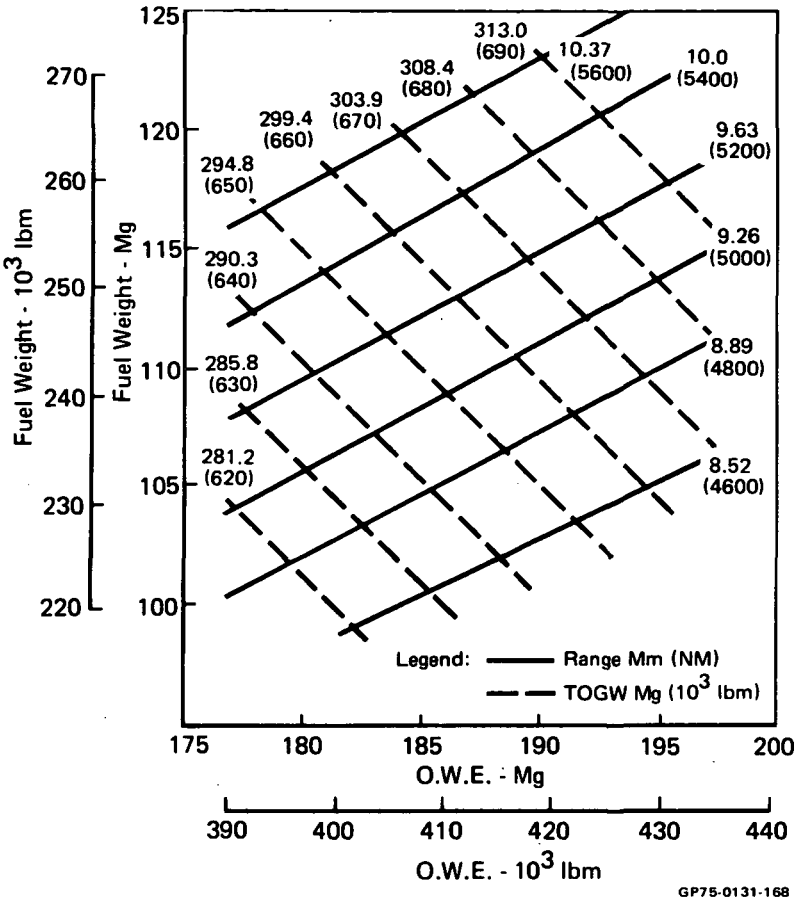

Notes:

1. Changes in O.W.E. (including total fuel weight) must reflect a 9% increment for a structural growth factor.
2. Changes in total and/or usable fuel weight may be read directly.

FIGURE 66
RANGE SENSITIVITY, CONCEPT 3

the actively cooled moldline panels. These panels require good thermal contact along the panel ends and sides to insure no detrimental hot spots.

The average gas temperature was determined during thermal protection system analyses by assuming convection from the surface panels to the N_2 gas and convection from the gas to the tankage insulation/gas interface. Figure 67 summarizes the amounts of N_2 used for Concept 1 during each phase of the flight, including the initial ground hold. The ground hold condition requires approximately 60 percent of the 411.6 kg (907.5 lbm) of nitrogen used by the purge system.

Based on this quantity of nitrogen purge gas, weights were established for a pressurized storage bottle, valves, lines, etc. The resultant purge system weight for Concept 1 was determined to be 597.4 kg (1317 lbm). Concepts 2 and 3 purge system weights were ratioed from the Concept 1 value using applicable tankage region wetted surface areas.

During the integral tankage TPS tradeoff study discussed in Section 8.3, allowances were made for purge system weight requirements. Concepts displaying air gaps as part of the TPS were charged with a 0.59 kg/m^2 (0.12 lbm/ft^2) weight allowance. Other concepts were felt to require some purging, such as through the air gaps between panel feeder lines and insulation, although the surface leakage areas involved were quite small. These concepts were charged a nominal 48.8 g/m^2 (0.01 lbm/ft^2) weight allowance for a purge system.

CONDITION	TIME MINUTES	N_2 USED KILOGRAMS	(POUNDS MASS)
Ground Hold	60.0	247.0	(544.53)
Climb	23.5	43.5	(95.98)
Cruise (M = 6)	64.0	39.6	(87.30)
Descent to Loiter	18.3	17.0	(37.40)
Loiter (M = 0.8)	20.0	44.4	(97.80)
Descent	6.1	20.2	(44.46)
Total GN_2 Used		411.6	(907.47)

FIGURE 67
PURGE SYSTEM NITROGEN GAS USAGE, CONCEPT 1

9. DESIGN OBSERVATIONS AND CONSIDERATIONS

In addition to the primary tasks of sizing the airframe's active cooling system and defining the fuselage tank thermal protection design concepts, certain other design aspects were evaluated to assist in establishing realistic structural arrangements and insure thermodynamic adequacy of the designs. The definition of the structural interface between the fuselage and the engine nacelle module required consideration of thermodynamic characteristics. An evaluation of panel joint designs was also performed to verify their adequacy for controlling the local surface temperatures.

9.1 ENGINE NACELLE THERMO/STRUCTURAL CONSIDERATIONS

As discussed in Section 4.3, original surface heating analyses conducted for the Concept 1 aircraft considered the effects of cooling the engine air induction system and the engine nacelle outer surfaces including the external ramps. It was recognized that the inner surfaces of the panels would be exposed to heating from the engine inlet. The high heating rates imposed on the inlet duct walls of hypersonic aircraft tend to drive hot structure design temperatures to unacceptable levels. For example, at Mach 6, surface temperatures approach 1700 K (2600°F), which would necessitate the use of heavy refractory materials.

For this study, it was assumed that the inlet duct walls will be designed as cooled panels, permitting the use of lighter materials. By routing hydrogen fuel through these panels before passing it to the engines, wall temperatures compatible with superalloy capabilities can be achieved. Cooling the walls to even lower temperatures to permit the use of lighter materials such as titanium has been shown to require more heat sink than is available at cruise engine fuel flowrates.

As a result, it was assumed in this study that the inlet duct walls were superalloy constructions cooled to approximately 1144 K (1600°F). It was assumed that the fuel passing through the inlet panels had already passed through the airframe's active cooling system heat exchanger. Consistent with the Reference (4) definition of "adequate fuel flow for vehicle cooling", no concern was given to verifying that adequate heat sink was available.

The heat transfer by radiation from the "cooled" inlet duct walls, at 1144 K (1600°F), to the backside of adjacent nacelle panels, at an average

of 366 K (200°F), was estimated to be nearly one half that of the external aerodynamic heating. Since that heating rate would significantly affect the size of the active cooling system, it was decided to minimize the effect by insulating the backside of the inlet duct walls so that the radiation heat transfer to the surface panels was reduced to an arbitrary level of one tenth that of the external surface heating. A 1.52 cm (0.6 in) layer of 56.1 kg/m^3 (3.5 pcf) fibrous insulation was determined to satisfy this goal. The weight of this insulation was reflected in the nacelle weights. Figure 68 indicates the thermo/structural considerations involved during the cooled nacelle analyses.

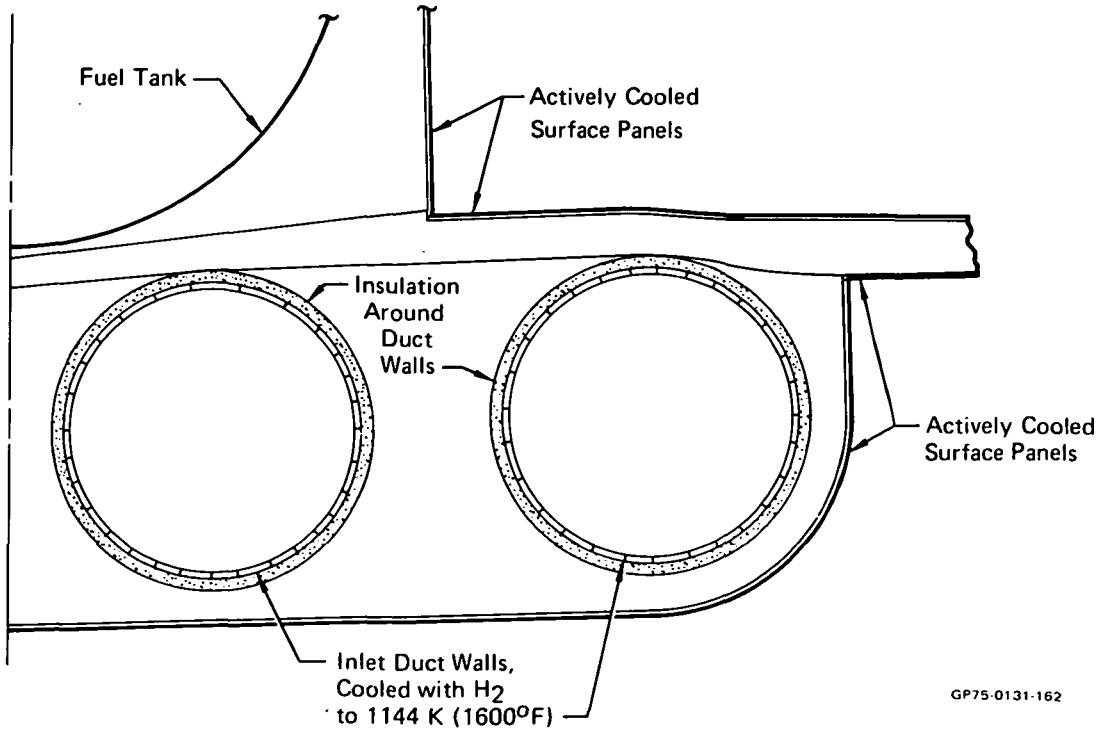

FIGURE 68
THERMO/STRUCTURAL DESIGN - COOLED NACELLE, ORIGINALLY PROPOSED FOR CONCEPT 1

However, as concluded in Section 4.3, active cooling of the nacelle surface panels was not justified, and the final designs of Concepts 1, 2 and 3 all incorporate a relatively "hot" nacelle structural design. These designs assume that the inlet duct walls are cooled only to a level consistent with superalloy material capabilities as discussed above. In fact,

the weight of all the nacelle structure reflects material densities typical of superalloy materials.

Since the nacelle surface panels are not cooled structure, there is no necessity to provide insulation completely around the inlet duct walls. Still, the lower surface of the fuselage at the nacelle interface and, in the case of Concepts 1 and 2, a portion of the upper wing panels, are exposed to radiation heat transfer from the upper duct walls. Therefore, it was assumed that an insulation blanket is located across the fuselage/nacelle interface surfaces to eliminate significant heat transfer. These considerations are summarized in Figures 69 and 70. Since heat transfer to the lower fuselage surface in the nacelle interface region is minimal, due to the insulation protection, the fuselage structure in these regions was assumed to be of conventional design, with no requirement to cool the interface area.

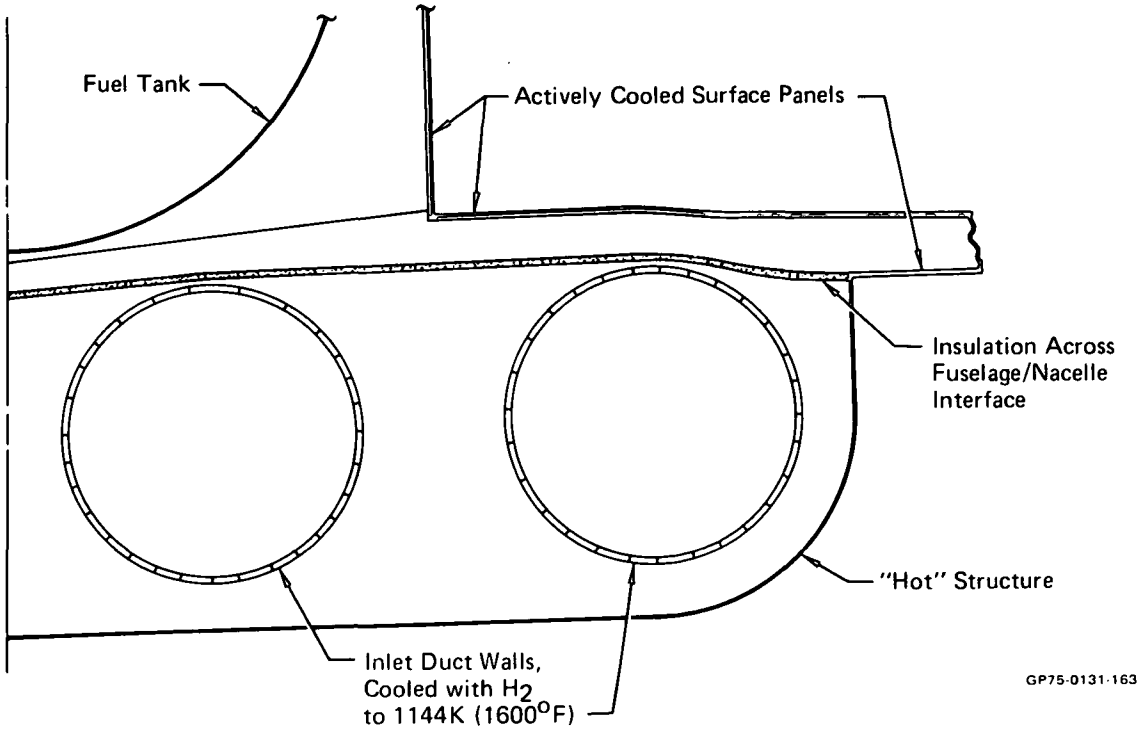

FIGURE 69
THERMO/STRUCTURAL DESIGN - "HOT" NACELLE CONFIGURATION, FINAL CONCEPTS 1 AND 2

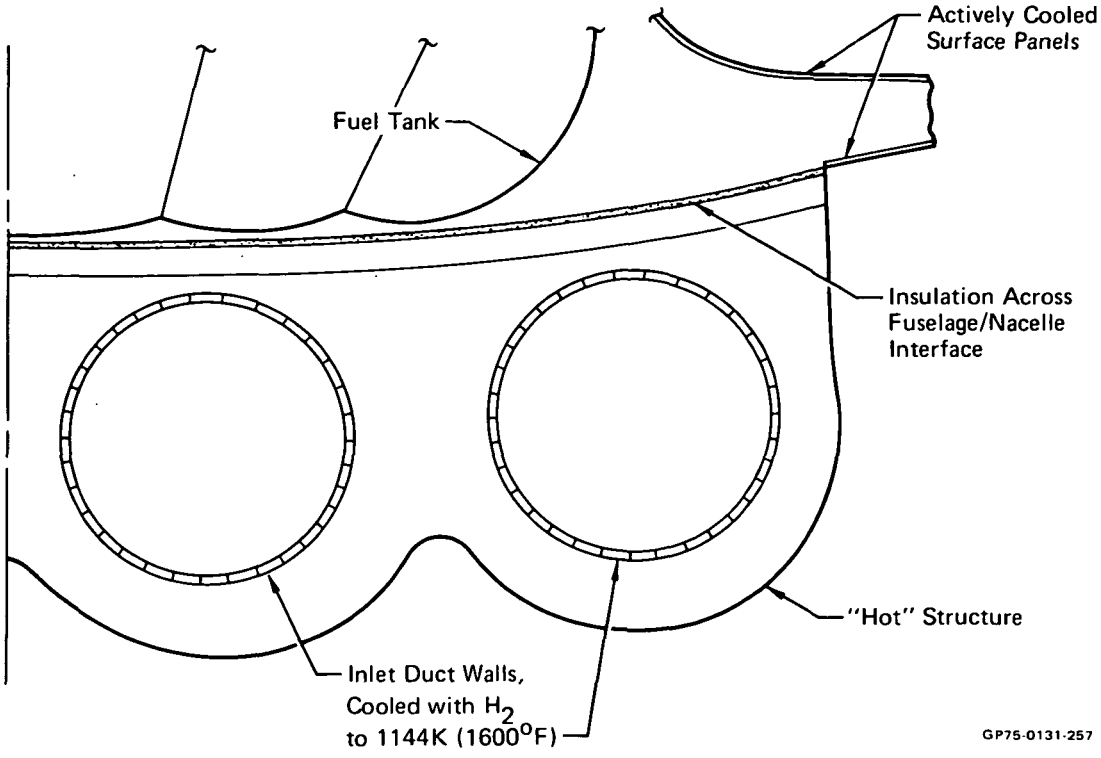

FIGURE 70
THERMO/STRUCTURAL DESIGN - "HOT" NACELLE CONFIGURATION, FINAL CONCEPT 3

9.2 COOLED STRUCTURAL PANEL JOINT DESIGNS

Analyses discussed in Section 5.1, and information derived from Reference (6), confirmed that surface temperatures in the panel skin between tubes and above the panel manifolds would not exceed 394 K (250°F). However, an additional analysis was required to confirm that surface temperatures were acceptable in the panel joint regions.

The actively cooled panel joint designs proposed for Concepts 1, 2, and 3 are significantly different, as indicated in Figure 71. However, the effects can be compared by analyzing the exit manifold end of the panels, where coolant and structural temperatures are at a maximum. Surface heating rates and coolant convective heat transfer coefficients experienced by panel manifolds and feeder lines at the forward end of the fuselage/tank area were used for this comparison.

In Concept 1 the actively cooled panels are primary load-carrying structural members. Loads are transmitted between panels by splice plates

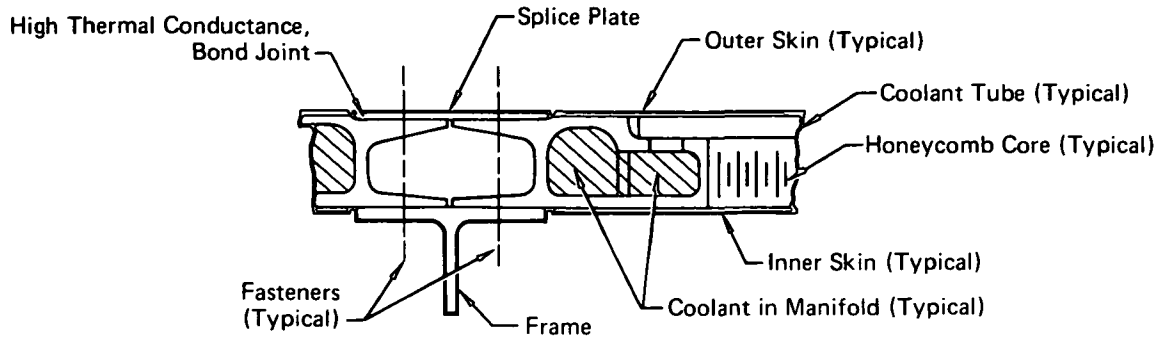

Concept 1 Panel Joint Design

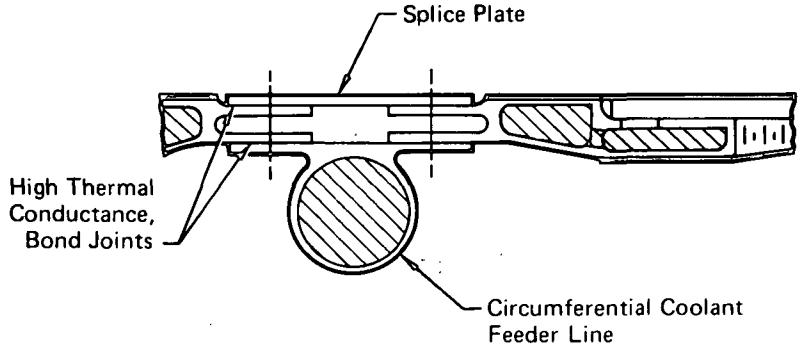

Concept 2 Panel Joint Design

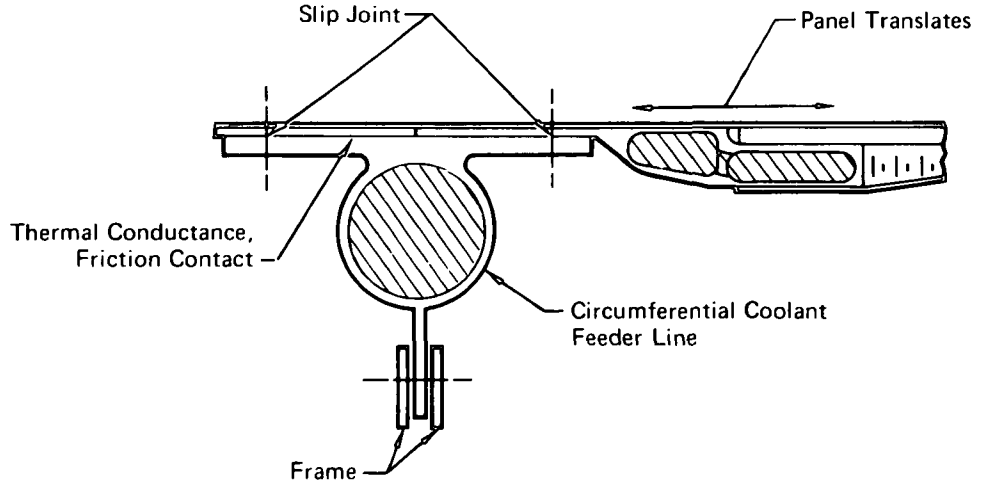

Concept 3 Panel Joint Design

GP75-0131-66

FIGURE 71
ACTIVELY COOLED PANEL JOINT DESIGNS

on both sides of the panels. At the manifold ends of the panels, fuselage frame outer caps serve as the inboard splice plates. These are permanent splice joints, and a high thermal conductance can be obtained by using a high conductance adhesive bonding agent. This interface treatment and the close proximity of adjacent panel manifolds insure maximum temperatures of approximately 339 K (150°F) at the mid-point of the external splice plate.

In Concept 2, the actively cooled panels over the fuel tank are "semi-structural". They are structurally assembled to each other, as in Concept 1, but their assembly to the aircraft induces significantly lower panel loading than in Concept 1. For this reason the panel thickness can be reduced to less than half that used on Concept 1.

At the manifold end of these panels, the coolant feeder line is employed as a fuselage frame and is used in combination with an outboard splice plate to transfer loads between panels. These rigid joints permit use of a high conductance bond similar to that employed on Concept 1. However, the distance of the outboard splice plate from the panel manifolds and the feeder line presented a potentially more critical design. Nevertheless, the maximum surface temperatures were determined not to exceed 366 K (200°F) on the Concept 2 splice plate.

The Concept 3 actively cooled panels are non-structural and are required only to transmit local air loads to the integral fuel tank for redistribution. At the manifold ends of the panels the circumferential coolant feeder lines were used as local panel supports. Local deflections were accommodated by slip joints around the periphery of each panel. These slip joints incorporate slotted holes in the coolant feeder line flanges to allow them to slide along the panel manifold flanges. Since no adhesive bond can be applied thermal conductance is low. The manifold flanges are thick enough, however, to provide an efficient heat path to the coolant in the panel manifolds. Also, the coolant in the feeder lines provides an efficient heat sink despite the low interface thermal conductance. As a result, maximum surface temperatures of only 350 K (170°F) were calculated for the Concept 3 panel joint area.

In conclusion, each of the structural panel joint designs proposed for the study aircraft satisfies the requirement for maintaining surface temperatures below 394 K (250°F).

10. CONCLUSIONS AND RECOMMENDED AREAS FOR FUTURE INVESTIGATION

Certain conclusions were derived from the active cooling system analysis which were not obvious at the initiation of the study. Although no unexpected trends were found, the study did provide insights into the significance of various parameters that had not previously been established. These conclusions provide a basis for subsequent analytical/research study requirements.

10.1 CONCLUSIONS

o Basic mission-related design requirements and assumptions must be given careful consideration, since active cooling system characteristics are very sensitive to certain factors. In particular, this study pointed out the following:

a. Selection of the design condition is critical. - As pointed out in Section 4.2, the aerodynamically desired ascent trajectory would have resulted in a 34% increase in cooling system weight and a net range loss of 289 km (156 NM).. While not considered in this system, design requirements imposed by flight maneuvering allowances could also significantly affect cooling system design and should be judiciously established.

b. Minimization of ground hold requirements is desirable. - Approximately 1/3 of the total hydrogen fuel boiloff (loss of usable fuel) and 60% of the nitrogen used by the purge system occur during a one hour ground hold.

o Even if an unlimited fuel heat sink is available, active cooling of the entire airframe surface may not be warranted. Section 4.3 summarizes a tradeoff between a cooled and a hot structure engine nacelle module. It was concluded that the higher structural weight of the hot structure design was more than offset by the reduction in cooling system weight. The hot structure nacelle design resulted in a 137 km (74 NM) gain in range. It is logical to assume that other regions with locally high average heating rates would display similar trends. A cursory comparison was made of hydrogen flowrate requirements. Based on a nominal cruise engine fuel flowrate of 15 kg/s (33 lbm/sec), the estimated heat sink available at the start of cruise is approximately 52% of that required to cool the Concepts 1 and 2 aircraft and 62% of that required by Concept 3. While fuel heat sink capacity will vary during cruise with engine demands, these percentages are representative.

Since the designs already reflect a hot nacelle structural design, it is obvious that to be compatible with the available heat sink: (1) large areas of the fuselage, wings, or vertical tail could not be cooled or (2) cooling requirements on a unit area basis must be reduced by using structural materials with higher design allowable temperatures or by shielding the structure.

o Performance sensitivities developed for these aircraft indicate that TPS fixed weight increases of up to 1.61 kg (lbm), for Concepts 1 and 2, and 1.87 kg (lbm), for Concept 3, that result in a savings of 1 kg (lbm) in usable fuel are justified.

o The weights of active cooling systems are high enough to influence aircraft sizing significantly. Trade-off studies to evaluate methods of reducing coolant flowrate requirements are warranted. Obviously, reducing distribution line sizes, hence residual coolant, by operating at higher pressure, etc. offers the greatest weight savings potential. The location of major components, such as the primary heat exchanger, was shown to be an important consideration. The necessity to provide a means of modulating coolant flowrates to minimize coolant pumping power penalties, as noted in Reference (5), was confirmed in these studies.

o TPS configurations employing internal insulation which can be permeated with gaseous H_2 are noncompetitive with alternate configurations. The degradation in thermal conductivity due to permeation requires excessive insulation thickness.

o TPS configurations employing an internal purged gap are attractive. Although the void area requires purging, the weight of the purge system is more than offset by the thermal resistance afforded by the gap. The gap provides a thermal barrier with little weight or volume penalty.

o Direct hydrogen-cooled surface panels cannot be justified except for high heat flux areas such as engine walls. Although cooling system weight is greatly reduced, it is more than offset by increased insulation requirements or by the decrease in usable fuel. In addition, structural, maintainability, and producibility considerations indicate that the approach is not competitive.

10.2 RECOMMENDED AREAS FOR FUTURE INVESTIGATION

o Studies to match cooling requirements to available fuel heat sink capacity should be pursued, and realistic weight penalties should be established. The potential of combining insulation and active cooling in panel

designs should be evaluated. Feasible hot structure designs should be developed to determine the weight penalties associated with regions that cannot logically be convectively cooled. These studies may indicate that other approaches, such as water blankets. are competitive with the cooled panel approach and should be considered in more detail.

o The development of an effective hydrogen vapor barrier for internal fuel tank applications should be pursued. The use of internal insulation would eliminate the need for thermal strain relief caused by large temperature differentials between structural components permitting use of lighter and simpler structural concepts. It would permit consideration of arrangements that combine the structural surface panel/tank wall functions to save further weight. In addition, insulation properties would not be degraded, hence volumetric efficiency would be enhanced and weight lowered due to reduced insulation requirements.

o A program extending the development of multilayer, evacuated (super) insulation is also recommended. External application of this type insulation would improve volumetric efficiency and reduce thermal protection weight. However, this would not afford the structural advantages gained with an effective vapor barrier.

o Investigations of several methods that could result in active cooling system weight reductions are warranted. Trade-off studies involving the following considerations are suggested:

a. Reduce coolant flowrate requirements by maximizing allowable surface temperatures and outer skin thermal gradients. - While structural weight penalties may result, the tradeoff with cooling system weight should be clearly established. For example, designing for a 422 K (300°F) maximum temperature rather than 394 K (250°F) would reduce flowrate requirements by nearly 40%. Increasing the allowable skin thermal gradient from 56 K (100°F) to 72 K (130°F) would reduce the number of coolant tubes required by about 10%.

b. Optimize coolant system design pressure. - A system design pressure of 1.03 MPa (150 psi) absolute was chosen for this study. A higher design pressure would permit larger pressure drops in the distribution lines, hence smaller lines and less residual coolant. Obviously, higher design pressures

necessitate structural weight increases and increased pumping power. It is estimated that a design pressure between 1.38 MPa (200 psi) absolute and 1.72 MPa (250 psi) absolute, would have reduced system weight by about 907 kg (2,000 lbm).

c. Establish the significance of centralizing the location of major cooling system components. - As discussed in Section 7.2, the heat exchanger location for Concept 3 resulted in a significant weight penalty. The penalty involved in providing adequate volume for components at a more favorable location should be assessed.

d. Refine feeder line sizing technique. - Each feeder line could be sized to match the local available pressure drop between the main supply and return lines. This study considered only a constant pressure drop per unit line length in establishing feeder line sizes. It is estimated that by considering locally higher line pressure drops a weight savings in the order of 454 kg (1000 lbm) would be reflected with this refinement.

e. Consider alternate line routing schemes. - Both this study and Reference (5) recognized the infinite number of possible line routings. While no attempt was made during this study to find an optimum configuration, it seems logical that benefits could be derived.

11. REFERENCES

1. NASA CR-132668, "A Fuselage/Tank Structure Study for Actively Cooled Hypersonic Cruise Vehicles - Aircraft Design Evaluation," T. Nobe, 30 June 1975.
2. NASA CR-132670, "A Fuselage/Tank Structure Study for Actively Cooled Hypersonic Cruise Vehicles - Structural Analysis," A. H. Baker, 30 June 1975.
3. NASA CR-xxxx, "A Fuselage/Tank Structure Study for Actively Cooled Hypersonic Cruise Vehicles - Summary," C. J. Pirrello, 30 June 1975.
4. NASA Request for Proposal 1-08-4129, "A Fuselage/Tank Structure Study for Actively Cooled Hypersonic Cruise Vehicles," Exhibit A, 17 August 1973.
5. NASA CR-1918, "Design of a Convective Cooling System for a Mach 6 Hypersonic Transport Airframe", R. G. Helenbrook and F. M. Anthony, December 1971.
6. NASA Contract No. NAS-1-12919, "Design and Fabrication of an Actively Cooled Panel", 1974.
7. NASA CR-1916, "Design and Evaluation of Active Cooling Systems for Mach 6 Cruise Vehicle Wings", W. A. McConarty and F. M. Anthony, December 1971.
8. NASA CR-1917, "Evaluation of Active Cooling Systems for a Mach 6 Hypersonic Transport Airframe", R. G. Helenbrook and F. M. Anthony, December 1971.
9. Federal Aviation Regulations, Part 25, "Airworthiness Standards; Transport Category Airplanes"
10. NASA TND-2350, "Afterbody Pressures on Two-Dimensional Boattailed Bodies Having Turbulent Boundary Layers at Mach 5.98", July 1964.
11. MCAIR Report No. A299, "Multipurpose Strategic Reconnaissance Aircraft Study", February 1964.
12. WADC TR-57-619, "Cooling Methods and Equipment for Supersonic Aircraft," G. R. Werth, H. K. McCluer, and G. T. Fitchett, February, 1960.